UCRL-11172

University of California

Ernest O. Lawrence Radiation Laboratory

CONTROLLED THERMONUCLEAR RESEARCH
SEMIANNUAL REPORT
July through December 1963

Berkeley, California

DISCLAIMER

UCRL-11172
Research and Development UC-20 Controlled Thermonuclear Processes
TID-4500 (24th Ed.)

UNIVERSITY OF CALIFORNIA

Lawrence Radiation Laboratory
Berkeley, California

AEC Contract No. W-7405-eng-48

CONTROLLED THERMONUCLEAR RESEARCH SEMIANNUAL REPORT

July through December 1963

January 30, 1964

Printed in USA. Price $2.25. Available from the
Office of Technical Services
U. S. Department of Commerce
Washington 25, D.C.

CONTROLLED THERMONUCLEAR RESEARCH SEMIANNUAL REPORT

July through December 1963

Contents

*Preceding semiannual reports: UCRL-10852, UCRL-10607

CONTROLLED THERMONUCLEAR RESEARCH SEMIANNUAL REPORT

July through December 1963

Lawrence Radiation Laboratory
University of California
Berkeley and Livermore, California

January 30, 1964

I. PYROTRON (MAGNETIC MIRROR PROGRAM)

1. Introduction and Summary

Richard F. Post

Several events of major significance to the Mirror Program have occurred during the last report period. In the Toy Top experiment a detailed study has elucidated the relationship between the stability of the plasma against a transverse drift (m = 1 interchange instability) and the phenomena of "end conduction" and "line tying." It has been shown that a low-density cold plasma exterior to the mirrors is capable of adequately stabilizing the hot plasma against transverse drifts. This, as far as we know, is the first clear-cut experimental proof of stabilization by line tying, that is, stabilization by the flow of currents (along the field lines) between the confined plasma and an exterior conducting region. At the same time it is observed that high-order ($m >> 1$) flutes do not play an important role in the losses, at least while the plasma is hot and remains stable against the $m = 1$ drift. During the time that this drift is suppressed the dominant loss mechanism is charge exchange, apparently arising primarily from the presence of neutral gas associated with the formation of the stabilizing cold plasma itself. For this reason it is found that attempts to improve the vacuum environment of the confined hot plasma tend to destabilize it, since such attempts necessarily diminish the amount of cold plasma available for line tying. This latter result is perhaps not too surprising, however, since in the absence of line tying the compressed plasma should indeed be $m = 1$ unstable; finite-orbit stabilization is ineffective against $m = 1$ drifts and the chamber wall is too far removed to provide centering. Although the problem has been pinpointed, there appear several possible avenues to its solution, some of which are mentioned below.

One approach to controlling transverse drifts is suggested by the most recent experimental results obtained on Table Top. Recently reported studies with this machine have shown that density regimes exist in which a rapidly developing instability may occur, grossly similar to the $m = 1$ transverse drifts in Toy Top. However, by activation of six "stabilizing" bars, similar to those employed by Ioffe in the USSR, complete stabilization

of these drifts has been observed. This result represents an independent verification of the stabilization effect observed by Ioffe. Its significance lies not only in this fact but in the fact that an entirely different plasma regime was studied, lending more generality to the result. In the Table Top experiment, a "hot electron" plasma was used, one which possessed a substantial electric potential. The experiments show that equilibrium electric fields of plasma origin do not destroy the stabilizing properties of multipole fields, but do not yet prove that there are no effects of importance associated with the presence of electric fields.

The origin of the stabilizing effect that multipole fields exert on a mirror machine is explainable in terms of the so-called "minimum-B" principle, long known in other connections (for example in the "cusp" confinement geometry). The idea here is to alter the mirror containment field so that there exists a region between the mirrors where the vacuum magnetic field has a local nonzero minimum. A low-β plasma confined in such a field should theoretically be stabilized against gross instabilities (such as $m = 1$ drifts), since it is resting at the bottom of a magnetic potential well. Strong multipole fields (produced by longitudinal bars) superimposed on the usual mirror field is a simple example of a field with a local nonzero minimum, and is the one first tested by Ioffe. Recently Harold Furth of this laboratory has made a theoretical study of the properties of minimum-B vacuum fields and has shown that there exists a wide class of such fields which are axially symmetric, in contrast to the multipole fields, which depart radically from axial symmetry. The new symmetric fields described by Furth (forms of which were also discovered by Andreoletti in France) in some cases closely resemble ordinary mirror fields of the types which we have been studying. It seems possible that these new fields may have substantial advantages over multipole minimum-B fields. A computation program is under way to determine practical coil systems that can be used to generate the new symmetric fields.

We believe that the impact of the "minimum-B" principle will be very large in our work, and are taking steps to incorporate tests of it into every element of the program. However, because of the somewhat restrictive conditions which the requirement for "minimum-B" places on the design of mirror containment fields, we are at the same time attempting to find what compromises, if any, can be made without losing stability. Finding answers to this latter question may become a matter of considerable importance, not only to the Mirror program but to other approaches as well. The alternatives to the use of pure minimum-B fields are: (a) shaping of the mirror fields to achieve stability according to hydromagnetic theory (the so-called "max $\int d\ell/B$" criterion), and (b) finite-orbit stabilization, coupled with suppression of $m = 1$ modes by other means. In matter of fact the present experiments on Alice are steps in this direction; future Alice experiments will be aimed at elucidation of both (a) and (b).

In the present Alice experiments a new milestone of sorts has been passed. Following recent improvements in beam and vacuum the experiments have now clearly demonstrated that under normal circumstances the density achieved is not limited by these two purely "technological" considerations, but is instead now limited by cooperative effects. Specifically the evidence appears to point to the existence of an $m = 1$ rotating flute-like

instability. Thus we see that in all three mirror machine experiments, Toy Top, Table Top, and Alice, one sees evidence of a particular gross instability, one of the simplest possible form, and precisely that one least affected by finite-orbit stabilization effects. Though this would be discouraging if one had hoped to avoid this difficulty by chance, the similarity of the instability effects demonstrated by these three dissimilar experiments encourages one to believe that a solution applying to all will be found. The direct evidence of $m = 1$ stabilization now demonstrated in Table Top gives added weight to this hope. What lies beyond the successful stabilization of the presently observed instabilities is not known, but we feel that there is no reason to be pessimistic about the future at this time.

2. MULTISTAGE HIGH-COMPRESSION EXPERIMENTS

Frederic H. Coensgen, William F. Cummins, Robert E. Ellis, William E. Nexsen, Jr., and Arthur E. Sherman

Toy Top III S

Operation of Toy Top III S during the past six months has greatly increased our understanding of the evolution and decay of the hot-ion plasma in this device. New information has been obtained primarily as the result of three developments.

First, the successful development of a plasma camera has enabled us to study the complete cross section of the plasma flux beyond the far mirror. The camera replaces a 54-channel probe array. This simplification has made possible some correlation of the end-flux data with the neutron, light, and peripheral-probe data.

Second, operating conditions have been found for which the trapped plasma exhibits a strong, easily recognizable transverse drift. This drift is evidenced by the coincidence of a rapidly rising signal from a wall probe located at the center of the containment section, a sudden increase in light from the containment chamber, and a sharp decrease of the neutron production rate. In a number of instances time-resolved plasma camera photographs were obtained at approximately the same time as the probe signals. In each instance these pictures show a rather irregular plasma cloud extending outside the limiting flux tube in the direction of the probe on which the large ion-current signal was received.

The third development is the discovery and investigation of methods by which the plasma contact with the wall could be delayed or eliminated; i.e., for certain conditions the wall bombardment during the compression cycle could be prevented or made to appear from one operation to the next. The control appears to depend on the density and duration of the plasma external to the containment chamber. This plasma forms a conducting link between the contained plasma and the vacuum chamber walls, and can thus limit the magnitude of the E_θ fields. This limitation in turn limits the transverse drift velocity, which is proportional to $E_\theta \times B_z$. We believe these data constitute the first positive evidence of the effect of external plasma on the stability of mirror containment systems; i.e., of the often

discussed "line tying" effects. These results as well as the fact that the fields are so symmetric that the magnetic aperture is nearly equal to the 9-inch bore of the vacuum chamber lead us to interpret the observed drift as a low-order (m = 1 or 2) hydromagnetic instability rather than a drift induced by field asymmetries. The observed tendency of the drift to occur predominantly in one direction is probably due to a slight asymmetry of the field and is not inconsistent with the instability interpretation.

Recent results have not altered the conclusions presented in the June 1963 semiannual report. These are essentially summarized in the statement that the general shape of the neutron histogram is determined primarily from a competition between the compressional and heating effects of the rising magnetic field and the loss of energetic ions due to the charge exchange. However, we now interpret histogram "fine structure" such as flat tops, ragged or broken peaks, abrupt changes of slope, etc. as evidence of hydromagnetic instabilities. In fact a large part of the data from past operation--which has been obtained from the various probes and probe arrays, light monitors, and neutron detectors--appears to be consistent with the presence of a low-order instability. The fluctuation of the data from one operational cycle to the next as well as its dependence upon operating condition can be ascribed to differences in the conductivity and lifetime of the external plasma. These factors affect the magnitude of the transverse drift velocity as well as the time of wall contact and hence strongly influence the character and the consequence of the plasma-wall contact thus producing the observed variations of the data.

If these explanations are adopted it becomes necessary to postulate the presence of some stabilizing mechanism from the beginning of the compression, for the plasma-wall encounter discussed above occurs at least 40 μsec after the magnetic compression is initiated, whereas the theoretical growth rate of the hydromagnetic instability is of the order of 1 μsec. Previously it was hypothesized that the late plasmas from the injectors and the plasma lost through the mirrors were responsible for the absence of a detectable m = 1 instability. In addition to these effects it appears likely that the initial wall bombardment gives rise to a third source of early external plasma. Such bombardment is known to occur. The longitudinal variation of the bombardment has been determined throughout the 9-inch chamber by means of a movable wall probe. Peripheral probe arrays at the 9-inch to 18-inch transition and at the center of the containment region have been used to study its azimuthal variation. Plasma is first detected at these locations about 12 μsec after the injectors are fired, and persists from 5 μsec to more than 100 μsec, depending primarily upon the longitudinal position. It is postulated that the wall bombardment causes the desorption of approximately 1/2 monolayer of gas from the transition end of the 9-inch vacuum chamber. Not only does this gas quickly raise the neutral background pressure to the 10^{-5} torr range, but also forms a low-temperature partially ionized plasma through photoionization and interaction with the injected energetic plasma. Consequently when the pulsed magnetic fields are applied there is a ready supply of charged particles which can be accelerated by the induced E_θ fields. Some of these particles can gain sufficient energy so that they contribute to the continued formation of a low-temperature plasma through further desorbing impacts with the walls and through ionization of the desorbed gas.

Just after the compression is initiated the following plasma components are probably present: (a) a trapped plasma within the containment chamber, (b) a streaming plasma from the injectors, (c) a cold plasma column between the mirror and the vacuum chamber walls, (d) the cold plasma sheath which is formed as just described, and (e) the leakage flux of the contained plasma through the mirrors. That portion of the injected plasma which is not reflected by the first mirror but which flows through the containment volume is referred to as a streaming plasma. The term "cold plasma column" is used to distinguish that portion of the plasma outside the first mirror which arises due to reflection of part of the injected plasma at this mirror and by reflection at the converging field in the transition region. Lifetimes of the cold plasma (b), (c), and (d) are limited to a few tens of μsec as the regenerating mechanisms die out, that is, as the plasma ejection from the injectors ends and the electric field which leads to regeneration of the cold plasma sheath decreases. In the absence of a regenerating mechanism the cold plasma lifetime is of the order of the ion transit time from the mirror to the wall. Thus the stabilizing effect of the external cold plasmas is limited to times of the order of 50 μsec. However, the transverse drift velocity is still limited by the plasma losses through the mirrors. As calculated from an expression derived by Rosenbluth, this velocity for the normal III S operating conditions is $\approx 10^4$ cm/sec. If the density of the contained plasma is less the drift velocity can be faster. Unstable operation to Toy Top III S was obtained through a series of changes which in retrospect all tended to lower the density and conductivity of the various cold plasmas and which lowered the density of the trapped plasma. Subsequently operations that increased one or more of these densities reversed the tendency for instabilities to develop.

It can be predicted that as the efforts toward cleaner walls progresses the trapped plasma will exhibit greater tendency to develop instabilities. This will be due to the inhibition of cold plasma formation and a decrease in the end loss rate, which is now probably dominated by the loss of cold ions left in the containment region as a result of charge exchange.

Upon our returning from the conference on "Mirror Confinement" held at Fontenay-aux-Roses in July, 1963, the LRL mirror machine program was intensively reviewed and as a result was to some extent reoriented toward "minimum B" geometries. Part of this reorientation was the decision that the initial 2X experiment should be built with a multipolar winding. Effectively, the first stage of the 2X operation has been dropped. As a large fraction of the bank 6 energy is needed to activate the multipolar field it is necessary to complete this construction before operating in the 2X location. This change of plans together with a support level far below that predicted last June has delayed the initial operation in this area.

The fields of several mirror-multipolar configurations have been determined by use of the MAFCO code developed by Walton A Perkins for the 7090 computer. Satisfactory mirror quadrupole systems have been designed, but work is continuing in an effort to design circularizing transitions outside the containment region. If circularization is possible the contamination problems will be simplified, as the plasma lost through the mirrors could be diverted to large-area "dumps" rather than bombarding the walls in the vicinity of the contained plasma. Such circularizers would also allow the

use of the methods we have developed for observing the plasma lost through the mirrors and perhaps would also result in a simplification of the injection problem.

At present the electronic and electrical installation is at least 95% complete. The remaining work includes completion of the transmission and crowbar systems for the multipolar magnet, installation and alignment of the pulsed and dc magnets, transfer of the dc power and bank-charging power from the Toy Top area, and finally removal and reinstallation of 1566 μF of the Toy Top capacitors.

All metal vacuum-chamber parts, forepump system, roughing system, and diffusion pumps have been procured and are in operation. Molybdenum gettering has been tested. Evaporators and liquid nitrogen cooled liners for the end sections are on order.

With the exception of the multipolar windings all dc and pulsed magnets have been constructed and are being installed. When this installation is completed the power will be switched from the Toy Top area and magnetic field testing will begin in the 2X area.

Injector Development

This work is proceeding as a one-man (John E. Stanko) effort. A coaxial gas-fed injector based on the LASL designs have been developed. Most of the effort so far has been directed toward improving the reliability and lifetime over that of our earlier models. Recently gas-fed injectors have been tested in magnetic fields up to 2000 G. Reliable measurements of the high-energy spectra were possible only after a new electrostatic analyzer was added to the magnetic analyzer, replacing the electrostatic grid system used previously. The present equipment yields a differential measurement which (although tediously) allows the impurity spectrum to be determined. Ion energy spectra and impurity content are being determined as a function of initial gas loading. Mean D^+ energies are of the order of 10 kV and the contamination by electrode material is of the order of 50%. As in the standard Toy Top injectors the impurities are slower and time-of-flight discrimination may be possible. As yet the angular distributions have not been determined nor have we attempted to trap the plasma in a compression experiment.

3. TABLE TOP III

Plasma Stability Studies with Complex Mirror Machine

Walton A. Perkins and William L. Barr

Preliminary stability studies have been made for the magnetic field configuration formed by adding a hexapole set of longitudinal line cusps to a simple mirror machine; i.e., a magnetic field configuration similar to that used by Ioffe, et al.[1] Previous experiments[2] with similar apparatus (but without hexapole coil) showed that a flute-type instability occurred under a wide range of conditions.

The general experimental apparatus is the same as that used previously,[3] but the containment region has been modified as shown in Fig. I-1. The mirror coils were 36-cm-diameter eight-turn coils. The hexapole coil was connected in series with the mirror coils so that they would have the same rise and decay times. A six-turn hexapole coil (wound so that all conducting arcs at the ends are in the same direction) gave a reasonable wall mirror ratio of

$$a_{\perp} = \frac{|B| \text{ at chamber wall (between bars)}}{|B| \text{ on axis in midplane}} = 1.44$$

Perhaps a most useful number is the ratio of $|B|$ for the last closed isobar[4] inside the chamber to $|B|$ on axis in midplane. Here that ratio is $R_w = 1.34$; R_w is essentially the mirror ratio for the magnetic well.

The axial mirror ratio was 1.7 without hexapole and 2.0 with hexapole (owing to the end arcs). The combined magnetic field system had a rise time of 650 μsec and a decay time of 8 msec, with a peak axial field in the midplane of 10 kG.

The vacuum chamber was made of glass to allow penetration of the pulsed magnetic field. The copper conductors of the hexapole coil were potted in an epoxy fiber glass (hollow) cylinder with three slots on one end to allow insertion of the glass chamber.

In these experiments a "hot electron plasma" (10 to 25-keV) was formed by plasma injection followed by magnetic compression. The electron energy has not yet been measured in the combined field (with hexapole), but we have reason to believe that it is not very different from that found in the earlier experiments with a simple mirror machine.[2]

---

1. M. S. Ioffe and E. E. Yushmanov, Nuclear Fusion, 1962 Supplement, Part II, p. 177.
2. W. A. Perkins and R. F. Post, Phys. Fluids 6, 1537 (1963).
3. See Fig. 2, reference 2.
4. J. B. Taylor, Phys. Fluids 6, 1529 (1963).

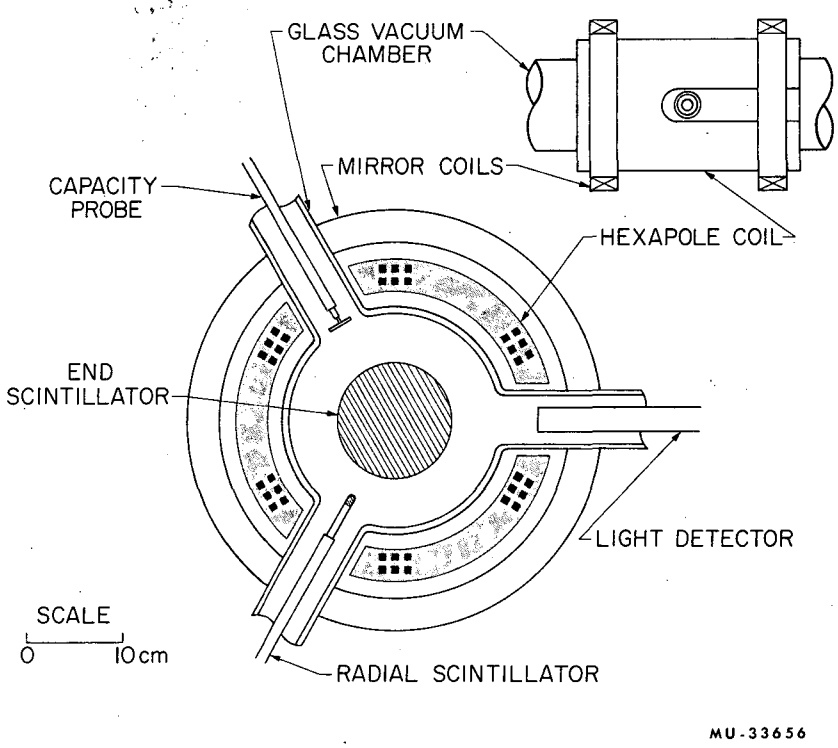

Fig. I-1. Diagram showing side and cross-section view of containment region.

The end scintillator, radial scintillator, light monitor, and capacity probe are the same as those used in previous experiments.[2]

Figures I-2, I-3, and I-4 show the signals obtained on the four detectors for different experimental conditions with and without hexapole coil. From the end scintillator signals, the density is estimated to be from 10^8 to $10^9/cm^3$ for Figs. I-2 and I-3, and about $10^{10}/cm^3$ for Fig. I-4.

At low injected density (Figs. I-2, I-3) without hexapole, occurrence of the flute instability can be clearly seen from the radial and capacity probe signals. The capacity probe signals show the eccentric rotation of the charged plasma column, while the radial probe signals are caused by the collision of the plasma column with this probe as it rotates ($\approx$ 2-μsec period) around the chamber. With hexapole coil no instability signal is detected by the radial scintillator. (The early hump is magnetic field pickup--notice the difference in scope gain.) The late hump on the radial scintillator signals, peaking at about 7.5 msec, is caused by plasma reaching the detector as the magnetic field decays. This signal does not have a periodic line structure. At these injected densities this hump (there are later humps) always occurs at the same time for a given position of the radial scintillator, which suggests that the plasma is expanding outward from the same initial radius on every shot. Plotting the position of the radial scintillator versus the time that the hump occurs and extrapolating to zero time, one finds that the peak of the hump starts at a radius of about 3.5 cm. A simple calculation shows that all plasma should have been compressed to a much smaller radius. Therefore this result indicates that the plasma is expanding to about 3.5 cm radius (by an instability mechanism) and then stopping. Other evidences of an internal instability were obtained from the oscillations seen on the capacity probe signals (see Fig. I-2) and from sharp drops in the light signal (not shown in the figures), which comes from a 1.3-cm-radius region about the axis, with no corresponding collection of particles by the radial scintillator. This type of phenomena is not unexpected, since with a hexapole (in contrast to a quadrupole) the field at first decreases with distance from the axis. In this particular case the magnetic field does not start increasing until a radius of about 3.5 cm is reached.

At higher injected density without hexapole (Fig. I-4) the instability appears at about 200 μsec. A sharp drop occurs in the end scintillator and light, and a large spike (usually composed of 5 to 10 bursts) appears on the radial scintillator. After this burst the plasma is usually quiescent for some milliseconds. With hexapole this early instability disappears and no evidence of the instability is seen. The internal unstable behavior disappears or diminishes at high injected densities; the 7.5-msec hump disappears from the radial scintillator signal, although there are later humps (not shown).

Figure I-5 shows results obtained with a different capacitor bank connected to the hexapole coil from that connected to the mirror coils. The variations of the two fields with time are shown in the top traces of Fig. I-5. In the left-hand set of traces the hexapole field is turned on at about 1.6 msec and stops the transport of plasma to the radial scintillator. At the right (Fig. I-5) the mirror and hexapole coil rise at about the same time. However, the hexapole current decays faster than that of the mirror coils, and the plasma becomes unstable late in time. The capacity probe again shows the eccentric rotation. However, rather than causing a large radial loss, as

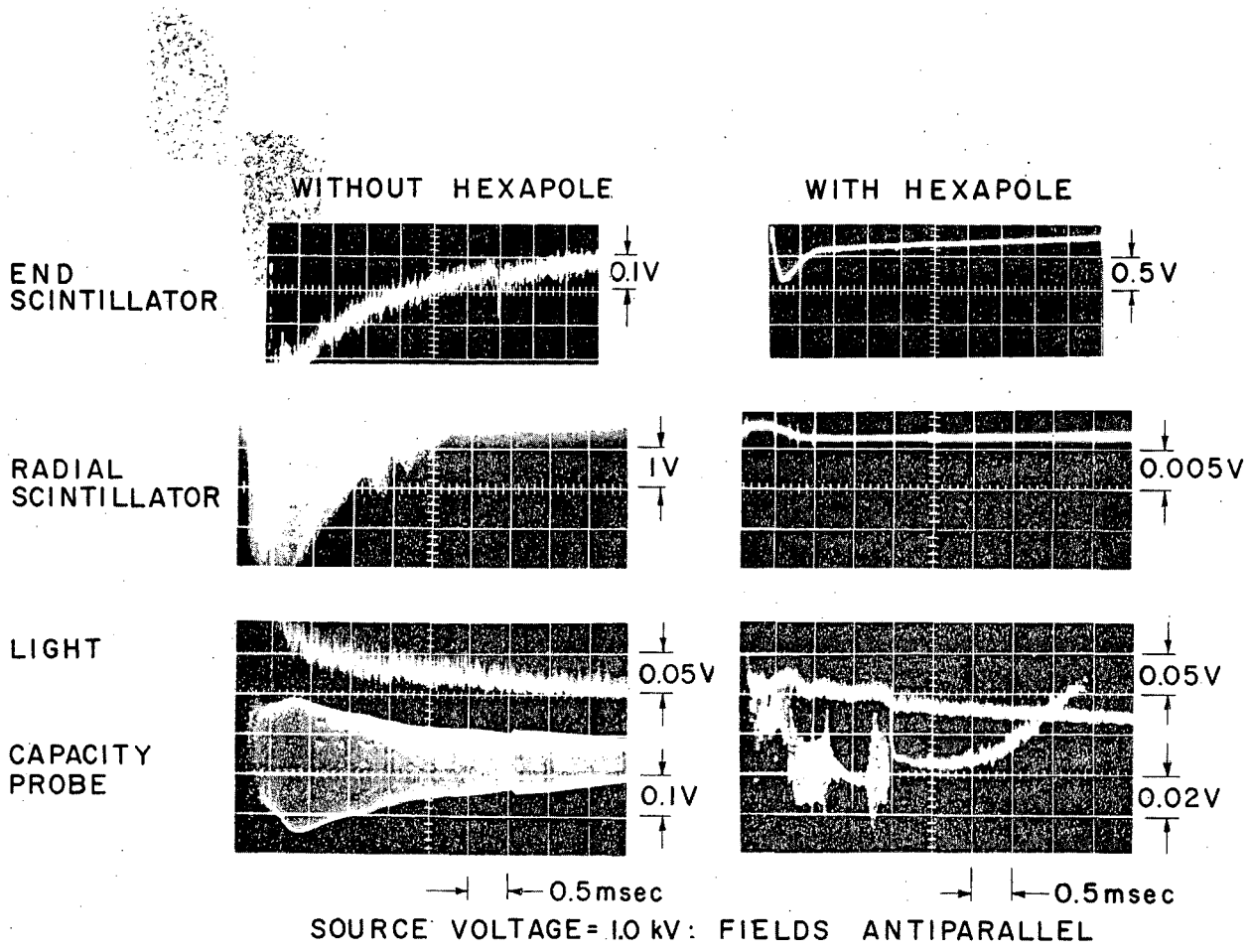

Fig. I-2. End scintillator, radial scintillator, light, and capacity probe signals for a source voltage of 1.0 kV and initial field (100 G) antiparallel to mirror field.

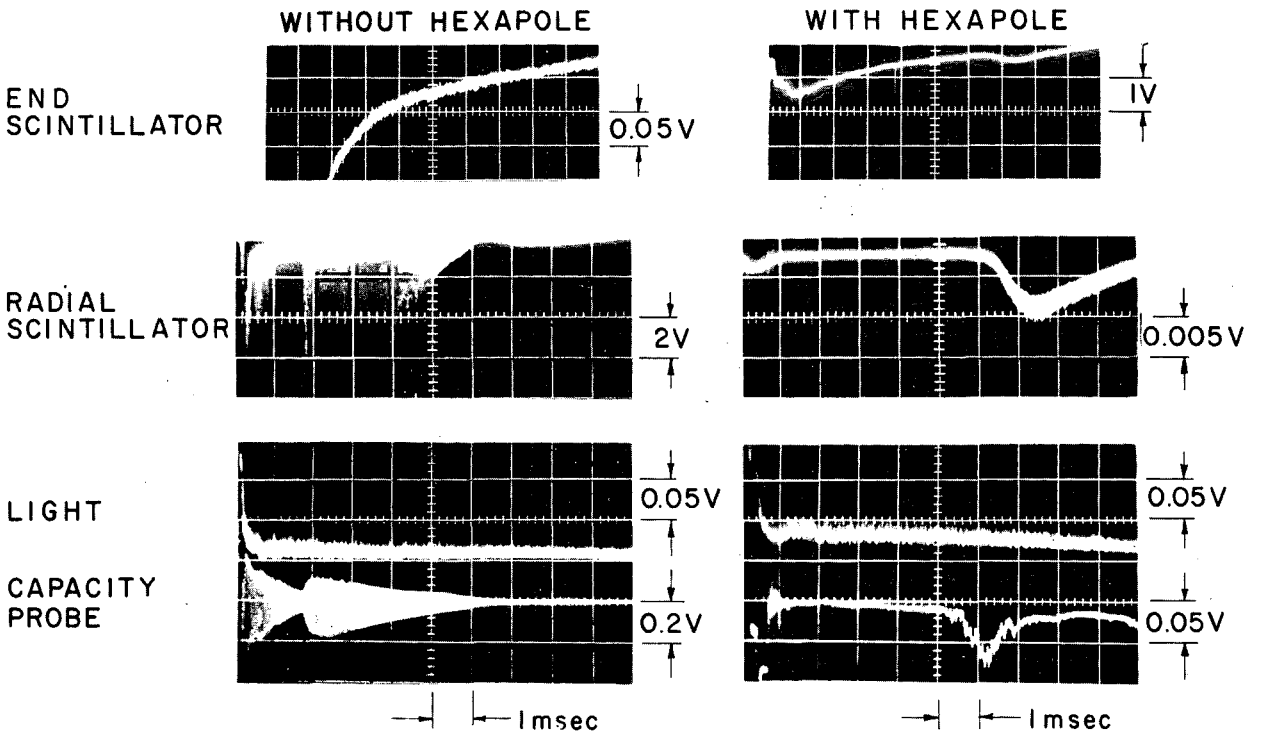

Fig. I-3. End scintillator, radial scintillator, light, and capacity probe signals for a source voltage of 2.0 kV and initial field (20 G) parallel to mirror field.

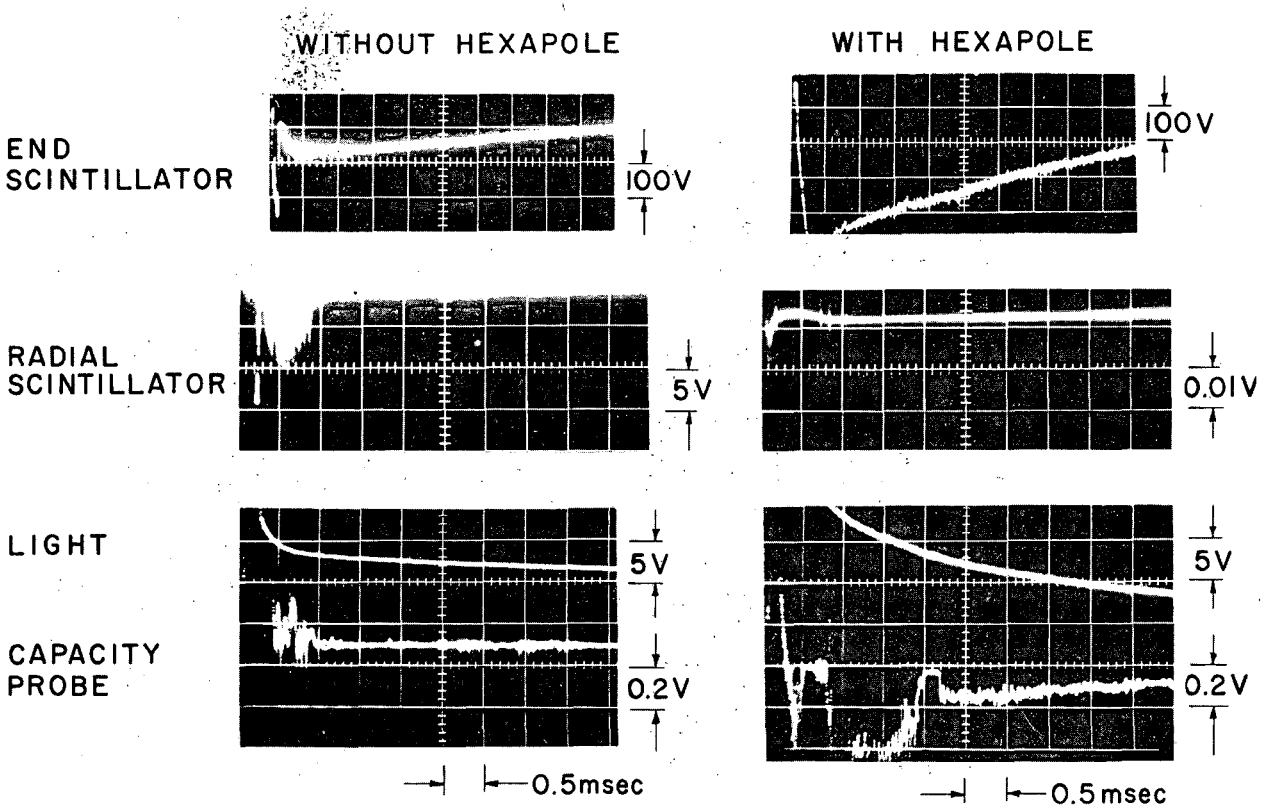

Fig. I-4. End scintillator, radial scintillator, light, and capacity probe signals for a source voltage of 3.0 kV and initial field (100 G) antiparallel to mirror field.

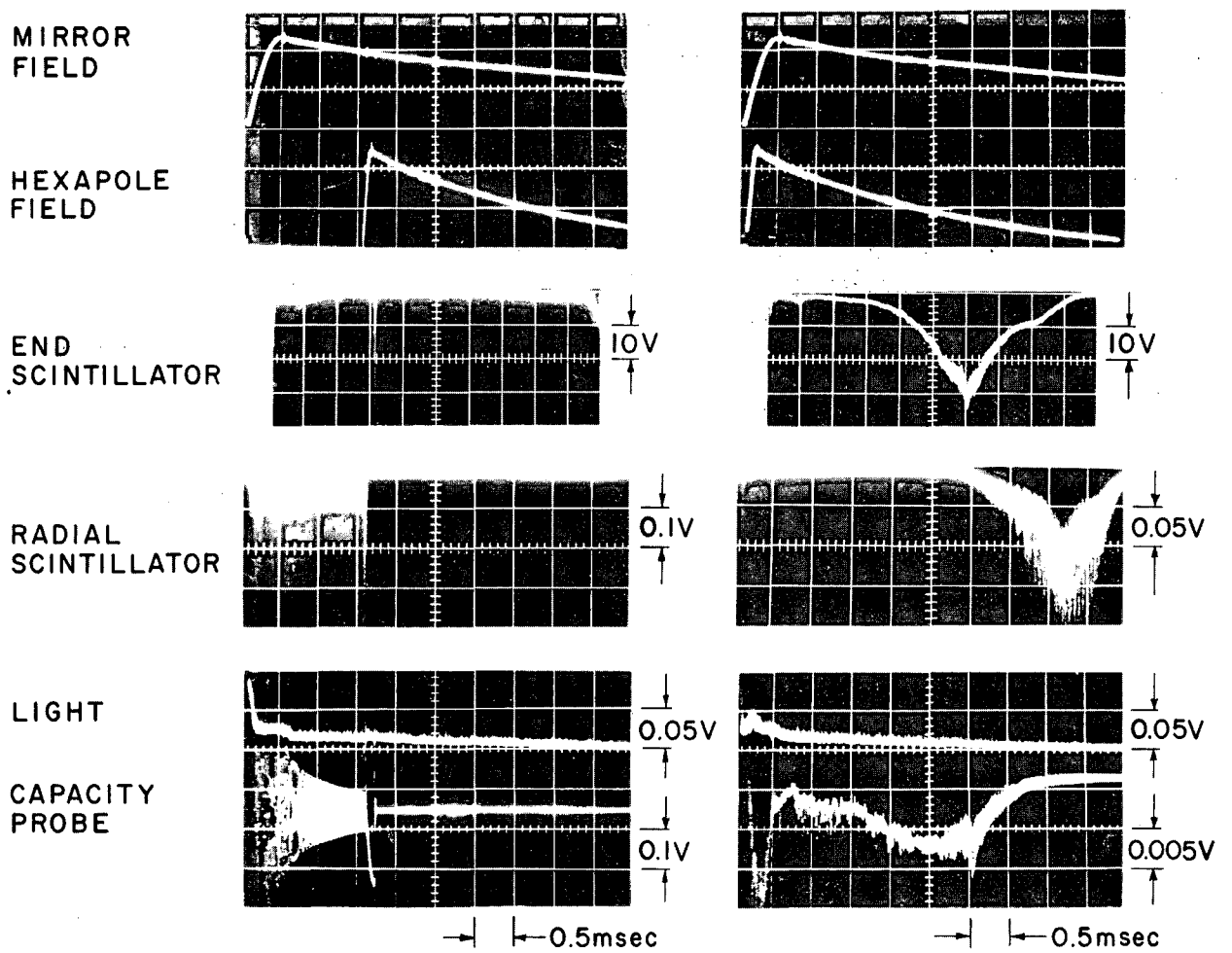

Fig. I-5. Probe signals when the mirror and hexapole coils are connected to separate capacitor banks.

would have been expected, most of the plasma seems to escape out the end. Note the rotational fine structure on the end signal. (This end loss occurs irrespective of the direction of the current in the end arcs of the hexapole, showing that it is not simply the result of changing the mirror ratio.) This suggests that the velocity distribution that remains trapped in a simple mirror machine and a complex mirror machine are not the same.

The radial expansion of plasma with time (see radial scintillator signal with hexapole, Fig. I-3) as obtained by varying the position of the radial scintillator is faster than one obtains by a calculation assuming that $\pi r^2 B$ = const. This could be due to a slow transport across the field lines, but more likely results because $\pi r^2 B$ = const. is a poor approximation in this complex field geometry. This effect and the results obtained with different rise and decay times for the mirror and hexapole indicate that in order to properly interpret the data, one must have knowledge of the trajectories of the individual particles as these complex fields are changing with time.

Although these results are preliminary, we can say in summarizing that the hexapole coil was shown to have a strong stabilizing effect and all evidence of rapid transport of plasma to the walls disappears.

4. ALICE (ENERGETIC NEUTRAL ATOM INJECTION)

A. Alice Plasma Experiments

Charles C. Damm, James H. Foote, Archer H. Futch, Jr., Andrew L. Gardner, Frank J. Gordon, Angus L. Hunt, and James F. Steinhaus

Introduction

The rebuilding of the Alice injector line was completed early in this report period. Initial operation was delayed by failure of two mirror magnet coil sections, and all operation during this period was with only three-quarters of each coil. The mirror ratio then dropped from 1.43 to 1.34, but no significant difference in the observations was detected on this account. Despite improvement in the trapping-chamber pressure the average density remains in the range below 10^8 ions/cm^3, and a density limitation other than by charge-exchange loss is indicated. New observations lead to a measure of the plasma radial distribution. Additional measurements have also been made of the plasma potential and the radio-frequency signals.

Plasma Density

The adjustable beam collimators added to the injector line allowed a trimming of the beam edges to reduce scattered beam in the trapping region. By reducing the collimator size to 0.8×2.0 in. the pressure increase during admission of the beam was reduced from 1.3×10^{-10} torr/mA to about 2.5×10^{-11} torr/mA. The total beam injected decreased by about 30% so that a net gain was realized. Also, because of the smaller collimator opening and a reduced operating pressure in the neutralizer region, the molecular streaming now appears to contribute less than 5×10^{-10} torr at the magnetic mirror axis. Thus with a base pressure of 4×10^{-10} torr and an injected beam of 40 mA, the operating pressure is estimated to be between 1.5 and 2×10^{-9} torr. This represents an improvement by a factor of 3 over previous operation. With a constant Lorentz trapping fraction and a slightly reduced beam, the density should have increased by a factor of almost 3. No increase at all was observed. The measured average density of 0.5×10^8 ions/cm^3 is lower by a factor of more than five than the density calculated by using a trapping fraction of 3.7×10^{-5} together with the measured vacuum and beam. In accordance with our previous interpretation,[1] the density apparently increases until the boundary of an unstable region is reached. Particle losses other than charge-exchange then hold the density at this level. A recent treatment of this problem by Rosenbluth[2] yields a density for onset of instability in reasonably good agreement with the experimental value. Unfortunately we cannot as yet account for the particle loss quantitatively, either radially or axially, so that the particle bookkeeping is incomplete.

---

1. Charles C. Damm, James H. Foote, Archer H. Futch, Jr., Andrew L. Gardner, Frank J. Gordon, Angus L. Hunt, and James F. Steinhaus, in Controlled Thermonuclear Research Semiannual Report, UCRL-10852, June 1963, p. 19.

The density fluctuations reported previously are still observed, but it now appears that the average density, even on the peaks, is well below the level expected if charge-exchange losses dominate. We cannot now maintain the tentative explanation that these density increases represent a jump to the upper stable region predicted by theory. Further light is shed on these fluctuations from measurements of the radial plasma density distribution.

Radial Density Distribution

We now have preliminary results obtained with the Radial Profile Detector (RPD).[3] The data reported here were acquired with the RPD grids biased to accept ions of all energies and to reject electrons. Because charged particles tend to follow magnetic field lines, any radial variations of the ions produced in the plasma should be maintained as they travel out through the mirror to the various RPD collector plates. The particles arriving at the plates originate over a range of positions along the Z axis. We expect most of the ions detected to result from charge-exchange collisions of fast trapped ions with the background gas. The observed distribution should therefore reflect the fast-ion distribution, if the gas density is uniform.

An example of the results obtained with the RPD is given in Fig. I-6, top. The two curves shown correspond to times before and after a 50% increase in the signal seen by our principal fast-atom detector (Fig. I-6, bottom) which is sensitive to the charge-exchange fast atoms that leave the plasma radially near the median plane.[4] The higher level in the fast-atom detector signal thus is correlated with a filling in of the radial profile at the smaller radii. This correlation is consistently found in our data. Part of this increase in the central RPD signals is apparently due to an axial expansion of the plasma. Evidence for this comes from our second fast-atom detector, located 9 cm off the median plane and shielded from the portion of the plasma that is near the median plane. Its signal level rises sharply with the signal increases discussed above. However, besides this axial expansion, there is also an increase in the central density, as demonstrated by the rise in signal of the median-plane fast-atom detector.

The radial profiles have shown that one cannot assume a density distribution independent of radius, as would be expected from Lorentz trapping. (Profiles taken at various orientations, and also sudden profile changes during a shot, show that background gas density variations do not cause the main radial variations observed.) The nonuniformity of the measured radial distributions is one more demonstration of the complex behavior of the plasma.

---

2. Marshall N. Rosenbluth, Paper J1, American Physical Society, Division of Plasma Physics Meeting, San Diego, November 6-9, 1963; and private communication.
3. This diagnostic tool was described and shown schematically in Controlled Thermonuclear Research Semiannual Report, UCRL-10852, June 1963, Fig. I-10, p. 29-30.
4. The position of this fast-atom detector is shown in Controlled Thermonuclear Research Semiannual Report, UCRL-10294, June 1962, Fig. I-5, p. 17.

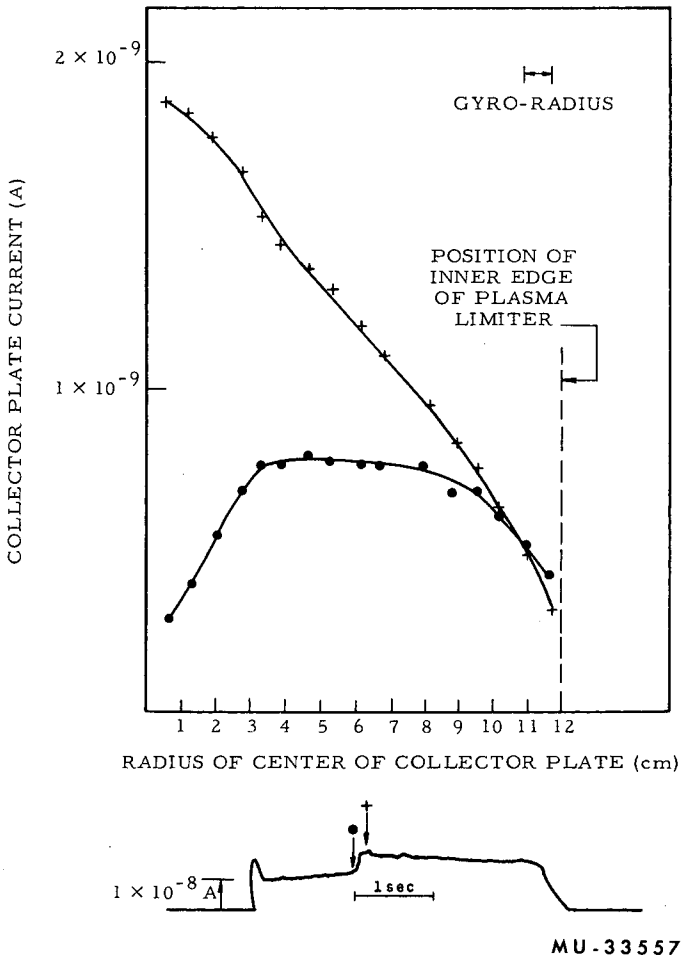

Fig. I-6. Top: Radial profile of the plasma before (●) and after (+) a major increase in the signal of the fast-atom detector. The horizontal (radius) scale has been transformed to the median plane. Thus the radius given for each collector plate is the radius at the median plane of the magnetic-field line that passes through the center of the plate.

Bottom: Fast-atom-detector signal, with arrows showing points at which profiles were measured.

Possible difficulties with the interpretation of the RPD signals include these factors:

1. Ions formed by any process register equally well, so that for instance, gas ionization by electrons could contribute to the signal. This correction is estimated to be small.

2. The RPD signals are time-averaged (≈ 0.1 sec), and are space-averaged over a range of axial positions. A faster amplifier should improve the time resolution but the space averaging is more difficult to eliminate.

Plasma Potential Measurements

Additional plasma potential measurements have been made of the plasma in the Alice experiment. The Faraday cup detector used to measure the Li^+ beam transmitted through the plasma has been modified by the addition of three high-transmission tungsten screens in front of the detector. This modification makes it possible to measure the energy of the thermal ions escaping from the plasma. Since these ions should arrive at a grounded detector with an energy equal to the plasma potential, measurement of the slow ion energy gives an independent estimate of the plasma potential.

In the absence of rf oscillations and under the present operating conditions, the thermal ion current to the Faraday cup is not much larger than the electrical noise current. However, during rf activity the thermal ion current is considerably larger, and reasonable measurements of the plasma potential have been made under these conditions with this technique. Figure I-7 shows how the current to the Faraday cup varied as the biasing voltage on the center screen was increased from -1800 to +1500 volts. Our interpretation of the observed Faraday cup current is as follows: With the screen voltage highly negative only ions are collected. As this voltage increases the current remains essentially constant until the voltage passes through zero. At this point electron collection begins and the Faraday cup current drops to a new level. The current again remains essentially constant until a voltage equal to the plasma potential is reached and the slow ions are prevented from reaching the detector. The plasma potential is taken to be the voltage at which the slow ions begin to be biased from the detector.

Figure I-8 shows the plasma potential during rf activity as a function of the gas pressure as indicated by an ionization gauge. Helium gas was admitted to vary the pressure. The magnetic field was 25 kilogauss. The crosses indicate measurements taken by the Li beam technique.[5] The measurements were made with the Li beam passing along the axis through the center of the plasma. Measurements indicated by the circles were obtained by determining the voltage necessary to prevent the detection of thermal ions as described above. Figure I-8 shows reasonable agreement between the two methods for measuring the potential.

5. A. F. Waugh and A. H. Futch, Jr., A Method for Continuous Measurement of Plasma Potential over a Range of 0 to 4 kV, UCRL-7414, June 1963 (unpublished).

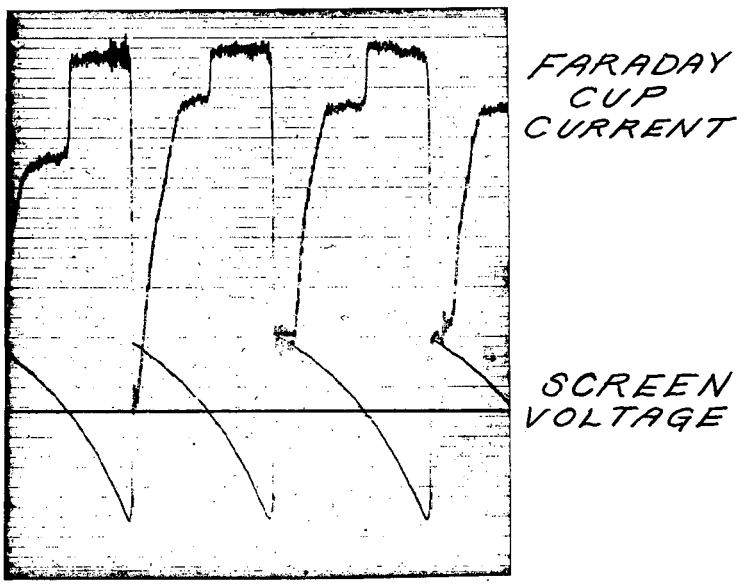

Fig. I-7. Faraday cup current and screen voltage as a function of time. The top curve shows the current to the Faraday cup as the bias voltage was varied from -1800 V to +1500 V, as indicated by the bottom curve.

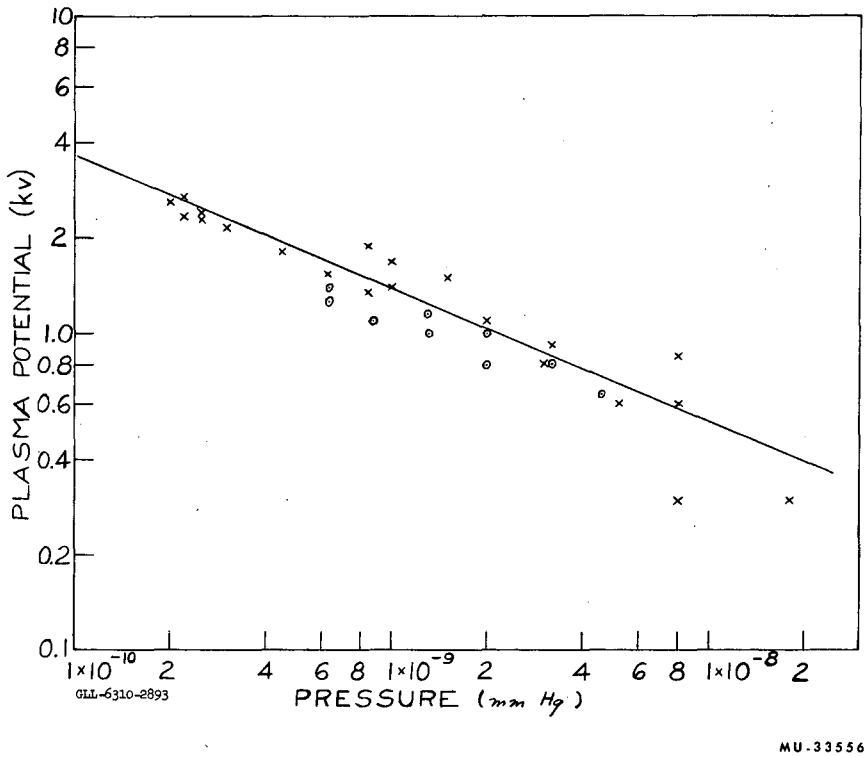

Fig. I-8. Plasma potential vs pressure. Measurements indicated by x were made by the Li beam technique; measurements indicated by ◌ were determined by biasing the thermal ions from the Faraday cup.

Measurements have also been made with the lithium beam and Faraday cup moved radially to a position 2 inches from the center of the plasma. During these measurements also the magnetic field was 25 kG. In this position the plasma potential increased in the usual manner for approximately the first 50 msec of the beam pulse. At this time the potential suddenly began to oscillate between a rather low potential and approximately 1 kV. In order to further investigate the oscillations in the plasma potential, the lithium beam energy was set at a steady dc level of 1 kV and the transmission to the Faraday cup observed. Observations of this current showed that the beam was strongly modulated or turned completely on and off, in phase with the low-frequency oscillations observed on the radial antenna.

These observations are consistent with an off-axis plasma column rotating with a frequency determined by the ∇B and electric field drift velocity of the ions.

Radio-Frequency Activity

The rf fields generated near the ion gyrofrequency have been studied further through the use of loop antennas oriented in two perpendicular planes. A balanced electrostatic shield is employed to achieve cancellation of the effects of currents induced by radial electric fields. Although a variety of signals are observed the following trends seem noteworthy:

1. The usual sustained activity at central fields of around 12 kG or less exhibits an H field that is predominantly axial.

2. At central fields around 25 kG, the very strong oscillation that frequently occurs, usually for periods less than a second, has an H field that is principally azimuthal. These periods are also characterized by increased plasma potential (from lithium ion-beam measurements) and increased ion density (from measurements of fast neutral atoms emitted).

3. The oscillations frequently show definite small departures from the "mean" gyrofrequency, and occasionally show a splitting into two frequencies with a difference of a few percent. Such variations may yield valuable information about changes in the volume distribution of the plasma. Correlations with the signals from the radial profile detector are being studied.

4. Limited observations have shown that the rf signal is sometimes substantially modulated at the low frequency related to precession of the ions. Simultaneously with these loop antenna measurements at the midplane, modulated rf signals were seen in varying amounts on three collectors selected from the array of 17 incorporated in the radial profile detector. (Tuned lines were employed to achieve sufficient rf sensitivity.)

Improved instrumentation has recently been installed which permits simultaneous spectrum-analyzer viewing of H_θ and H_Z (with a raster presentation) over a much wider frequency range. Brief observations capable of revealing any appreciable radiation at subharmonics of the ion gyrofrequency have detected none. Some second-harmonic content is sometimes observed, but in general the signal is rather sinusoidal except for the low-frequency modulation previously noted.

B. Ion Source Development

Frank J. Gordon

A series of runs was made in which the distance from the ion source arc column to the exit slit was the only controlled variable. The range was from 0 to 30 mils. Several observations were made:

1. Total drain on the accelerating voltage power supply goes up sharply as the distance approaches zero, showing increased ion output.

2. A "runaway" condition on the accelerating voltage power supply current (drain) prohibited peaking of such parameters as hydrogen gas supply to the arc, arc current, and accelerating slit adjustment as the distance approached zero.

3. Focused-ion output peaked in the neighborhood of 20 mils.

A series of troubles terminated these experiments before optimum parameters could be definitely established.

One run with an accel-decel slit system (ions accelerated to 27 keV, then decelerated down to 20 keV) showed possibly better focusing and gas efficiency, but further work is needed.

Installation of an auxiliary source on Alice is progressing.

C. Cold Plasma for Beam Trapping

James F. Steinhaus and Norman L. Oleson†

In a continuing effort to obtain an effective cold plasma for purposes of stabilization and enhanced breakup in Alice, two concepts are presently being pursued. The occluded-gas titanium-washer source, while producing a high percentage of contaminant heavy ions and excessive neutral particles (about 10% of total particle density in the plasma column appears to be neutral), nevertheless has an attractive hydrogen ion density output ($\approx 10^{14}$ per cc). It is felt that the disadvantages of such a gun might be overcome by injection at 90° to the coil axis and slightly off the midplane of a cusped magnetic field geometry where contaminant particles could be excluded from the trapping region and multiple guns could be used. Hardware to examine such an injection scheme is being acquired.

Another injection concept, the one being examined at present, utilizes a gun similar to the Homopolar Gun I developed in Berkeley by Klaus Halbach, William Baker, and Kenneth Ehlers et al., and recently described in UCRL-10206-Revised.[1] This is a modified version of the Homopolar V device using neutral gas injection and a rotating plasma. Although the kinetic temperature of plasma from the Berkeley gun is in the kilo-electron-volt range, we expect that it can be operated at lower energies and could be

† U. S. Naval Postgraduate School, Monterey, California.

1. Klaus Halbach and William R. Baker, Lawrence Radiation Laboratory Rept. UCRL-10206-Revised, December 9, 1963 (unpublished).

suited for our purpose. Primary emphasis is being placed on an azimuthally symmetric plasma of large volume and high purity, providing adequate containment is achieved.

Such a gun has been built and is now being tested in Livermore. Although ideal operating conditions have not yet been obtained, preliminary observations indicate that the gun is operating in the proper mode, i.e., energy is being put into the plasma, with proper back voltages being observed, rather than into internal low-resistance paths. Electron densities in excess of $10^{13}/cm^3$ have been measured with microwave techniques at the gun exit, but the neutral gas input has not yet been optimized.

Measurements that will determine the basic applicability of the homopolar gun to Alice will be containment time of the rotating plasma of a density of 10^{10} ions/cm^3 or greater. To prevent excessive charge-exchange losses, this time must be at least comparable to the e-folding time of neutral gas pumping in Alice. This measurement is proceeding.

D. Alice Diagnostics

Archer H. Futch, Jr., and Andrew L. Gardner

Semiconductor Detector

Preliminary results have been obtained with one of the small semiconductor detectors operating on the Alice experiment. This detector has an active area of 7 mm^2 and is not affected by the magnetic field of Alice. By placing the detector and the shielded preamplifier close to each other and cooling the detector with liquid nitrogen, the detector noise has been greatly reduced. With the detector cooled and biased at 100 volts, the spread (full width at half-maximum resolution) due to amplifier and detector noise was less than 5 keV. Density measurements obtained with this detector are in reasonable agreement with measurements based on the emission of secondary electrons by fast atoms.

It may also be possible to use this detector to measure the energy of the trapped ions in the plasma. A significant change in the energy of the trapped ions would be detected by a change in the pulse-height spectrum of fast atoms resulting from charge-exchange collisions.

Microwave Measurements of n_e

An attempt will be made to measure the average electron density by means of a transmission measurement at around 9 Gc. A single horn will be used in conjunction with a focusing metallic reflector dish which will not be appreciably affected by a coating of molybdenum from the getter filament in the Alice chamber. More than half of the launched power is expected to be retrieved after the double pass through the plasma. A direct calibration of phase shift for the overall system is planned by imparting a small movement to the reflector. Various factors could frustrate the actual measurement, but preliminary tests indicate the system should be capable of detecting an average density of less than 10^8 electrons/cm^3.

E. Vacuum and Surface Studies

Angus L. Hunt and Charles C. Damm

Surface Bombardment

The bombardment of titanium sheet with a deuteron flux of 1 to 5 $\mu A/cm^2$ at energies from 10 to 18 keV, coupled with observation on the evolved gas composition as a function of temperature, has resulted in an improved beam-termination method in Alice.

The observations on titanium may be summarized as follows: In the temperature range 80°K to 300°K the incident deuteron beam is retained by the titanium with essentially no evolution of molecular deuterium from the surface. At higher temperatures, to 300°C, the incident beam is still trapped by the titanium. The formation of a bulk titanium deuteride is probably the cause of the marked retention of the incident beam at these higher temperatures. The evolution of methane and carbon monoxide during the ionic bombardment increases with the temperature of the titanium. The evolution of trapped deuterium becomes large at temperatures above 400°C. These observations are similar to those reported by Simonov and others[1] for higher deuteron fluxes of 2 mA/cm^2 at 20 keV.

In the previous beam termination method in Alice the energetic neutral beam was terminated on a water-cooled copper target. The resulting low-energy molecular gas was removed by a continuously deposited water-cooled titanium getter film and a diffusion pump. This technique resulted in a locally high neutral-particle density at the copper target and a low-energy return flux of neutrals from the copper target toward the plasma, which contributed to the neutral-particle density in the plasma chamber.

The experience with titanium bombardment suggested that if the neutral Alice beam were to strike a titanium target at liquid nitrogen temperature the beam would be trapped within the titanium and the return flux along the beam greatly reduced or eliminated. It would also be necessary to minimize the temperature increase of the titanium surface to prevent the evolution of methane and carbon monoxide, as well as provide a method for increasing the titanium target temperature to greater than 400°C so that at appropriate intervals between the plasma experiments the target could be degassed of the trapped hydrogen or deuterium.

It was found that these conditions could be met by a 10-mil-thick titanium sheet thermally connected to a liquid-nitrogen-cooled copper block of sufficient heat capacity to restrict the temperature to a maximum of 0°C during the 5 to 10 sec the 50-ma 20-keV neutral beam was incident on the target. The titanium sheet was resistively heated to temperatures greater

1. V. A. Simonov, G. F. Kleymenov, A. G. Mileshkin, and V. A. Kochnev, Paper No. 255, Conference on Plasma Physics and Controlled Nuclear Fusion Research, Salzburg, Austria, September 1961, AEC-tr-5589.

than 400°C by eliminating the liquid nitrogen flow to the copper block and concurrently passing 400 amperes through the sheet.

As an additional improvement in pumping evolved gas, the copper substrate for the deposited titanium film was cooled to liquid nitrogen temperatures.

It was found that these improvements allowed termination of the beam with a measurable pressure increase within the beam burial chamber of less than 10^{-8} torr during beam injection, compared with the previous 10^{-7} torr.

Magnetron Pressure Gauge Application to Alice

As previously reported, a magnetron gauge promised to be applicable to operation very close to the plasma chamber within the return flux of the mirror field. It was found that stable operation could not be obtained within the tolerances required to measure the small pressure changes (within the 10^{-10} torr range) during neutral beam injection. Unpredictable changes in electron density within the gauge appeared to be a function of the rate of increase of magnetic field, and the average value of the field, as well as a function of the pressure.

F. "Minimum-B" Magnetic Field Configurations for Alice

Richard F. Post

Experiments are being planned to investigate the use of "Minimum-B" mirror fields in the Alice experiment. In connection with these plans calculations have been made of the field configurations generated by various coil systems. Examples of two general types of minimum B fields have been studied. The first is a quadrupole field, similar in basic configuration to the one being studied in Table Top by Perkins (see I. 3 of this Progress Report). The second general configuration studied is the axially symmetric "disc" geometry of Furth[1] and Andreoletti.[2] This is one that appears to be of special interest.

Following a suggestion of Perkins, the first quadrupole field studied is one generated entirely by the use of "modular" circular coils, placed as shown in Fig. I-9. Although not particularly efficient in its present form, such a configuration has, for us, the considerable practical advantage that it can be assembled from existing coils and can be added to the present Alice system with a mimimum of changes. An example of the calculated field line configuration and the contours of constant B for such a quadrupole coil array is shown in Fig. I-10 for a particular set of operating currents dictated by practical considerations. Mirror ratios are indicated by the circled numbers, and magnetic field strength (in arbitrary units) is indicated by the small numbers adjacent to each contour. The locations of the coils are also shown.

1. Harold P. Furth, Phys. Rev. Letters 11, 308 (1963).
2. J. Andreoletti, Euratom Meeting on Mirror Confinement, Paris, (Fontenay-aux-Roses), France July 15-19, 1963.

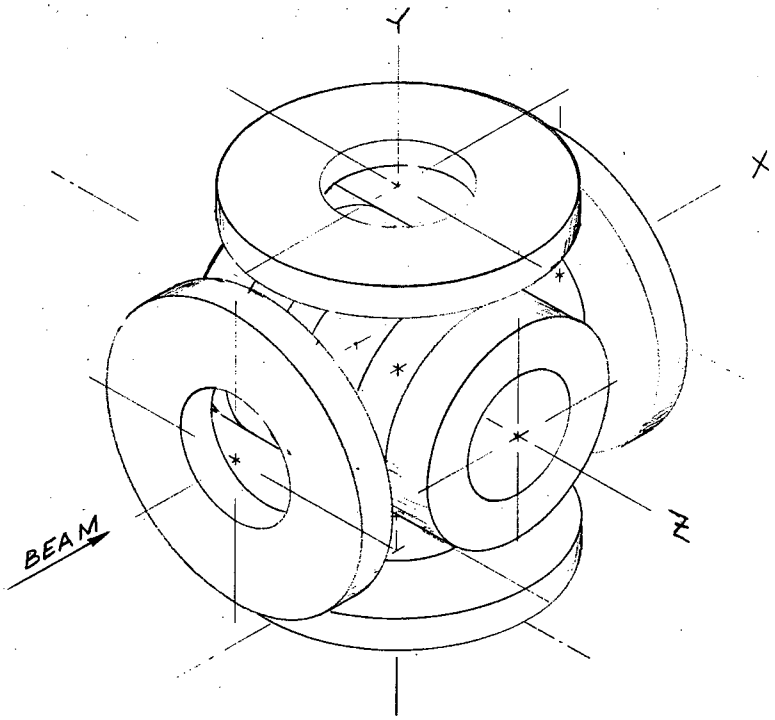

Fig. I-9. Schematic drawing of modular quandrupole coils.

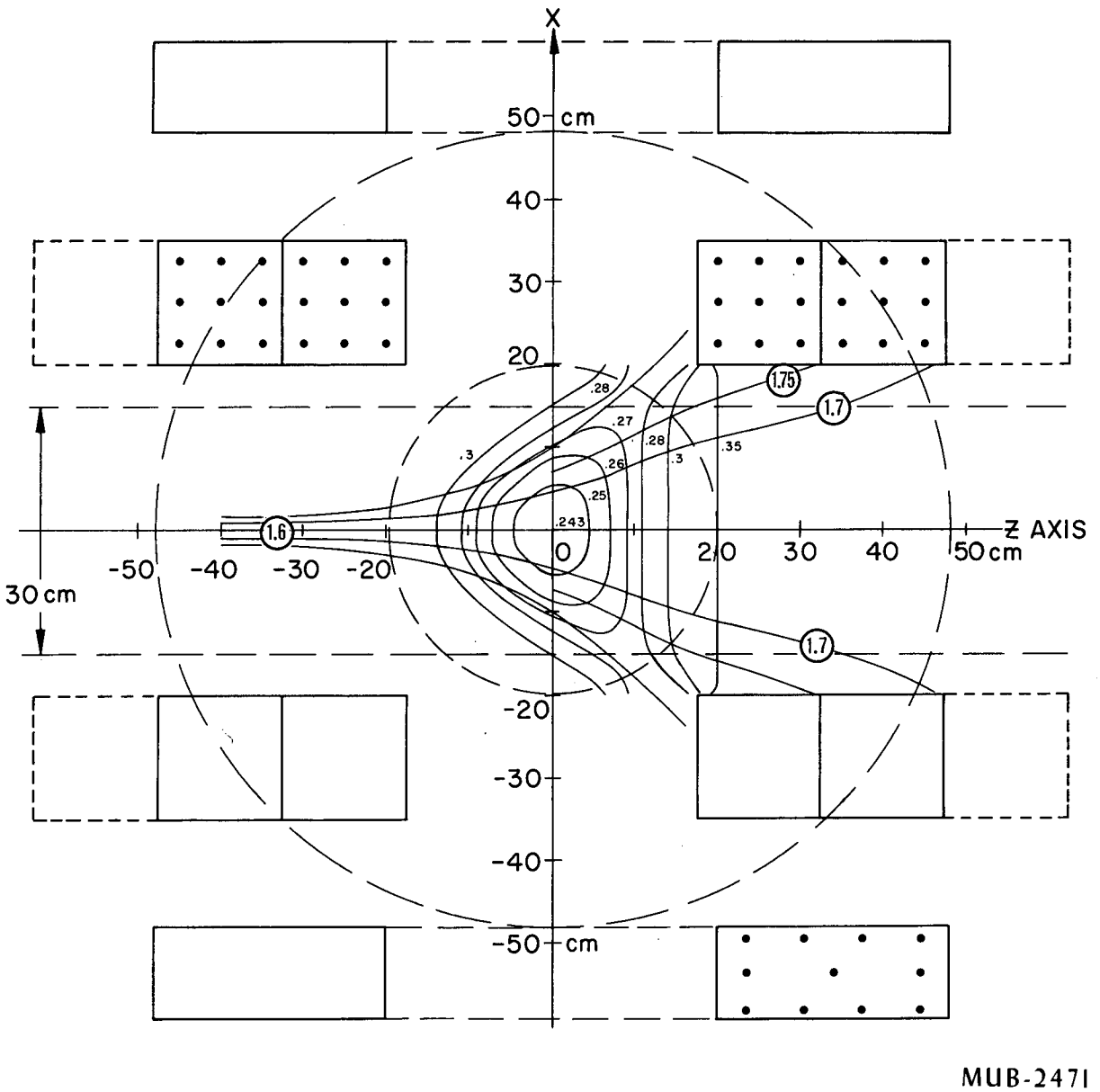

Fig. I-10. Field lines and contours of constant B for modular quadrupole coil systems.

In this example a reasonable volume of closed minimum B contour is achieved. However, not all this volume is available for plasma confinement, as only the field lines for which mirror ratios are indicated have usable ratios at both ends. The last of these lines passes well under the last closed contour of constant B.

An example of the field configuration of a "disc" minimum-B field is shown in Fig. I-11. The shapes of the field lines are shown, together with the coil locations and relative currents. The presence of the coils nearest the axis was shown to be very advantageous in reducing the total power required and in producing a better configuration, as compared with the first structures considered by Andreoletti. Calculations presently under way are aimed at still further optimization of the field shape, particularly in increasing the usable volume of closed B contours.

The calculations have all been performed with the magnetic field code developed by Perkins and previously reported.

G. Finite-Orbit Effects and the Stability of "Hollow" Plasma*

Richard F. Post

Finite-orbit effects[1] can modify the hydromagnetic stability properties of confined plasma provided certain scaling relationships are satisfied, theoretically stabilizing all interchange modes except a simple transverse drift (m =1). For complete stability against interchanges, one must either surround the plasma by a conducting shell[1] or else find configurations that are intrinsically stable. In particular, one may search for plasma density-temperature spatial distributions for which simple transverse plasma drifts are energetically unfavorable. By using conventional hydromagnetic theory, it has been found that in open-ended axially symmetric systems such as the mirror machine, a special class of "hollow" or napkin-ring-shaped plasma satisfies this criterion. Furthermore, if the mirror machine is turned "inside out" (field lines convex toward the axis, with a least one mirror near the wall) a wider class of such distributions is found.

To calculate the stability, the artifice of an effective "g." determined by the field curvature, has been used in the hydromagnetic equations. This model, although approximate, has been shown by past experience to predict the essential features of the stability. The two general types of field configurations that were studied are illustrated in Fig. I-12. The upper configuration is that of the ordinary mirror machine; for it the effective "g" is pointed outward (field lines convex toward the axis). The lower configuration (an example of the "inside out" mirror machine alluded to earlier) can be achieved by a relatively simple rearrangement of the field coils.

---

*Based on paper presented at the 5th Annual Meeting of the Division of Plasma Physics, San Diego, California, November 6-9, 1963.

1. M. N. Rosenbluth, N. A. Krall, N. Rostoker, Nuclear Fusion, 1962 Supplement, Part 1, p. 143.

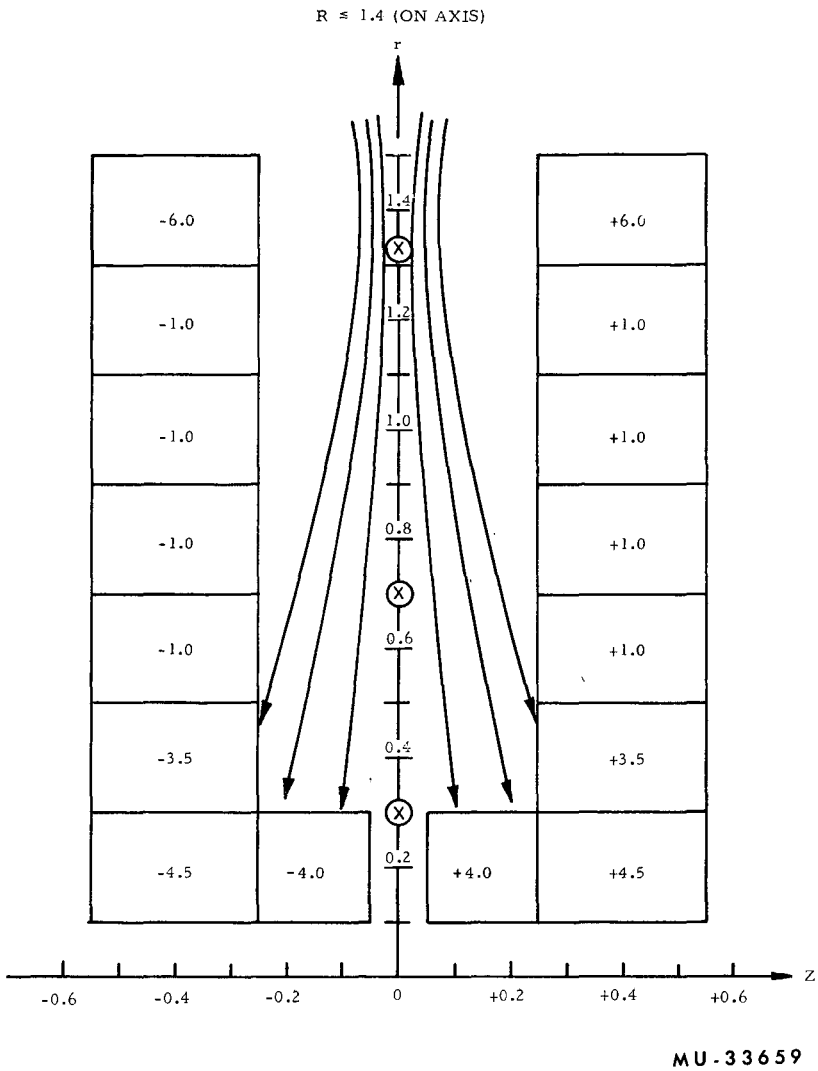

Fig. I-11. Field lines and coil configuration for an example of a disc machine.

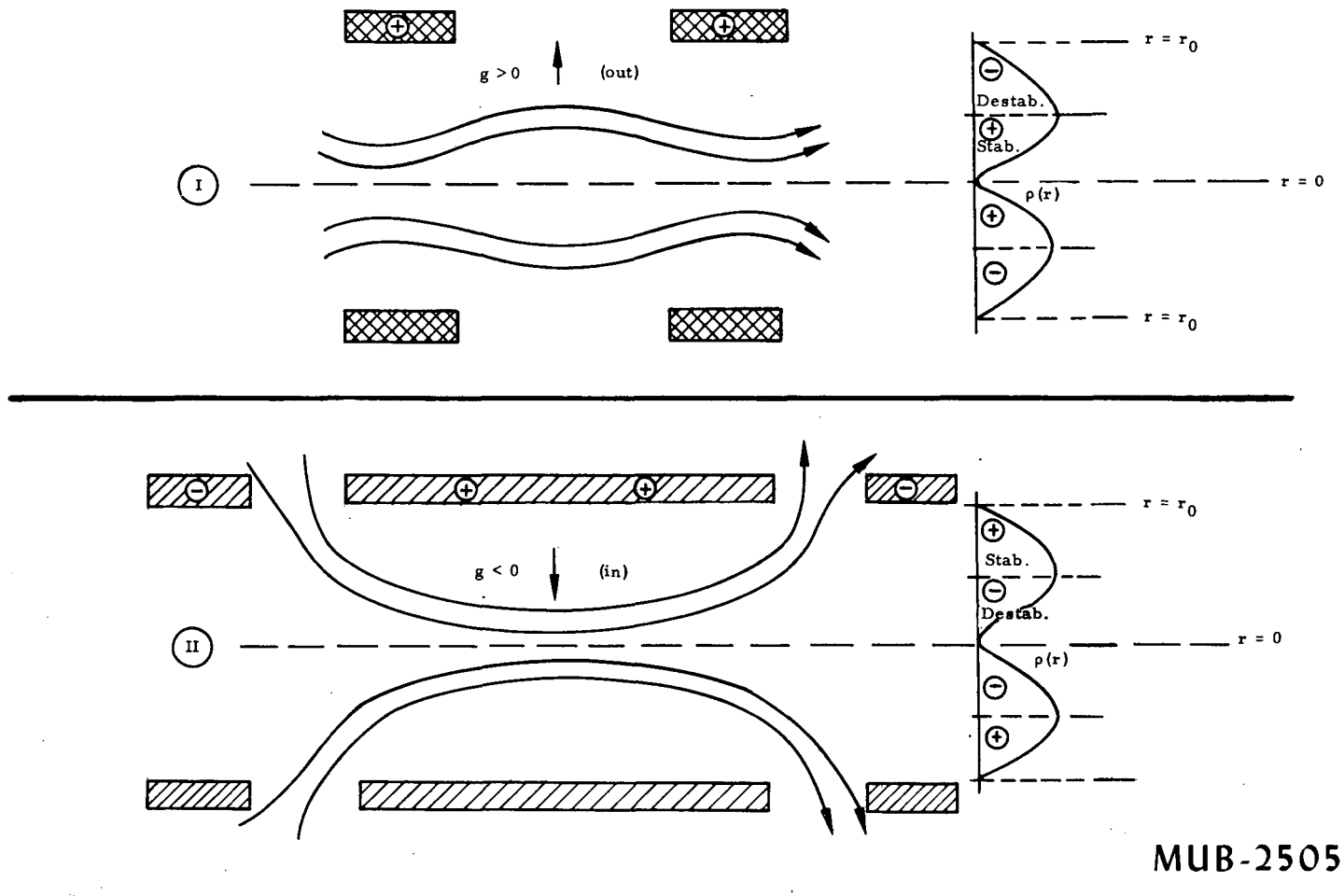

Fig. I-12. Schematic of field lines and stability properties for normal and "inside out" mirror machines.

With the standard δw formalism,[2] the appropriate hydromagnetic integral expression for δw is

$$\delta w = -\frac{1}{2}\int d\tau\, (\underline{\xi}\cdot \underline{\text{grad}}\,\phi)\,(\underline{\xi}\cdot \underline{\text{grad}}\,\rho) > 0 \quad \text{stable},$$
$$\underline{\text{div}}\,\underline{\xi} = 0. \qquad (1)$$

For a simple transverse displacement, $\xi_r = \xi_0 \sin\theta$, so that

$$\delta w = \frac{\pi}{2}\,\xi_0^2 \left\langle \int_0^{r_0} r g(r) \frac{d\rho}{dr}\, dr \right\rangle > 0 \quad \text{stable}, \qquad (2)$$

where the average is taken along a field line; $g(r) = -d\phi/dr = v^2/P(r)$; and $P(r)$ = radius of curvature of the field lines.

It can be seen from (2) that stability against m = 1 displacements is determined by the average sign of the product of g and the density gradient, weighted by a factor r. The integral can also be written in the form

$$\delta w = \frac{\pi}{2}\,\xi_0^2 \left\langle \int_0^{\rho_0} r(\rho)\, g(\rho) d\rho \;\Big|_I + \int_0^{\rho_0} r(\rho)\, g(\rho) d\rho \;\Big|_{II} \right\rangle .$$

where I and II refer respectively to the regions inside and outside the point of maximum density of the hollow distribution.

A simple and convenient distribution to study is the thin "napkin ring," i.e., a plasma cylinder localized in radius. For this case, ignoring the axial dependence, we may expand the relevant quantities in terms of distance from the mean radius, r_0; i.e., take $r = r_0 + x$, $x \ll r_0$. Then

$$g(r) = g_0(r_0) + g' x + g'' x^2 + \cdots ,$$
$$\rho(r) = \rho(r_0) + \rho' x + \rho'' x^2 + \cdots . \qquad (3)$$

Taking as an example the parabolic density distribution, $\rho(x) = \left[1-(x/\epsilon)^2\right]$, with $x \leq \epsilon$, one finds

$$\delta w = -4\left\{\frac{\epsilon}{3}\left[g_0 + r_0 g'\right] + \frac{3}{10}\left[g'' + r_0 g\right] + \cdots\right\} .$$

2. I. Bernstein, E. Frieman, M. Kruskal, and R. Kulsrud, Proc. Roy. Soc. (London) A244, 17 (1958).

Thus if $\epsilon << 1$, $\delta w > 0$ if $[g_0 + r_0 g'] < 0$.

If $g_0 > 0$ (ordinary mirror machine), for stability this requires $g' < 0$ and $|\Delta g|/g_0 > (\epsilon/r_0)$, i.e., g must decrease across the cylinder by a sufficient amount. This could in principle be accomplished by field shaping or by a negative radial temperature gradient.

On the other hand, if $g_0 < 0$ (inside-out mirror machine) and if $g'/g_0 \geq 0$, then $\delta w > 0$ for all g'. If $g'/g_0 < 0$, $|g'| < |g_0/r_0|$ is also required for stability.

One thus finds a much wider class of "stable" distributions for the inside-out mirror machine than for the ordinary case. This is a general result, arising from the "r" weighting factor in the stability integral. Parenthetically, it should be noted that plasmas confined between inside-out mirrors are automatically hollow, since there are no mirrors on axis.

The above calculations of course do not alone prove the possibility of overall stability of hollow plasmas against interchange modes. They suggest, however, that properly chosen plasma distributions, with allowance for scaling requirements, could be adequately stable, provided finite-orbit effects are able to stabilize all modes higher than m = 1.

H. Theoretical Considerations

Archer H. Futch, Jr., and V. Kelvin Neil

As a guide to the interpretation of some of the measurements observed on the Alice plasma, Poisson's equation has been solved for an arbitrary charge distribution, $\rho(r,z)$, inside an infinitely long grounded cylinder of radius b. Assuming that the charge density, $\rho(r,z)$, is a function of r and z only, then we obtain the following solution for the potential of a plasma column of length ℓ,

$$\phi(r,z) = 4\pi \sum_s \frac{J_0(\lambda_s r)}{b^2 \lambda_s J_1^2(\lambda_s b)} \int_{-\ell/2}^{\ell/2} e^{-\lambda_s |z-z'|} \times \int_0^b \rho(r',z') J_0(\lambda_s r') r' dr' dz', \qquad (1)$$

where the λ_s's are determined by the condition that the potential ϕ is zero at r = b. The above equation has been coded for an IBM 7090 computer so that numerical solution may be easily obtained.

Equation (1) enables one to determine the charge density from measurement of the plasma potential provided the spatial dependence of the charge distribution is known. The electron density may then be determined from the charge density using a measured value for the ion density. If one makes the approximation that ρ is a constant and calculates the difference between the

ion and electron densities necessary to satisfy Eq. (1) for a $\phi(0, 0)$ of 2 kV, then one finds that this difference is approximately 4×10^7 particles/cc. This difference is approximately the same as the measured ion density, which is estimated to have an average value between 2×10^7 and 8×10^7 ions/cc.

Crude calculations have also been made of the frequency with which ions and electrons oscillate in the potential well determined by Eq. (1). The calculated electron oscillation frequency was approximately equal to the ion cyclotron frequency at a magnetic field of 12 kG. Oscillations of this nature may explain the large bursts of radiation at the ion cyclotron frequency which have been found experimentally to occur at magnetic fields of 12.5 kG and 25 kG.

Attempts are now being made to obtain a self-consistent solution of $\phi(r, z)$ and of the proton and electron densities. The procedure used is to pick an initial $\phi(r, z)$ and determine the proton and electron densities that result from particles formed by a source term and moving in orbits determined by the adiabatic invariant conditions. The charge distribution resulting from the time-averaged particle orbits will then be fed into Eq. (1) and a new potential determined. This iterative procedure will be repeated until a self-consistent solution is obtained. This procedure should result in a prediction of the plasma spreading that results from the measured potential.

II. ASTRON PROGRAM

Nicholas C. Christofilos, Ross E. Hester, John D. G. Rather, William A. Sherwood, Ross L. Spoerlein, Paul B. Weiss, and Robert E. Wright

The major effort of the Astron group this report period has been directed toward the completion and starting of operation of the Astron facility.

Since the successful operation of the accelerator most of the effort has been applied to finishing the installation of the power supplies and electronic controls for the Astron field coils. The controls provide the possibility of creating any desirable mirror shape along the Astron tank and the ability to change this shape during buildup of the E layer.

The mechanical assembly of the Astron, the installation of the decelerating resistors, etc. has been completed.

A variety of diagnostics, including the closed-circuit television hook-up to observe the plasma luminescence, has been installed.

Finally on December 20, 1963, 10 years and 2 months since the conception of the E layer, the Astron facility began operation.

A beam of electrons (4 MeV, 60 A) was injected into 100 microns of argon. The beam traveled a helical path of approximately 100 meters and hit a target 22 meters away from the injector. No trapping was attempted. A plasma of approximately $10^{12}/cm^3$ was generated by the electron beam. No instabilities have been observed.

The conclusion from this first experiment is that it may be possible to inject the electrons in the presence of a plasma of 10^{10} to 10^{12} density to avoid excitation of the tank modes.

No other experiments were done in 1963. Operation was resumed on January 6, 1964. The results of this experiment, though, will be reported in the next semiannual report.

A brief outline of the contemplated experimental work for the first half of 1964 is:

1. Study of trapping and confinement of single electron pulses in a variety of gases at a wide range of pressure.
2. Study of the influence of a cold plasma (10^{10} to 10^{12} density) in quenching instabilities or in preventing the existence of instabilities.
3. Trapping of a sequence of pulses, thus establishing an E layer of 10 to 20% of its full strength, and study of its properties under a variety of conditions.

III. LIVERMORE PINCH PROGRAM

Dale H. Birdsall, Stirling A. Colgate,
Harold P. Furth, Charles W. Hartman, and Richard H. Munger

1. LEVITRON

Operation

The objective of levitron operation has been to explore the mechanism and control of the instability leading to plasma loss. Since the leading possibility for instability excitation still remains the anisotropic velocity distribution associated with $J_{||}$ (current density parallel to the local magnetic field), a major objective has been the formation and heating of a plasma with small $J_{||}$.

In earlier levitron experiments, the induction of appreciable $J_{||}$ was unavoidable during formation of the basic vacuum magnetic field configuration: namely, since the magnetic fields must necessarily be transient and since B_θ and B_z have different radial dependences, an $E_{||}$ of 0.05 V/cm is produced during the rise of the fields. The combination of this electric field and the near-perfect single-particle-confinement properties of the sheared magnetic surfaces causes the base vacuum of 10^{-6} mm Hg to break down. Because of the small-port construction of the levitron (to reduce magnetic field perturbations), additional pumping could not easily have improved the vacuum, but the development and operation of a retractable liquid-helium cold finger (Fig. III-1) has proved successful. A cold rod of copper 4 in. long $\times$ 0.5 in. in diameter, cooled from an external reservoir, provided a pumping speed for air as well as deuterium consistent with a sticking probability greater than 80%. This rod and reservoir, extracted from the toroidal vacuum chamber 1 second before a discharge, results in the predicted 30-fold improvement in base vacuum. This is sufficient so that no electric breakdown occurs during the rise in the magnetic fields. The possibility now exists of injecting plasma or neutral gas near peak vacuum field, and heating by non-Ohmic means.

Plasma Potential Measurements

In attempting to understand the plasma loss mechanism during Ohmic heating we have measured the drain current to the wall necessary to change the plasma potential.

A helical tungsten filament of 5 cm^2 area was introduced into the plasma discharge 4 cm from the wall (Fig. III-2) and biased 200 volts positive or negative by a capacitor with a series resistor and ignitron switch. The plasma potential was monitored by a small floating probe 3 cm from the wall, inserted 90 deg around the torus from the filament. Figure III-3 shows typical potential and current traces for the conditions of plasma formation of Figs. III-4 and III-5. It is observed that the plasma potential can be forced positive or negative with a current of 400 to 500 amperes lasting for a millisecond. The possibility that the residual drain current represents the electron thermal and runaway loss along the distorted lines of force is being investigated.

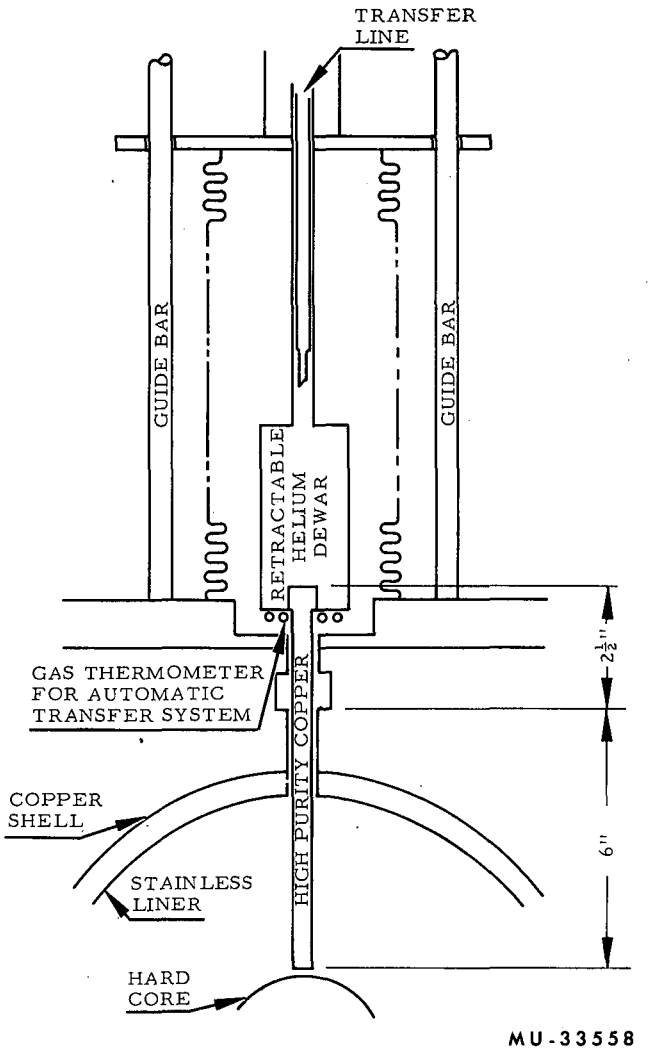

Fig. III-1. Liquid helium trap.

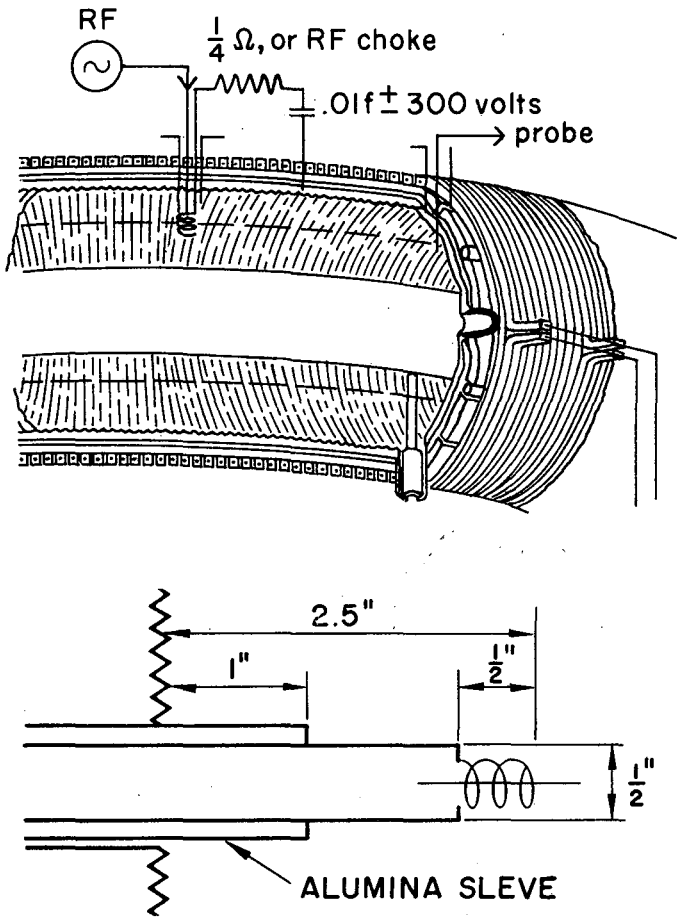

Fig. III-2. Filament dc bias and rf probe.

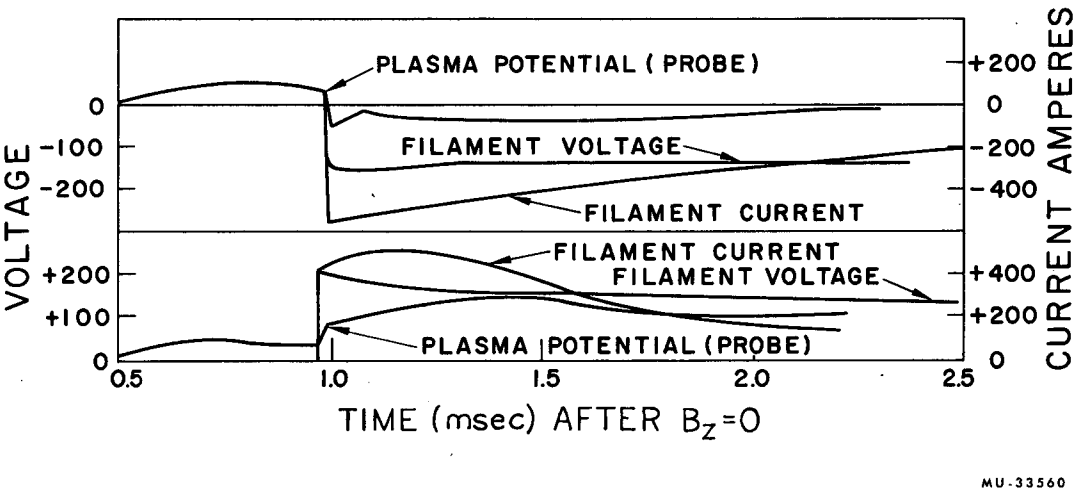

Fig. III-3. Bias potential and current measurements.

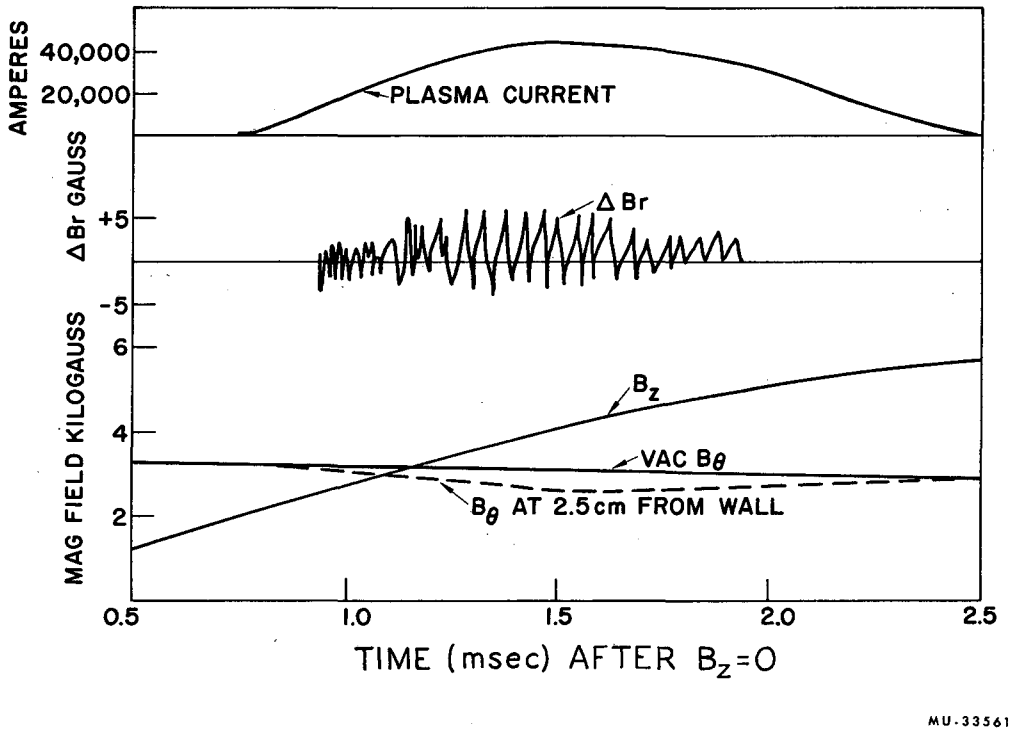

Fig. III-4. Magnetic fields and plasma current.

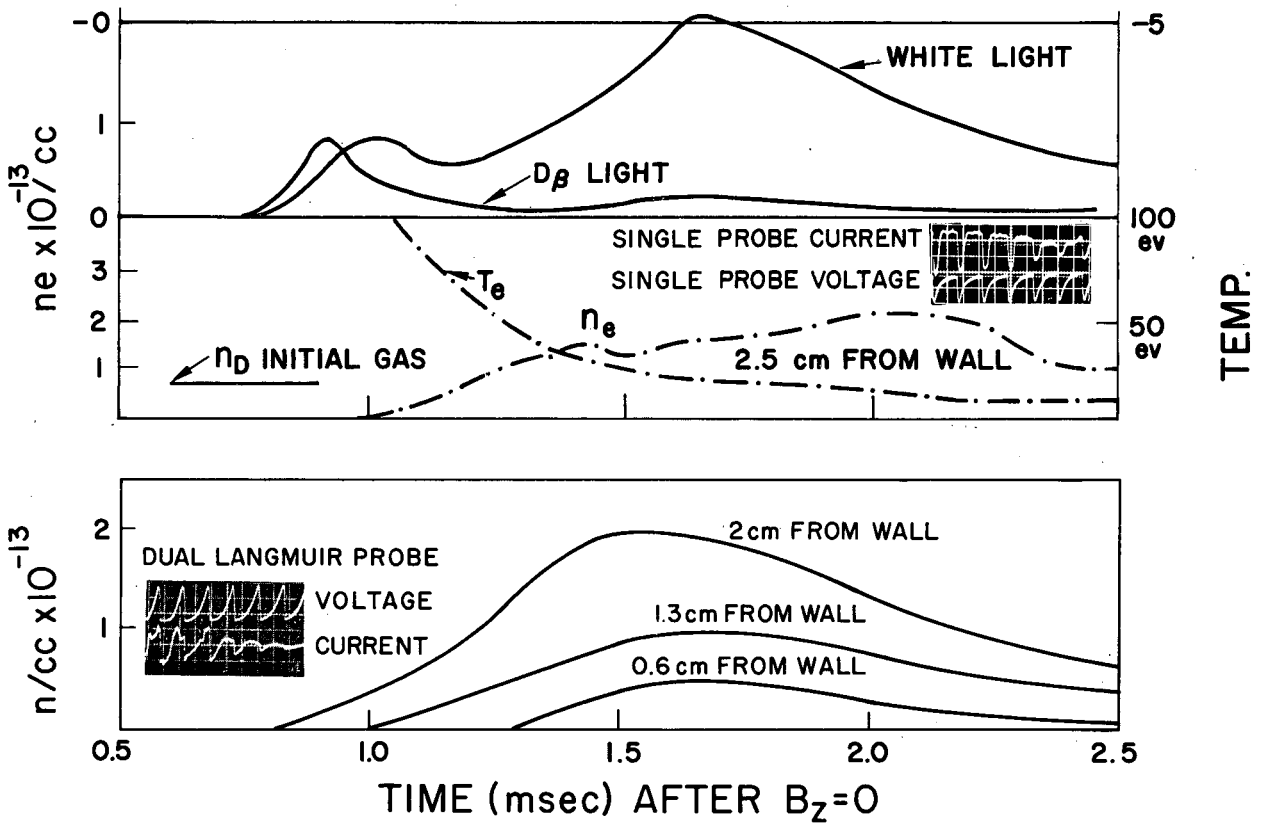

Fig. III-5. Plasma density and light.

Langmuir probe measurements made with the circuit and probes of Fig. III-6 gave the results of Fig. III-5. The plasma diffusion to the wall would appear to have a characteristic time constant of 300 to 500 μsec.

Rf Heating Experiments

Rf heating is being applied in the range 3 to 10 Mc and 10 to 100 kW. For the initial experiments, a hot filament like that in Fig. 2 has been used to apply a radial rf electric field.

The present power level has been too low for operation with neutral pulsed gas injection. Therefore, the procedure has been to allow a weak Ohmic heating during buildup of the confining magnetic field. In the interval of 3 msec about peak field the discharge ordinarily stops, but the plasma can be maintained by application of the rf. The observed rf impedance of ≈1 ohm agrees with calculated impedances for excitation of hydromagnetic waves. Rf currents of order 100 A have been used. With a cold filament rectification results, and the plasma potential swings sharply positive. With a hot filament the rectification ceases, and the plasma potential swings negative by about 100 V, indicating preferential loss of ions. The plasma-confinement properties are being stuided.

Plasma Source Development

A major limitation to the usefulness of the plasma source described in an earlier report[1] was frequent arcing along B between metal surfaces external to the hollow cathode. To avoid this difficulty various designs have been investigated and several causes of arcing have been identified. Primarily, it was found that the choice of refractory metals for electrodes is important. Ta was found to be especially susceptible to arc spot formation and eroded badly, indicating a similarity to low-boiling-point metal-vapor arcs. The vaporization limit of spot formation appears to result from the low thermal conductivity of Ta. Arcs formed on Mo and W show little erosion and are strongly dependent on the presence of surface contaminants.

The most stable design arrived at is similar to that described previously. It consists of a W ribbon filament 4 mm wide placed 3 mm behind a Mo Pitot tube 2.5 mm i. d. and 4 mm long, and a washer Mo anode with 3 mm aperture. The filament ribbon is the cathode and the Pitot tube is allowed to float. Only the hot W surface of the cathode is intercepted by magnetic field lines passing through other electrodes.

Operation of the source is quiescent and arc-free provided the filament temperature is above about 2500°C. Under these conditions the total arc drop is about 100 V at 10 to 30 A and the tube floating potential is 50 to 75 V. As the filament temperature is lowered the arc drop increases to 800 to 1000 V before an arcing limitation is encountered. The tube potential remains at 100 V, indicating the additional drop appears at a cathode sheath.

1. D. H. Birdsall, S. A. Colgate, H. P. Furth, C. W. Hartman, R. H. Munger, and R. L. Spoerlein, in Controlled Thermonuclear Research Semiannual Report, UCRL-10852, June 1963, p. 45.

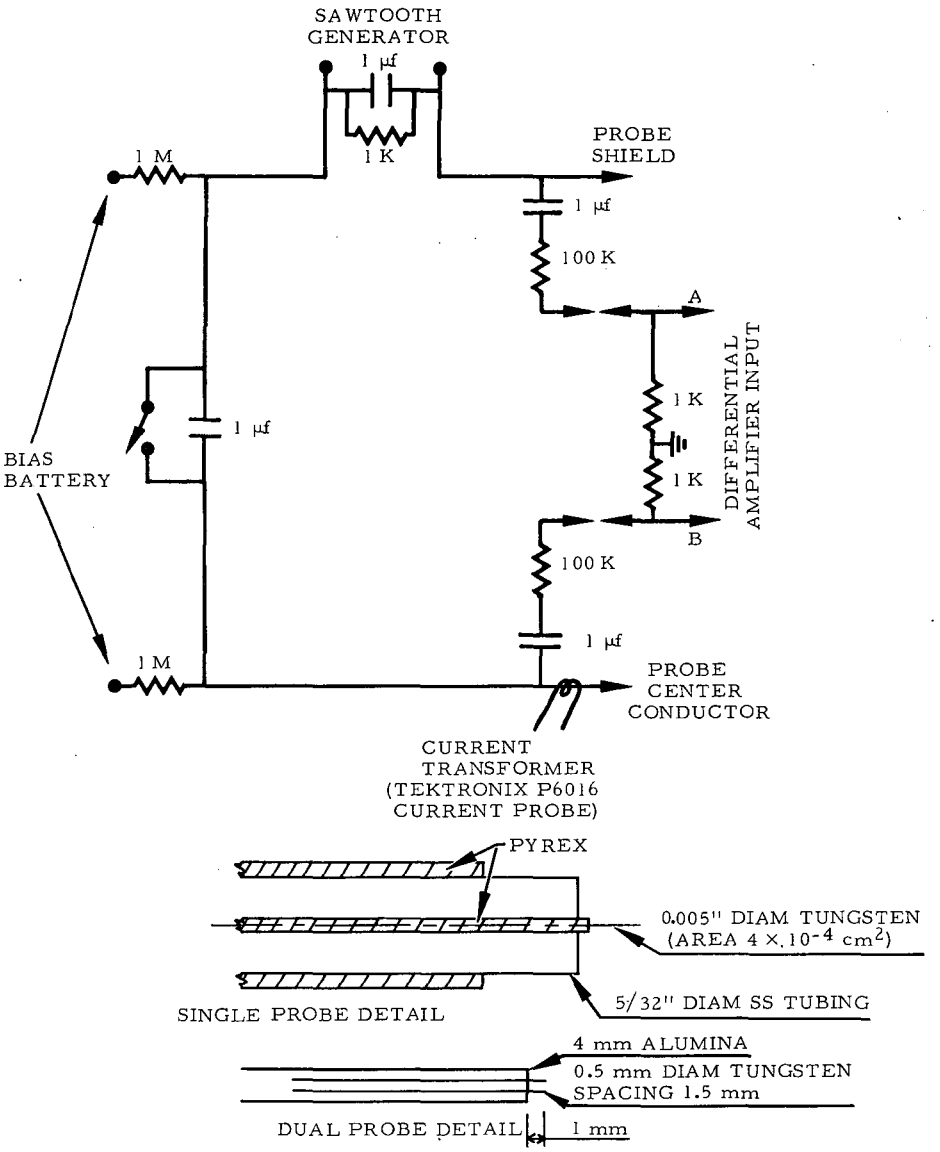

Fig. III-6. Langmuir probes and circuit.

Preliminary spectroscopic investigation of the plasma has failed to indicate impurities of electrode material.

Alkali Metal Plasma Experiments

Plasmas that correspond in many ways to the classical hot plasma of thermonuclear interest can be readily generated from alkali metal vapor by contact ionization. The close correspondence is especially evident in the areas of containment and stability, where meaningful experimental tests of magnetic bottles can be made. With this interest in mind, studies have been initiated to investigate contact ionization of alkali metals of low mass in order to minimize the magnetic field needed to provide a given number of Larmor radii.

An iridium cathode has been used thus far with Li and Na. The quoted thermionic work function for Ir is given as 5.3 to 5.4 volts, which is to be compared with the ionization potential of Li, 5.36 V, and of Na, 5.12 V. Preliminary results (at 0.1 mA/cm^2 Li ions) indicate that 10 to 50% of the Ir genode surface has a work function in excess of 5.36 V. At the same time, the electron work function evaluated by electron emission is about 4.5 V. The difference is attributed to patch surface contamination. The Li monolayer is removed at cathode temperatures in excess of 1800°C.

Hard-Core Experiment

An experimental study of plasma containment in the minimum-B, stuffed-cusp geometry has been initiated. This geometry combines the radially decreasing B_θ with radially increasing cusp fields, and should provide a comparison with the levitron, in which B decreases everywhere away from the hard core.

The design has been completed and the vacuum vessel is on hand. Continuous cusp fields up to 8 kG and pulsed hard-core fields (3/4 msec rise time) to 10 kG will be used. The central ring mirror is 15 in. radius, the length is 40 in., the hard core diameter is 4 in., and the mirror ratio is 2:1; rf heating at ω_{ci} and ω_{ce} will be used in conjunction with the plasma source.

Theoretical

An explanation has been found for the levitron instability. The measurements previously reported[1] on the autocorrelation lengths and the field structure of this mode were consistent with the finite-resistivity "gravitational" and "rippling" modes.[2] The $J_\parallel$-dependent rippling mode has appeared considerably more plausible than the β-dependent gravitational mode, since the amplitude of the instability is better correlated with $J_\parallel$ than with β. Previously, the rippling mode has appeared theoretically inadmissible, however, since thermal conductivity along field lines can easily wipe out the local resistivity perturbation on which the rippling mode depends.

2. H. P. Furth, J. Killeen, and M. N. Rosenbluth, Phys. Fluids 6, 459 (1963).

The problem has been resolved by taking proper account of the dJ/dt term in Ohm's law. As previously reported, this term can also give rise to the rippling mode, and leads to the same dispersion relation, where one need merely replace the usual resistivity η_0 by $\eta_0 + \eta_i$, where

$$\eta_i = \frac{\omega}{r_c n_e} ,$$

with $r_c = 3\times10^{-13}$ cm (the classical electron radius) and ω the growth rate of the mode.

In the levitron one has $\eta_0 \approx 10^6$ emu and $\eta_i \approx 10^5$ emu if all the electrons share in carrying the current, and if the observed $\omega \approx 10^5$ sec^{-1} is used. Under these conditions, the inclusion of η_i gives only a minor effect. A major effect, however, can be obtained if one takes note that the Ohmic heating current is carried preferentially by less than 10% of the electrons. This is plausible both theoretically and experimentally, and will shortly be measured by the energy-analyzer experiment.

The usual hydromagnetic analysis is then modified to include two fluids: the current-carrying electrons (with their neutralizing ions) and the cold electrons (with their neutralizing ions). If these two fluids are assumed to move together (being coupled by $\bar{B}_0$ perpendicular to $\hat{k}$) the analysis is simple, and yields the usual growth rate, with η_0 replaced by $(1/\eta_0 + 1/\eta_i)^{-1}$. This means that for $\eta_i >> \eta_0$ the dJ/dt effect precisely undoes the stabilization due to the thermal conductivity effect, and the instability grows as in the absence of both effects.

As η_i becomes large, the "collision-free skin depth" $s_i = (\eta_i/\omega)^{1/2}$ becomes comparable to the current layer thickness, and the current-carrying electrons are not strictly coupled to the cold electrons. In that case it appears possible to have a rippling mode leading to much stronger leakage of energetic electrons than of cold plasma. The parameters appropriate to this regime are almost being reached in the levitron.

When the levitron is operated so as to avoid the $dJ_{||}/dt$ effect, e.g., by use of non-Ohmic heating) the present dominant instability should disappear. This will permit us to examine whether there are any inherent instabilities (of the gravitational type) in shear-stabilized systems.

To prepare for the eventuality that shear stabilization is ineffective, we are studying toroidal systems stable by the $\int d\ell/B$ cirterion.[3] We have shown that this criterion is insensitive to finite-resistivity effects, and the a priori likelihood of stable confinement is therefore high.

In the approximation of long thin flux tubes, a "periodic quadrupole" solution[3] has been found for which $\int d\ell/B$ decreases toward the outside.

---

3. H. P. Furth and M. N. Rosenbluth, 5th Annual Meeting, Division of Plasma Physics of the American Physical Society, G-4, November 1963, San Diego, California.

An element of the torus (approximated as a straight section) is shown in Fig. III-7. To satisfy the conditions of the derivation, the axial scale must be elongated far more than shown in the upper model, and somewhat more than in the lower model. To improve on these somewhat impractical dimensions, the analysis is being relaxed so that $\int d\ell/B$ need have a negative outward gradient only near the outer periphery.

Higher multipole structures have been investigated, but it is found that (to the order in radius at which the multipole field first becomes effective, and for moderate multipole numbers) it is not possible to enclose the axis with closed surfaces of constant $\int d\ell/B$ having a negative outward gradient. It is possible to have stable "streamers" inside the multipole structure, and it may be possible to connect these streamers by rotational transform into a stable surface surrounding the axis.

Open-ended multipole-stabilized structures (Ioffe machines) have also been studied, by the same technique of expansion in radius. It is found that straight, infinite "Ioffe bars" in general give configurations having undesirable properties. By using mutipole coils (i.e., Ioffe bars plus azimuthal cross-connectors, suitably distributed) one can satisfy various prescriptions for symmetrizing field-line curvature, constant-B surfaces, etc. The electric field induced along magnetic field during compression has been calculated. Only for the quadrupole does $E_{\parallel}$ vanish to the order in r at which the multipole first becomes effective (i.e., r^2 for the quadrupole). The r^4 term for the quadrupole cannot be made to vanish identically, but the potential difference between the two ends of all field lines can be made to vanish to order r^4. (If there is no mirror effect on axis, the $E_{\parallel}$ can vanish to all orders for the quadrupole.) It has been found that the field-line equations for all multipoles can be integrated analytically at small radius. Explicit integrals for the adiabatic invariant J can thus be given.

An analysis demonstrating the existence of axisymmetric poloidal minimum-B mirror machines (Fig. III-8) has been published.[4] A preliminary report on the work prior to July 1 was given by Richard F. Post,[5] who has also been conducting calculations on a practical embodiment (see Mirror Program). The same basic idea has been reported by J. Andreoletti.[6]

4. H. P. Furth, Phys. Rev. Letters 11, 308 (1963).
5. R. F. Post, Euratom Meeting on Mirror Confinement, Paris, France, 15 July, 1963.
6. J. Andreoletti, Euratom Meeting on Mirror Confinement, Paris, France, 15 July, 1963.

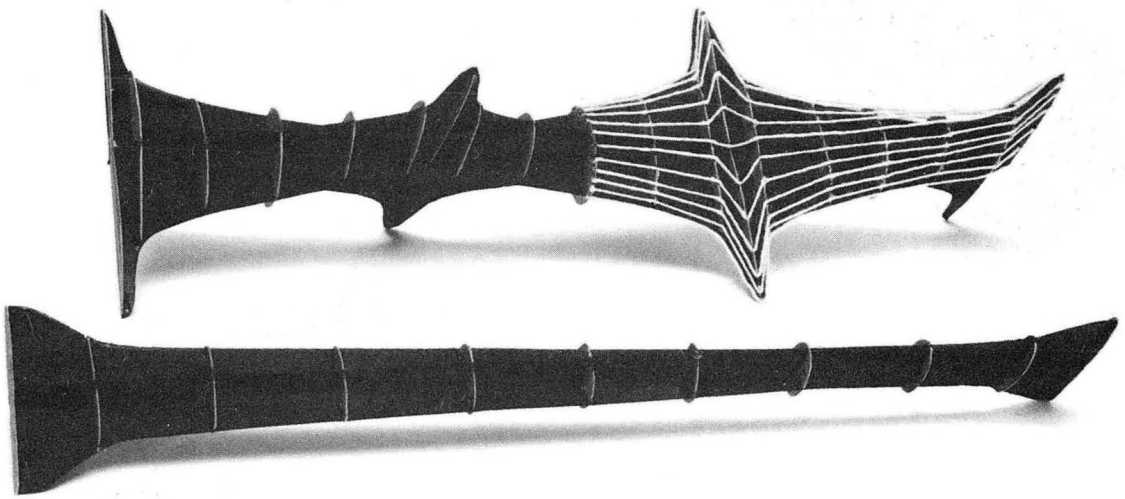

ZN-4187

Fig. III-7. Periodic quadrupole torous.

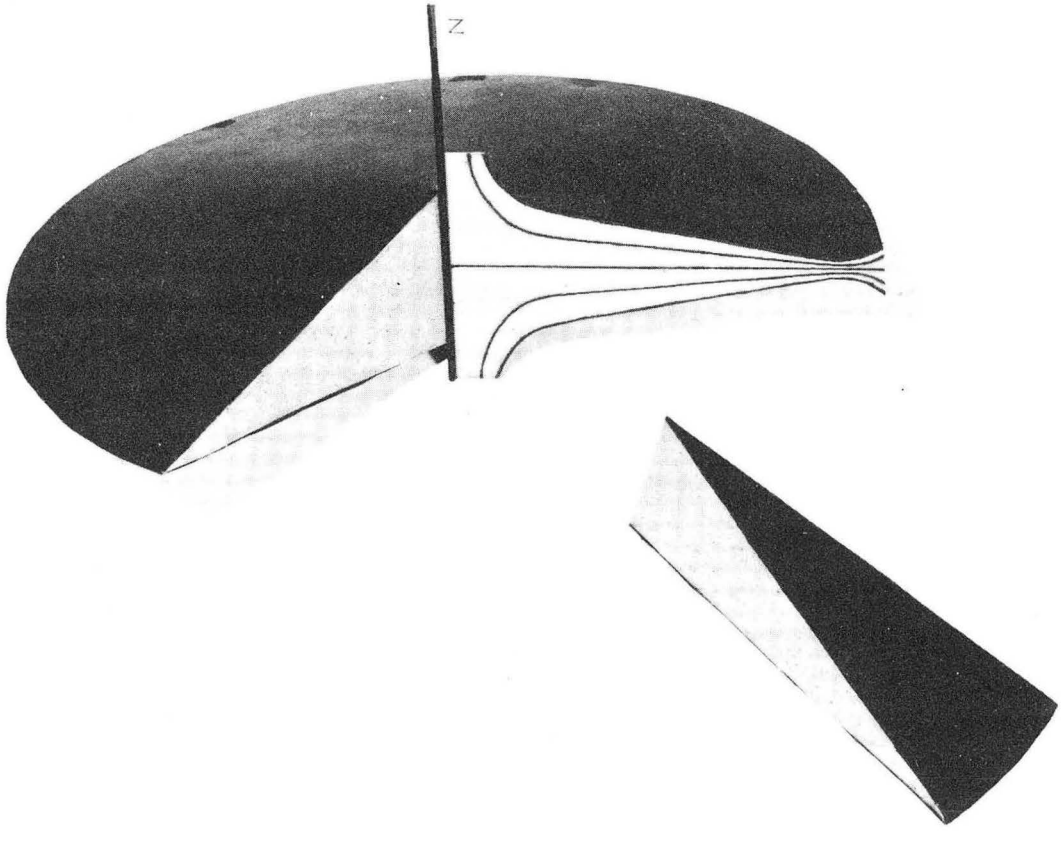

ZN-4186

Fig. III-8. Disc-type mirror machine. Excised sector resembles flux surface of quadrupole "Ioffe Machine."

IV. BERKELEY PLASMA RESEARCH

1. ROTATING-PLASMA RESEARCH

A. Production and Detection of Diamagnetic Signals in the Homopolar Device

Klaus Halbach

As a basis for the measurement and interpretation of diamagnetic signals in the Homopolar Gun I and the Homopolar V device, calculations have been made concerning the production and detection of diamagnetic flux changes produced in these devices. Because of their length, these calculations will be published in a regular UCRL report and only the results will be given here.

To obtain simple results, some simplifications have been made:
(a) We used the fact that the plasma produced by the two devices has a small β, i.e., the kinetic energy density of the plasma is small compared with the energy density of the externally applied magnetic field.
(b) It has been assumed that the plasma is azimuthally symmetric, a condition which should be fulfilled if the devices operate properly.
(c) It has been assumed that the plasma is uniform in the axial direction and that the length of the plasma is large compared with its diameter. Since this condition is usually not fulfilled experimentally, the formulas given below allow only an approximate interpretation of the experiments.
(d) The radial transit time of a MHD wave obtained from the spacing of the coaxial electrodes and the Alfvén velocity is assumed to be short compared with the rise time of a diamagnetic signal caused by the skin effect of the outer electrode; this condition is always fulfilled in our experiments.
(e) The thickness of the electrodes is assumed to be small compared with their radius, which is the case in both devices.

When the plasma is created, one expects to find a change of the magnetic flux that goes through the area inside the outer electrode. This flux change will, in general, have two components, one resulting from the rotation of the plasma and the other from the kinetic temperature of the plasma. Neglecting for the moment the azimuthal currents induced in the electrodes, the latter contribution can be expressed as

$$F_L = \frac{\mu_0}{B_0} \int_{r_1}^{r_2} \left\langle \frac{\rho v_L^2}{2} \right\rangle 2\pi r \, dr, \qquad (1)$$

with the following meaning of the symbols (all in mks units):

F_L = flux change because of Larmor motion,

B_0 = externally applied field,

r_1 and r_2 = radius of the inner and outer electrode,

r = distance of a volume element from the axis of the device,

$\left\langle \rho v_L^2/2 \right\rangle$ = Larmor energy density.

The Larmor energy density can be thought of as being the average value of one-half the product of the density ρ times the square of the Larmor velocity v_L of the ions at the time of their creation, since the original Larmor energy of the electrons can be neglected and since the total Larmor energy density is unaffected by the later energy transfer from the ions to the electrons.

The flux change resulting from the rotational velocity v_R of the plasma has the form

$$F_R = \frac{\mu_0}{B_0}\left(\int_{r_1}^{r_2} \frac{\rho v_R^2}{2}\, 2\pi r\, dr - \pi r_0^2 \int_{r_1}^{r_2} \frac{\rho v_R^2}{r}\, dr\right). \tag{2}$$

The second integral on the right side of Eq. (2) results from the fact that, because of the rotation, the magnetic field at the center electrode has to be smaller than at the outer electrode. If this field can penetrate the center electrode, one has to set $r_0 = 0$; in our experiments, however, this field cannot penetrate and one therefore has to set $r_0 = r_1$. In general, this term leads to only a small correction.

For our experimental parameters, the Larmor velocity and the rotational velocity of the ions should be approximately equal, so that both effects can be expected to contribute about equally to the total diamagnetic signal. It should be noted that although the flux changes resulting from rotational velocity and Larmor velocity are about the same, the diamagnetic field distributions within the plasma resulting from these sources are drastically different.

If no significant radial transfer of angular momentum takes place in the plasma, the first integral in Eq. (2) can be expressed in terms of the backvoltage V and the charge per unit of axial length, Q/L, that passed through the device during the initial discharge,

$$\int_{r_1}^{r_2} \frac{\rho v_R^2}{2}\, 2\pi r\, dr = \frac{1}{2}\, VQ/L\,. \tag{3}$$

This result can, of course, also be expected from energy considerations. Since Q is proportional to V/B_0^2, the total diamagnetic flux change has to be proportional to V^2/B_0^3 when the correction term in Eq. (2) can be neglected.

The induced azimuthal currents in the electrodes modify the actual flux changes in the plasma. We are not directly interested in the actual flux changes, however, but in the voltage induced in a single loop around the outer electrode. If we neglect the effect of the center electrode, it can be shown that the Laplace transforms of the plasma-generated flux change of $F(p)$ and the induced voltage $V(p)$ are connected through

$$V(p) = \frac{pF(p)}{\cosh\sqrt{p\tau_1} + p\tau_2 \sinh\sqrt{p\tau_1} \,/\, \sqrt{p\tau_1}}\,, \tag{4}$$

with $\tau_1 = \mu_0 \sigma x^2$; $\tau_2 = \mu_0 \sigma r_2 x/2$; σ, x, and r_2 are the electrical conductivity, thickness, and radius of the outer electrode. For the outer electrodes of Homopolar Gun I and Homopolar V, the time constants τ_1 and τ_2 are 5 μsec and 120 μsec.

Analysis of Eq. (4) shows that if F(t) is a step function of amplitude F_0, V(t) rises to 90% of its maximum, F_0/τ_2, in the time $3\tau_1/\pi^2$, and decays exponentially with the time constant τ_2. The rise time $3\tau_1/\pi^2 \approx 1.5$ μsec is due to the skin effect in the electrode, whereas the decay time τ_2 is the L/R time of the electrode. Since the electrode serves as an integrator with a sufficiently long time constant for our current experiments, an external integrator or pulse-shaping circuit is not used at present. Model experiments with a copper liner of equal dimensions confirm these calculations, but they show also that the shape of the decay function can be expected to depend somewhat on the length of the plasma. Calculations show that the center electrode also changes the decay function somewhat, but not enough to affect out present experiments noticeably.

B. Homopolar Gun I

Kenneth W. Ehlers and Klaus Halbach

Early in the report period we continued experiments with both mirrors energized. Fast-neutron measurements yielded results similar to the ones described in the Homopolar V section of the preceding semiannual report; the latest recorded fast neutrons appeared 200 μsec after the main discharge.

Diamagnetic signals yielded an energy density nkT_{kin} of the plasma between 10^{17} and 10^{18} eV/cm^3, as could be expected from the other experimental parameters. The diamagnetic signals reach their maximum value about 1 to 2 μsec after the main discharge, which is in agreement with the calculations described above. As a result of an external crowbar, the diamagnetic signal decreases by a factor of 2, which has to be expected if, originally, the Larmor velocity equals the rotational velocity and the latter is then removed by crowbarring. Shortly after the crowbar, the diamagnetic signal starts to decay, with a decay time of the order of 10 to 20 μsec. Since the plasma starts to spread axially, as shown by delayed diamagnetic signals farther removed from the valve region, this decay of the signal is certainly not entirely due to a genuine decay of the plasma.

After disconnecting the downstream mirror, we made the first measurements concerning the (axial) transfer velocity of the plasma. The delay of diamagnetic signals downstream gave maximum axial velocities of 2×10^5 m/sec, which is in agreement with the position of the gas valve in the magnetic field configuration, the discharge parameters, and the estimated original axial length of the plasma. The first appearance of light signals, measured with photomultipliers at different downstream locations, gave the same axial velocities. The delay between the maximum amplitudes of these light signals gave, however, only 1×10^5 m/sec axial velocity. This could tentatively be explained by the assumption that components of the plasma with lower initial energy would obtain lower axial velocities and would also emit more light than the high-energy components of the plasma.

C. Homopolar V

Klaus Halbach, Robert W. Layman, and G. Donald Paxson

To obtain better accessibility and allow the application of additional diagnostic methods, the Homopolar V device has been modified. The original coil arrangement has been replaced by two coils. They are each 14 in. long, have an i.d. of 11 in., and are separated to give a mirror ratio of 1.5. A new outer electrode has several windows to (a) allow microwave transmission experiments along cords at several axial locations, (b) measure microwave emission from the plasma, and (c) detect charged reaction products with a solid state detector, which, if successful, could ultimately lead to a spatially resolved measurement of the reaction rate in the plasma. We also hope that the absence of large amounts of epoxy will lead to a better detection of neutrons.

So far, the device has been operated only with H_2, in the hope that the later switchover to D_2 will give some information about the production of neutrons by wall bombardment. It also allowed us to make some qualitative γ measurements with a LiI counter. They show that the internal crowbar is always accompanied by a large burst of γ's, suggesting the acceleration of electrons to energies of the order of the applied voltages.

A diamagnetic loop gave signals that correspond, as in the Homopolar Gun I, to a density-temperature product of 10^{17} to 10^{18} eV/cm^3, which was roughly in agreement with the other experimental parameters. Although the diamagnetic signal increased with the applied voltage and decreased with increasing magnetic field, the proportionality to V^2/B_0^3 was not observed. Since we do not use a switch in series with the fast capacitors, it is possible that the amount of gas released by the valve until the breakdown occurs depends on the voltage and the magnetic field. To eliminate this possibility, we plan to install again this seris switch. The rise time of the diamagnetic signal was about 5 μsec, much longer than calculated, and the decay time was about 10 to 15 μsec. Since the main discharge current was also followed by an unusually high leakage current, we suspected a malfunction of the valve. Inspection of the center electrode and the fast valve showed azimuthal asymmetries which, we hope, were responsible for this unusual behavior. We have replaced the valve by a new one and will repeat these experiments in a month or so.

2. HYDROMAGNETIC WAVES AND ION CYCLOTRON HEATING

A. Ion Cyclotron Resonance Experiment

William R. Baker, Dennis Reilly, and John M. Wilcox

The plasma energy density in the magnetic beach region has been increased by a factor of 3 during this period, mainly as a consequence of reducing the impurity radiation.

First efforts were devoted to reducing the impurities introduced at the time of plasma formation. Plasma preparation with a hydromagnetic ionizing wave was useful in the Alfvén-wave work that was done at a pressure of 100 microns, but at the pressures below 1 micron that are appropriate for the magnetic beach the large dc currents associated with the hydromagnetic wave contribute to the impurity level. Therefore the rf oscillator is now used also for pre-ionization. A small capacitor is first discharged into the oscillator, giving a burst of rf energy that partially ionizes the plasma. The hydromagnetic impedance is then low enough to accommodate the main pulse of rf power. At present a sparker imbedded in the electrode must be fired at the same time as the initial discharge to achieve breakdown. There is evidence that this element is now one of the main sources of impurities.

The hypothesized breakdown mechanism consists of an ionization front, of the same diameter as the electrode, propagating down the axis from the electrode to the end plate, which is then followed by a radial breakdown in the beach region where the $\vec{E}\times\vec{B}$ force is largest. Evidence for this is given by the observation that the maximum intensity of the D_β light along a path normal to and intersecting the z axis at the beach occurs 30μsec before the maximum along a path parallel to the z axis at a radius of 2-1/4 in. Compare Figs. IV-1a and IV-1b.

The cylinder that contains the plasma is now made of tungsten 5 mils thick, which is heated by direct-current Ohmic heating to a temperature of 600°C. At this temperature the base pressure recorded by the Vac Ion pump is less than 10^{-7} mm Hg. The center electrode has a cap of deuterium-loaded titanium. A number of other electrode and wall materials were investigated. In each case the contaminant line radiation was observed with a monochromator or spectrograph. When the electrode or walls were made of stainless steel, the impurity level was considerably higher than at present. Molybdenum and tantalum were also found to be inferior to tungsten.

A glow discharge at 1 mm of deuterium was applied to the plasma chamber for several hours in an attempt to reduce the impurity level. The line radiation from impurities decreased to the limit of the detector sensitivity while the glow discharge was on, but when the magnetic beach was established after the glow discharge "cleaning" the diamagnetic signal had decreased considerably.

a

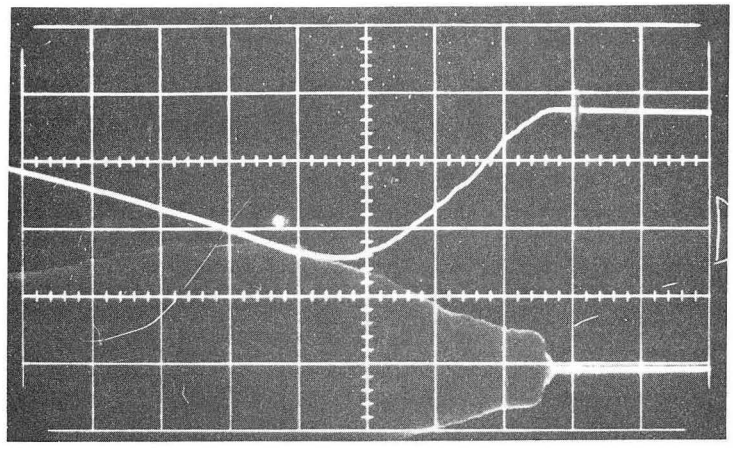

b

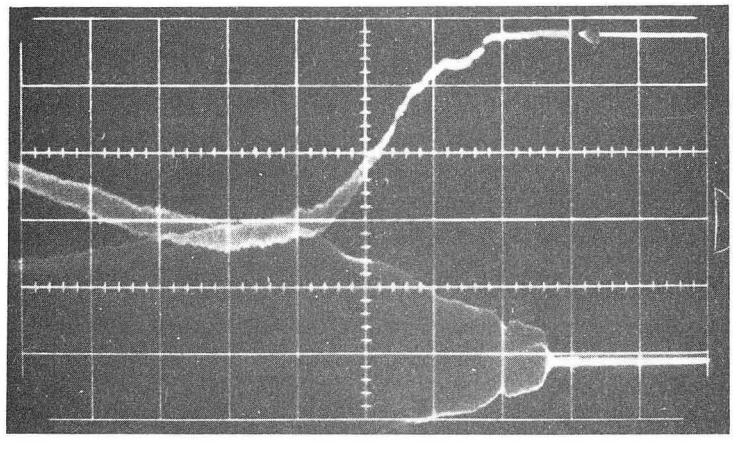

ZN-4131

Fig. IV-1. a. Top trace is D_β intensity along a path normal to and intersecting the z axis at the beach. Bottom trace is driving current, shown to provide time reference. Horizontal scale is 20 μsec/cm from right to left.

b. Top trace is D_β intensity along a path parallel to the z axis at a radius of 2-1/4 in. Bottom trace is driving current. Horizontal scale is 20 μsec/cm.

The end of the mirror opposite the driving electrode has contained a conducting screen so as to tie down the magnetic lines and perhaps inhibit the onset of instabilities. When this screen was replaced by a quartz plate the diamagnetic signal increased by a factor of 2. However, after a number of shots the signal decreased as impurities built up on the plate. This is in contrast to the situation with a screen, in which the holes acted as traps for the impurities. It is possible that the end screen is not compatible with a positive plasma potential for this hot-ion plasma. This point needs further investigation.

The present situation is shown in Fig. IV-2. Figure IV-2a shows the D_β line, which peaks at 110 μsec and is down to half amplitude after 200 μsec. Figure IV-2c shows the diamagnetic signal from a coil of five turns wound around the 5-mil tungsten cylinder. This signal increases with time until it reaches a maximum after about 270 μsec, and then drops off to a lower level. The peak corresponds to an energy content greater than 10^{16} eV/cm^3. The resonant nature of the peak is illustrated in Fig. IV-3. In Fig. IV-3a the beach field is adjusted so that the ion cyclotron frequency is approximately equal to the oscillator frequency. In Fig. IV-3b resonance has been eliminated by increasing the beach field by 10%. The voltage (Fig. IV-2b) and the current (Fig. IV-2a) applied to the driving electrode are also shown. The current increases for 180 μsec and then decreases, while the voltage is low during the time of high current loading.

The hydromagnetic ionizing wave, the glow-discharge "cleaning," and the sparker have all been shown to introduce impurities into the plasma by sputtering wall, electrode, and insulator materials. Another mechanism for sputtering is the acceleration of ions by a high plasma potential. Making both electrodes into electron emitters would serve to alleviate this problem by lowering the plasma potential.

After a few hundred microseconds the contact of the electrodes with the plasma seems to become less effective. This is perhaps the principal limitation on further heating at present. This limitation could be attacked by changing the electrode sizes, using a puff valve to increase the gas density in the region of the electrodes, and making both electrodes into electron emitters.

B. The Contact Problem in the Ion Cyclotron Resonance Experiment

Wulf B. Kunkel

In the ion cyclotron heating experiment at Berkeley (Hothouse II) the radio-frequency power is transmitted via concentric electrodes that permit conduction current to pass directly into and out of the ionized gas. In principle, this arrangement should provide excellent coupling between the oscillator and the plasma, and, indeed, from various measurements in the past, substantial energy transfer has been inferred, although the terminal energy content of the plasma remained disappointing.[1] The recent success in the lowering of the impurity level and the accompanying temporary increase of the observed energy density have stimulated a re-evaluation of the

1. Refer to all preceding Controlled Thermonuclear Research Semiannual Reports, e.g., UCRL-10852, July 22, 1936, p. 62.

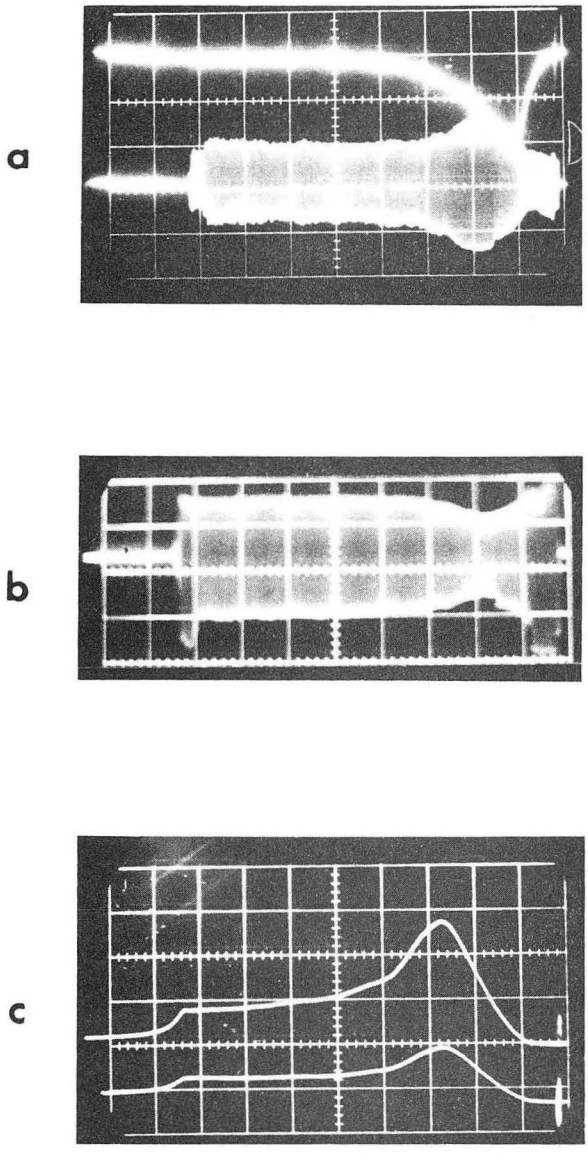

Fig. IV-2. a. Top trace is D_β intensity along a path normal to and intersecting the z axis at the beach. Bottom trace is electrode current at 450 A/cm. Horizontal scale is 100 μsec/cm.

b. Electrode voltage at 2 kV/cm. Horizontal scale is 100 μsec/cm.

c. Diamagnetic signal at 5 G/cm. Top trace is from coil located near center of magnetic mirror, and bottom trace is from coil 4 in. away from center.

a

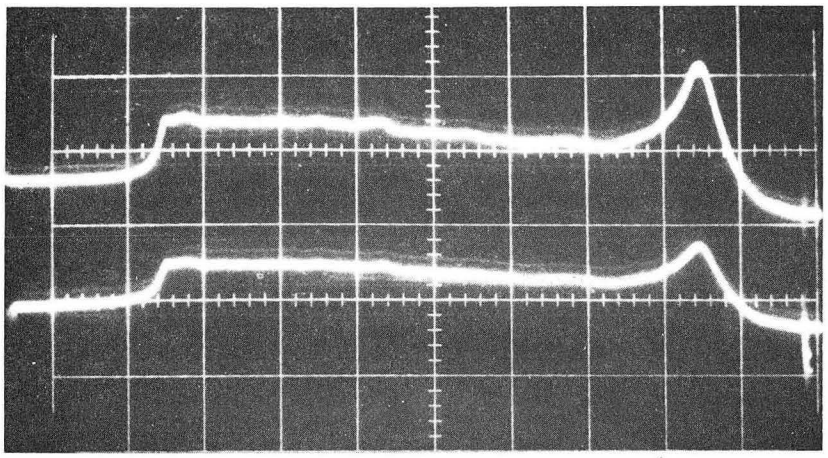

b

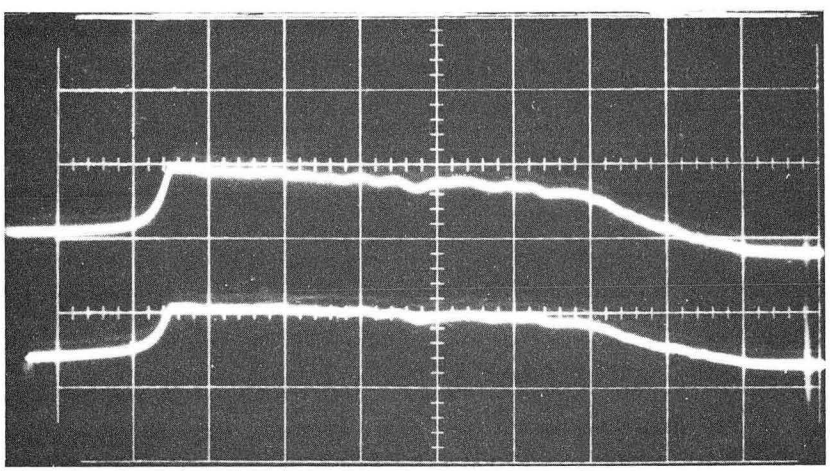

ZN-4133

Fig. IV-3. a. Diamagnetic signals showing resonance at beach. Horizontal scale is 200 μsec/cm.
b. Diamagnetic signals with beach magnetic field increased 10% above resonance field. Horizontal scale is 200 μsec/cm.

other probable limitations of this particular heating scheme. The considerations dealt primarily with the nature of the electrical contact, and of the resulting thermal contact, between the plasma and the electrodes. The conclusions may be summed up as follows:

Electrical Contact

1. For proper operation both electrodes must be capable of emitting electron currents at least as large as the required radio-frequency current.

2. Reliance on electron emission from cathode spots on cold electrodes is inadvisable because the resulting irregularities are likely to enhance cross-field diffusion.

3. Some tendency toward rectification of the alternating current is unavoidable because the metal-plasma contacts have nonlinear characteristics, which will probably always differ for the two electrodes.

4. As a consequence of 3, the metal wall (or liner) must be isolated for rf currents to prevent the shunting out of the outer electrode.

Thermal Contact

5. It should be easy to make the mean free paths long compared with the gyro radii. Thus the magnetic field is strong enough to ensure radial containment as long as instabilities do not produce anomalous diffusion. Axial confinement (mirror effect), on the other hand, requires that the mean free path be long compared with the length of the machine. In Hothouse II this occurs when $T_i^2 > 10^{-10} n_i$, where T_i is the ion temperature in volts and n_i is the number of ions per cubic centimeter. Also, the neutral density must be well below 10^{13} cm^{-3}.

6. Lack of axial containment means that the plasma streams axially to the ends of the machine. The resulting effects depend entirely on the rate at which material returns. If the collision frequency remains high a stationary state is reached as soon as the axial component of the particle pressure gradient is zero. In this case the energy loss can be described as heat conduction, which can be estimated from kinetic theory.

7. If the ion temperature and the ion-temperature gradient in a fully ionized gas exceed those of the electrons by a factor of $(m_i/m_e)^{1/7}$, the heat is conducted primarily by the ions. This condition may be assumed to exist in Hothouse II. Substitution of the appropriate parameters yields a peak ion temperature of about 50 volts for a dissipation of 1 megawatt. The electron temperature will, of course, be much lower.

8. The above value can be exceeded in a steady state only if the conduction loss is reduced by effective mirror confinement. In that case, however, space-charge limitations in the region between the confined plasma and the driving electrodes may come into play. Possible solutions of this contact problem are still being investigated.

9. From the above remarks it can be concluded that the most important quantity that would have to be carefully monitored in any future experiment would be the ion density. Without reliable information about the ion density a meaningful interpretation of other observations in this experiment is exceedingly difficult.

C. Computer Model of Ion Cyclotron Resonance Experiment

Gordon W. Hamilton

The measurements of amplitudes and phases of ion cyclotron waves that have been previously reported[2, 3] are susceptible of various interpretations because of the possible excitation of both the torsional and compressional modes. In order to resolve this ambiguity and also to provide an improved theoretical model for wave propagation in nonuniform conditions, a numerical analysis has been undertaken, using a realistic computer model simulating the geometry and plasma conditions of the Hothouse II experiment.

In order to make contact with the analytic theory[4] the computer model is based upon the same set of magnetohydrodynamic equations as has been solved analytically with the assumption of uniform magnetic field and plasma density and temperature. These equations are basically the macroscopic equation of motion, the generalized Ohm's law, and two linearized Maxwell's equations

$$nm \frac{\partial \underline{v}}{\partial t} = \underline{j} \times \underline{B}_0 , \tag{1}$$

$$\underline{E} + \underline{v} \times B_0 = \underline{\underline{\eta}} \cdot \underline{j} + \frac{1}{en} \underline{j} \times \underline{B}_0 , \tag{2}$$

$$\nabla \times \underline{b} = \mu_0 \underline{j} , \tag{3}$$

$$\nabla \times \underline{E} = - \frac{\partial}{\partial t} \underline{b} . \tag{4}$$

This set of four equations involves four unknown dependent variables associated with the ion cyclotron waves: $\underline{E}$, the wave electric field; $\underline{b}$, the wave magnetic field; $\underline{v}$, the macroscopic plasma velocity; and $\underline{j}$, the current density. The known functions of position are $\underline{B}_0$, the external magnetic field; n, the ion density; and $\underline{\underline{\eta}}$, the resistivity tensor. The remaining symbols are constant (m, the ion mass; e, the ion charge; and $\mu_0 = 4\pi \times 10^{-7}$ Henry/meter).

The approximations on which these equations are based are described in Ref. 4 and are valid for this experiment. We make the further assumptions

2. Forrest I. Boley, Alan W. DeSilva, Peter R. Forman, and Gordon W. Hamilton, in Controlled Thermonuclear Research Semiannual Report, UCRL-10294, July 20, 1962, p. 45.
3. Forrest I. Boley, John M. Wilcox, Alan W. DeSilva, Peter R. Forman, Gordon W. Hamilton, and C. N. Watson-Munro, Phys. Fluids 6, 925 (1963).
4. Alan W. DeSilva, Experimental Study of Hydromagnetic Waves in Plasma (Ph. D. Thesis), UCRL-9601, March 17, 1961.

of axial symmetry and monochromatic time dependence (i.e., $\partial/\partial\theta = 0$ and $\partial/\partial t = -i\omega$). The four equations can be combined into one equation in which the only dependent variable is $\underline{E}$ (a vector with three complex components) and in which the two independent variables are the cylindrical coordinates r and z. This is a complex elliptic partial differential equation.

Such an equation can be solved by various matrix iteration methods,[5] which begin with the construction of a grid system in the r-z plane and the approximation of the spatial derivatives by difference equations, with use of physically realistic boundary conditions. In effect, with a grid system of about 1000 mesh points, the problem is reduced to the solution of a system of about 6000 simultaneous linear equations. With mathematical advice from the Berkeley and Stanford computer centers, it was decided to solve this system by the line block over-relaxation method, which is a well-understood iteration technique providing the most rapid rate of convergence to a solution by successive approximations.

The first attempt to solve this system revealed a computational instability, in which a pattern of standing waves appeared that was amplified by each iteration. It has been discovered that the condition of charge neutrality may be imposed to suppress the instability. Charge neutrality can be deduced from Eq. (3) with no further assumptions, thus making possible the simplification $\nabla \times (\nabla \times \underline{E}) = -\nabla^2 \underline{E}$. This modification of the model is now being made. After agreement with the analytic theory is established with use of uniform conditions, the input parameters $\underline{B}_0$, n, and electron temperature will be altered to simulate actual experimental conditions.

D. Steepening of Large-Amplitude Alfvén Waves

Peter R. Forman and Forrest I. Boley

For frequencies far below particle resonances the hydromagnetic waves induced in cylindrical geometry by an oscillatory radial electric field are mainly torsional, and propagate along a constant axial magnetic field B_0 with the azimuthal wave magnetic field component b_θ dominant. Such waves, with amplitudes ($|b_\theta|/B_0$) $\ll 1$, propagate undistorted at very nearly the Alfvén velocity $V_A = B_0/(4\pi\rho)^{1/2}$, where ρ is the plasma mass density.

In this experiment, the wave amplitudes $|b_\theta|$ are as large as 0.6 B_0. To a good approximation, waves of such amplitude must satisfy the requirement

$$(B_0^2 + b_\theta^2)^{1/2}/\rho = \text{constant},$$

because of the plasma compressibility. To satisfy this requirement, the phase velocity $a^2 = dP/d\rho$ becomes

$$a^2 = \frac{B_0^2 + b_\theta^2}{4\pi\rho} .$$

5. R. S. Varga, Matrix Iterative Analysis (Prentice-Hall, Inc., Englewood Cliffs, N. J., 1962).

Thus when b_θ^2 is not small compared with B_0^2, the phase velocity depends upon b_θ because of the dependence of the magnetic pressure P upon the total magnetic field.

An initially sinusoidal wave field $b_\theta = |b_\theta| \exp[i(\omega t - k_0 z)]$ induced at $z = 0$ is increasingly distorted during propagation as points of larger b_θ overtake the lower portions of the wave. Steepening of the leading slopes results. Writing δ as the ratio of the slope of the steepened wave front to the corresponding slope of the unsteepened wave at $z = 0$, i.e., $\delta \equiv (\partial b_\theta/\partial t)/(\partial b_\theta/\partial t)_{z=0}$, then after propagation over a distance z one has

$$\delta = \left\{1 - \frac{zk_0}{2} \Big/ \left[1 + \left(\frac{B_0}{b_\theta}\right)^2\right]\right\}^{-1} ,$$

neglecting collisions. To compare this result with experiment, δ is measured as a function of b_θ/B_0.

These steepened waves have been observed with use of the Hothouse I device. The experimental arrangement for these observations is shown in Fig. IV-4. The plasma is prepared by propagation of an ionizing front as previously described.[6] For the experiments discussed here the device was operated with an axial magnetic field $B_0 = 8$ kG, an initial hydrogen pressure of 0.10 torr, and an ion density of approximately 4×10^{15} cm^{-3}. The large-amplitude waves are induced by discharge of the 1-μF 100-kV capacitor shown in Fig. IV-4. A 430-kc damped oscillation is produced thereby.

Wave magnetic fields are measured by using 2.4mm-diameter eight-turn calibrated pickup loops placed within 6 mm o.d. quartz tubes that are inserted longitudinally into the plasma. Such coils are placed at z = 10 cm and 30 cm at the radial position of maximum b_θ field. The voltage output and its time integral from these coils are used to determine $\partial b_\theta/\partial t$ and b_θ. Wave amplitudes ranging from about 500 G to 5000 G were produced with constant shape by varying the voltage to which the capacitor was charged.

Figure IV-5 is a plot of $(\partial b_\theta/\partial t)/b_\theta$ determined during the first quarter cycle of the propagated wave at $z = 10$ cm as a function of b_θ/B_0. In this plot b_θ is the wave amplitude at $z = 0$ determined with the aid of the measured attenuation of low-amplitude waves at $z = 10$ cm and 30 cm. Also shown in Fig. IV-5 is the corresponding steepening calculated from the collisionless theory and normalized to the lowest wave-amplitude value of $(\partial b_\theta/\partial t)/b_\theta$.

The steepening at $z = 10$ cm is quite close to that predicted from collisionless theory. However, additional measurements indicate that the steepening does not continue to increase at larger values of z, as expected from the expression for δ given above. For the largest wave amplitudes ($|b_\theta| \approx 5$ kG) the maximum value of $(\partial b_\theta/\partial t)/b_\theta$ is 5.0×10^6, and occurs at $z = 20$ cm. This value is 2.4 times the low-amplitude limit of this ratio.

6. William S. Cooper, Alan W. DeSilva, and John M. Wilcox, in Controlled Thermonuclear Research Quarterly Report, UCRL-9243, June 29, 1960, p. 78.

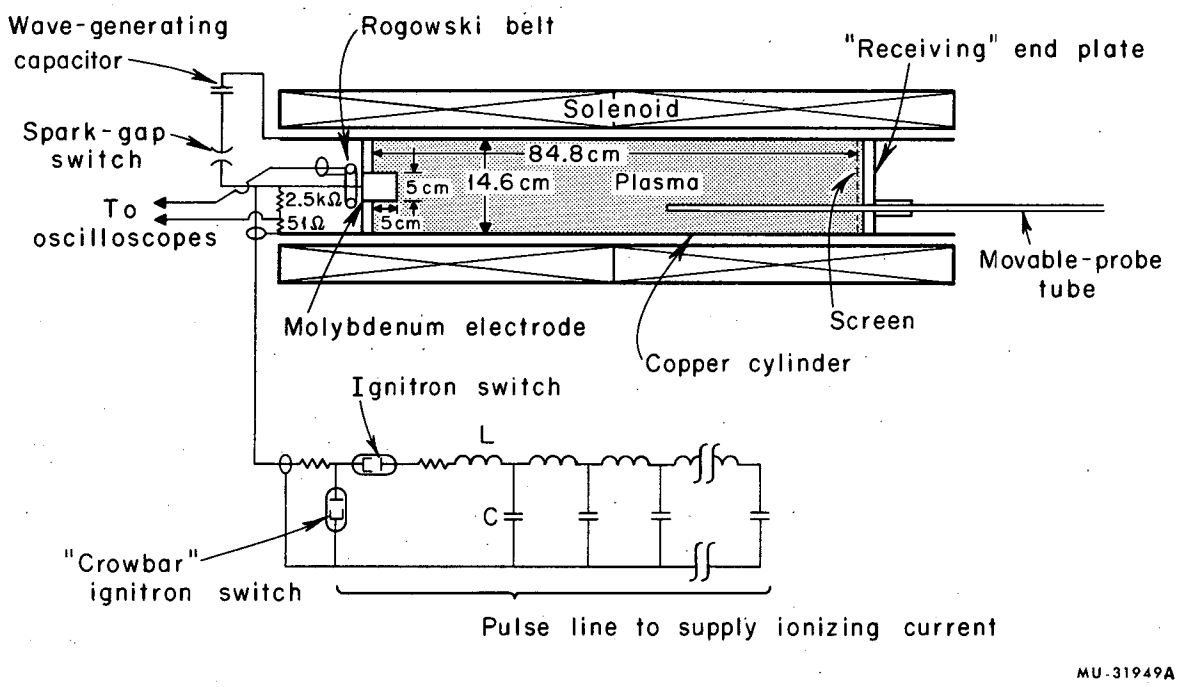

Fig. IV-4. Experimental arrangement.

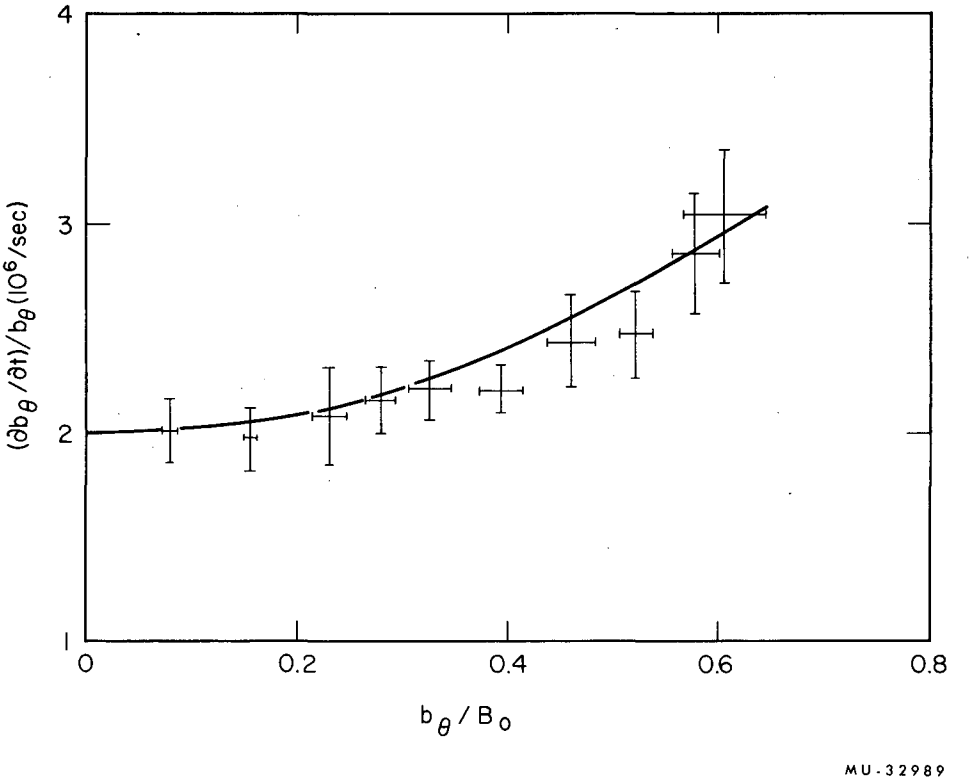

Fig. IV-5. Comparison of experimental values of $(\partial b_\theta/\partial t)/b_\theta$ at $z = 10$ cm with the corresponding results calculated from collisionless theory. The bars represent the rms deviations of the data. The solid curve representing the theory is normalized to the lowest wave-amplitude value of $(\partial b_\theta/\partial t)/b_\theta$.

3. HYDROMAGNETIC IONIZING FRONTS

Arthur R. Sherwood and Wulf B. Kunkel

As has been reported,[1] photographs of the luminosity pattern of the discharge and the signals from current buttons in the outer electrode of our annular system indicate that the apparatus is not producing the azimuthally symmetric ionizing fronts that we wish to study. Instead we observe spokes which "corkscrew" down the tube. In an attempt to promote an azimuthally uniform initial breakdown of the working gas, a radio-frequency oscillator was constructed and installed as a preionizer so that one could establish an rf discharge in the gas prior to the main discharge in the vicinity of its initial occurrence. This oscillator operated at a frequency of about 30 Mc and a power level of around 300 W, and it was coupled capacitively through the discharge region to the outer electrode. Although the use of the rf discharge had an observable effect on the main discharge, it did not help the production of uniform ionizing fronts.

Preliminary results with argon instead of hydrogen as the working gas are more encouraging. For example, with argon at a pressure of 0.015 torr, an axial magnetic field of 16 kG, a drive current of 20 kA, and without the use of the rf discharge, the luminosity pattern shows multiple spoking at first, which smooths into an azimuthally symmetric pattern in a few microseconds.

1. Arthur R. Sherwood and Wulf B. Kunkel, in Controlled Thermonuclear Research Semiannual Report, UCRL-10852, July 22, 1963, p. 85.

C. Computer Model of Ion Cyclotron Resonance Experiment

Gordon W. Hamilton

The measurements of amplitudes and phases of ion cyclotron waves that have been previously reported[2, 3] are susceptible of various interpretations because of the possible excitation of both the torsional and compressional modes. In order to resolve this ambiguity and also to provide an improved theoretical model for wave propagation in nonuniform conditions, a numerical analysis has been undertaken, using a realistic computer model simulating the geometry and plasma conditions of the Hothouse II experiment.

In order to make contact with the analytic theory[4] the computer model is based upon the same set of magnetohydrodynamic equations as has been solved analytically with the assumption of uniform magnetic field and plasma density and temperature. These equations are basically the macroscopic equation of motion, the generalized Ohm's law, and two linearized Maxwell's equations

$$nm \frac{\partial \underline{v}}{\partial t} = \underline{j} \times \underline{B}_0 , \tag{1}$$

$$\underline{E} + \underline{v} \times B_0 = \underline{\underline{\eta}} \cdot \underline{j} + \frac{1}{en} \underline{j} \times \underline{B}_0 , \tag{2}$$

$$\nabla \times \underline{b} = \mu_0 \underline{j} , \tag{3}$$

$$\nabla \times \underline{E} = - \frac{\partial}{\partial t} \underline{b} . \tag{4}$$

This set of four equations involves four unknown dependent variables associated with the ion cyclotron waves: $\underline{E}$, the wave electric field; $\underline{b}$, the wave magnetic field; $\underline{v}$, the macroscopic plasma velocity; and $\underline{j}$, the current density. The known functions of position are $\underline{B}_0$, the external magnetic field; n, the ion density; and $\underline{\underline{\eta}}$, the resistivity tensor. The remaining symbols are constant (m, the ion mass; e, the ion charge; and $\mu_0 = 4\pi \times 10^{-7}$ Henry/meter).

The approximations on which these equations are based are described in Ref. 4 and are valid for this experiment. We make the further assumptions

2. Forrest I. Boley, Alan W. DeSilva, Peter R. Forman, and Gordon W. Hamilton, in Controlled Thermonuclear Research Semiannual Report, UCRL-10294, July 20, 1962, p. 45.
3. Forrest I. Boley, John M. Wilcox, Alan W. DeSilva, Peter R. Forman, Gordon W. Hamilton, and C. N. Watson-Munro, Phys. Fluids 6, 925 (1963).
4. Alan W. DeSilva, Experimental Study of Hydromagnetic Waves in Plasma (Ph. D. Thesis), UCRL-9601, March 17, 1961.

of axial symmetry and monochromatic time dependence (i.e., $\partial/\partial\theta = 0$ and $\partial/\partial t = -i\omega$). The four equations can be combined into one equation in which the only dependent variable is $\underline{E}$ (a vector with three complex components) and in which the two independent variables are the cylindrical coordinates r and z. This is a complex elliptic partial differential equation.

Such an equation can be solved by various matrix iteration methods,[5] which begin with the construction of a grid system in the r-z plane and the approximation of the spatial derivatives by difference equations, with use of physically realistic boundary conditions. In effect, with a grid system of about 1000 mesh points, the problem is reduced to the solution of a system of about 6000 simultaneous linear equations. With mathematical advice from the Berkeley and Stanford computer centers, it was decided to solve this system by the line block over-relaxation method, which is a well-understood iteration technique providing the most rapid rate of convergence to a solution by successive approximations.

The first attempt to solve this system revealed a computational instability, in which a pattern of standing waves appeared that was amplified by each iteration. It has been discovered that the condition of charge neutrality may be imposed to suppress the instability. Charge neutrality can be deduced from Eq. (3) with no further assumptions, thus making possible the simplification $\nabla \times (\nabla \times \underline{E}) = -\nabla^2 \underline{E}$. This modification of the model is now being made. After agreement with the analytic theory is established with use of uniform conditions, the input parameters $\underline{B}_0$, n, and electron temperature will be altered to simulate actual experimental conditions.

D. Steepening of Large-Amplitude Alfvén Waves

Peter R. Forman and Forrest I. Boley

For frequencies far below particle resonances the hydromagnetic waves induced in cylindrical geometry by an oscillatory radial electric field are mainly torsional, and propagate along a constant axial magnetic field B_0 with the azimuthal wave magnetic field component b_θ dominant. Such waves, with amplitudes ($|b_\theta|/B_0$) $\ll 1$, propagate undistorted at very nearly the Alfvén velocity $V_A = B_0/(4\pi\rho)^{1/2}$, where ρ is the plasma mass density.

In this experiment, the wave amplitudes $|b_\theta|$ are as large as 0.6 B_0. To a good approximation, waves of such amplitude must satisfy the requirement

$$(B_0^2 + b_\theta^2)^{1/2}/\rho = \text{constant},$$

because of the plasma compressibility. To satisfy this requirement, the phase velocity $a^2 = dP/d\rho$ becomes

$$a^2 = \frac{B_0^2 + b_\theta^2}{4\pi\rho} .$$

5. R. S. Varga, Matrix Iterative Analysis (Prentice-Hall, Inc., Englewood Cliffs, N. J., 1962).

Thus when b_θ^2 is not small compared with B_0^2, the phase velocity depends upon b_θ because of the dependence of the magnetic pressure P upon the total magnetic field.

An initially sinusoidal wave field $b_\theta = |b_\theta| \exp[i(\omega t - k_0 z)]$ induced at $z = 0$ is increasingly distorted during propagation as points of larger b_θ overtake the lower portions of the wave. Steepening of the leading slopes results. Writing δ as the ratio of the slope of the steepened wave front to the corresponding slope of the unsteepened wave at $z = 0$, i.e., $\delta \equiv (\partial b_\theta/\partial t)/(\partial b_\theta/\partial t)_{z=0}$, then after propagation over a distance z one has

$$\delta = \left\{1 - \frac{zk_0}{2} \Big/ \left[1 + \left(\frac{B_0}{b_\theta}\right)^2\right]\right\}^{-1} ,$$

neglecting collisions. To compare this result with experiment, δ is measured as a function of b_θ/B_0.

These steepened waves have been observed with use of the Hothouse I device. The experimental arrangement for these observations is shown in Fig. IV-4. The plasma is prepared by propagation of an ionizing front as previously described.[6] For the experiments discussed here the device was operated with an axial magnetic field $B_0 = 8$ kG, an initial hydrogen pressure of 0.10 torr, and an ion density of approximately 4×10^{15} cm^{-3}. The large-amplitude waves are induced by discharge of the 1-μF 100-kV capacitor shown in Fig. IV-4. A 430-kc damped oscillation is produced thereby.

Wave magnetic fields are measured by using 2.4mm-diameter eight-turn calibrated pickup loops placed within 6 mm o.d. quartz tubes that are inserted longitudinally into the plasma. Such coils are placed at $z = 10$ cm and 30 cm at the radial position of maximum b_θ field. The voltage output and its time integral from these coils are used to determine $\partial b_\theta/\partial t$ and b_θ. Wave amplitudes ranging from about 500 G to 5000 G were produced with constant shape by varying the voltage to which the capacitor was charged.

Figure IV-5 is a plot of $(\partial b_\theta/\partial t)/b_\theta$ determined during the first quarter cycle of the propagated wave at $z = 10$ cm as a function of b_θ/B_0. In this plot b_θ is the wave amplitude at $z = 0$ determined with the aid of the measured attenuation of low-amplitude waves at $z = 10$ cm and 30 cm. Also shown in Fig. IV-5 is the corresponding steepening calculated from the collisionless theory and normalized to the lowest wave-amplitude value of $(\partial b_\theta/\partial t)/b_\theta$.

The steepening at $z = 10$ cm is quite close to that predicted from collisionless theory. However, additional measurements indicate that the steepening does not continue to increase at larger values of z, as expected from the expression for δ given above. For the largest wave amplitudes ($|b_\theta| \approx 5$ kG) the maximum value of $(\partial b_\theta/\partial t)/b_\theta$ is 5.0×10^6, and occurs at $z = 20$ cm. This value is 2.4 times the low-amplitude limit of this ratio.

6. William S. Cooper, Alan W. DeSilva, and John M. Wilcox, in Controlled Thermonuclear Research Quarterly Report, UCRL-9243, June 29, 1960, p. 78.

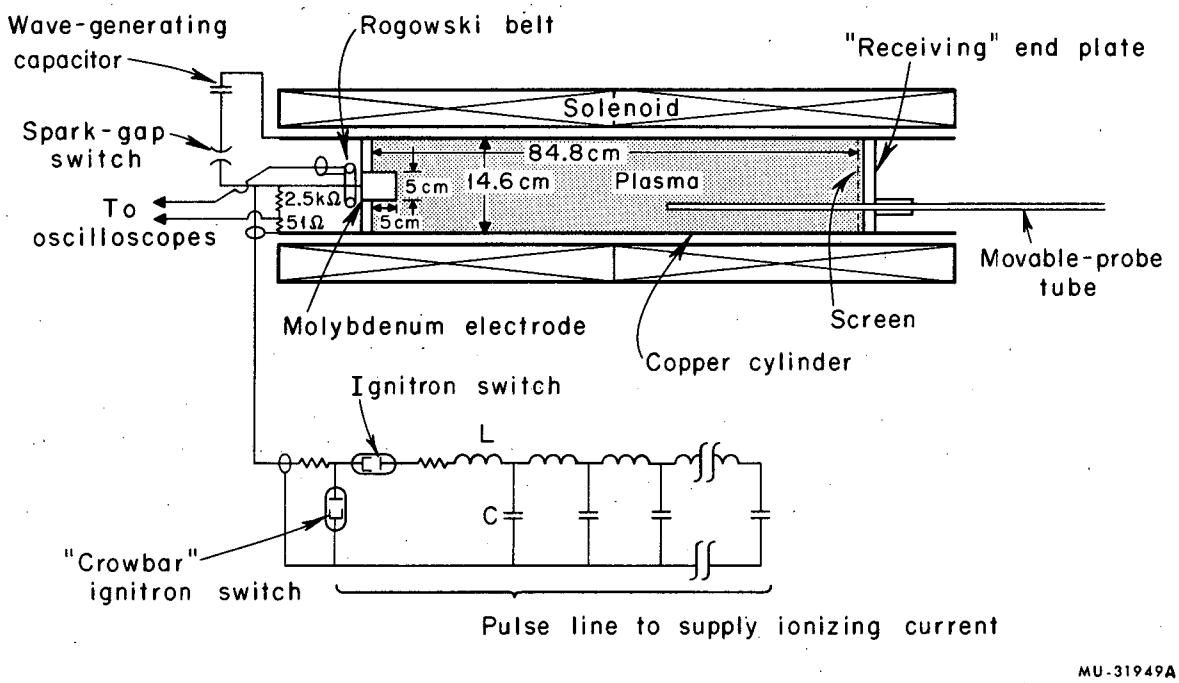

Fig. IV-4. Experimental arrangement.

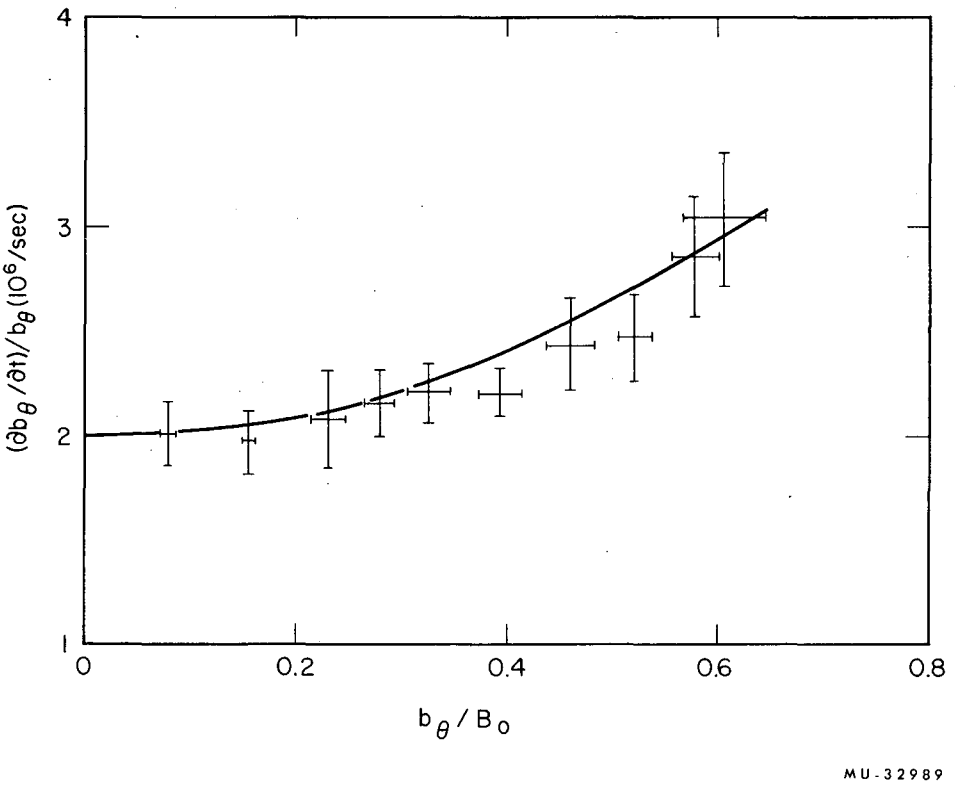

Fig. IV-5. Comparison of experimental values of $(\partial b_\theta/\partial t)/b_\theta$ at $z = 10$ cm with the corresponding results calculated from collisionless theory. The bars represent the rms deviations of the data. The solid curve representing the theory is normalized to the lowest wave-amplitude value of $(\partial b_\theta/\partial t)/b_\theta$.

3. HYDROMAGNETIC IONIZING FRONTS

Arthur R. Sherwood and Wulf B. Kunkel

As has been reported,[1] photographs of the luminosity pattern of the discharge and the signals from current buttons in the outer electrode of our annular system indicate that the apparatus is not producing the azimuthally symmetric ionizing fronts that we wish to study. Instead we observe spokes which "corkscrew" down the tube. In an attempt to promote an azimuthally uniform initial breakdown of the working gas, a radio-frequency oscillator was constructed and installed as a preionizer so that one could establish an rf discharge in the gas prior to the main discharge in the vicinity of its initial occurrence. This oscillator operated at a frequency of about 30 Mc and a power level of around 300 W, and it was coupled capacitively through the discharge region to the outer electrode. Although the use of the rf discharge had an observable effect on the main discharge, it did not help the production of uniform ionizing fronts.

Preliminary results with argon instead of hydrogen as the working gas are more encouraging. For example, with argon at a pressure of 0.015 torr, an axial magnetic field of 16 kG, a drive current of 20 kA, and without the use of the rf discharge, the luminosity pattern shows multiple spoking at first, which smooths into an azimuthally symmetric pattern in a few microseconds.

1. Arthur R. Sherwood and Wulf B. Kunkel, in Controlled Thermonuclear Research Semiannual Report, UCRL-10852, July 22, 1963, p. 85.

4. SHEET PINCH STUDIES

Oscar A. Anderson

The resistive instability study described in the preceding report[1] is now approaching completion. Optical diagnostics is finished and all the hardware for multiple-probe field-correlation measurements has been built and installed.

The previous report showed framing-camera photographs in which an initially uniform tubular pinch apparently breaks up into a number of filamentary pinches. Figure IV-6 in the current report helps to confirm this. In addition to the end-on views previously obtained, there are simultaneous views at angles of ± 10 deg from the tube axis. These show that the spots seen in the center view are indeed filaments extending from the top electrode to the bottom electrode. All the photographs in Fig. IV-6 were made on the same shot, at intervals of 0.3 μsec/frame. The first frame was exposed at pinch time, and the sixth frame near peak current. In this frame the current channels are disintegrating. The cathode fins, which were installed to reduce the flare effect,[2] are visible in the fifth and sixth frames.

Growth rates and wavelengths for the tearing mode in cylindrical geometry have been calculated by John Killeen.[3] He used the actual dimensions of the Triax tube and considered typical values for conductivity, mass density, and magnetic field. He finds good agreement with the experimental results, particularly for the fastest-growing wavelength.

Although the tearing mode in the small-amplitude limit behaves as predicted, it is not easy to understand its large-amplitude behavior. When the current channels into distinct filaments, one would expect an ordinary pinch instability to develop immediately. Framing photographs and preliminary probe measurements show that the secondary instability is indeed violent once it starts, with e-folding time considerably less than 0.1 μsec. But Fig. IV-6 shows that the onset is delayed by about 1.2 μsec. Even longer delays are found with other conditions.[1] Perhaps a nonlinear theoretical treatment is needed to explain this anomalous hydromagnetic stability.

H. A. B. Bodin has observed a similar stability for current rings caused by the tearing mode in the reversed-field θ pinch at Aldermaston.[4] His case is even more remarkable because of the higher temperature involved. In the θ pinch, unlike the Triax, there is a zero-order attraction of the current filaments to themselves, and in fact they coalesce before a secondary instability occurs.

1. Oscar A. Anderson, in Controlled Thermonuclear Research Semiannual Report, UCRL-10852, July 22, 1963, p. 88
2. Oscar A. Anderson, in Controlled Thermonuclear Research Semiannual Report, UCRL-10607, January 16, 1963, p. 69.
3. John Killeen, V.5 in this report.
4. H. A. B. Bodin, Resistive Instabilities in the Theta Pinch, paper E-11, APS Division of Plasma Physics Meeting, San Diego, California, November 6-9, 1963.

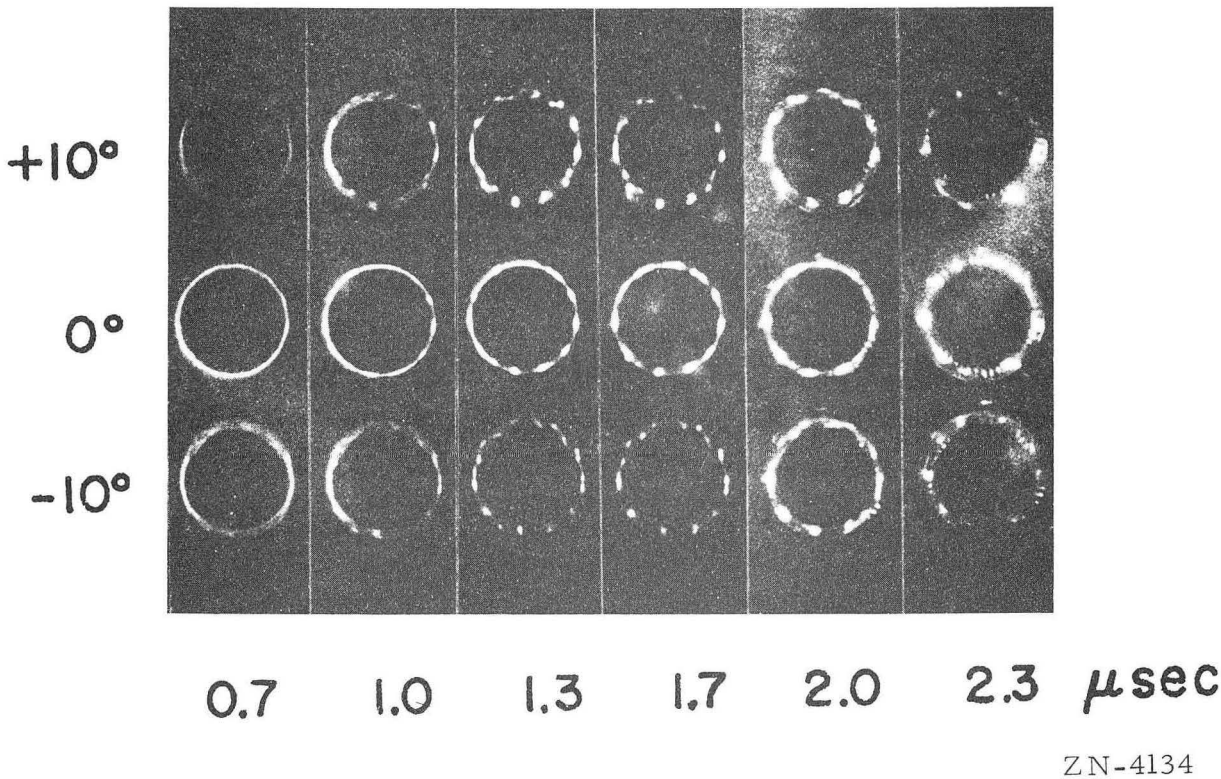

Fig. IV-6. Stereoscopic framing-camera photographs of Triax pinch, with helium at 125 μ Hg. Peak current: 1.5×10^6 A at 2.5 μsec.

The delayed onset of the secondary instability would be understandable if the current were channeled less strongly than the photographs seem to indicate. It is important to find how closely the light distribution as photographed in the Triax represents the actual current distribution. This is one purpose of the multiple-probe studies which will soon be under way.

5. GAS COLLISIONS AND DIFFUSIONS

Klaus H. Berkner, Vincent J. Honey, Robert V. Pyle,
J. Warren Stearns, and John C. Warren

A. Plasma Diffusion and Oscillations

1. Plasma diffusion across and along a magnetic field from a hollow cathode line source

Electron and ion density and temperature distributions in an argon plasma between an axial line source and a conducting cylindrical can 30 cm long and 20 cm in diameter have been reported previously.[1] This work has been extended to H_2 and He and to a longer container (67 cm).

(a) Radial density and temperature distributions

All the radial measurements are consistent with classical diffusion if the Zharenov or Tonks (f = 0) model is used. Anomalies in the electron temperature distributions are still observed.

(b) Axial distributions

Density distributions similar to those reported in Ref. 1 have been observed again in the longer geometry, namely the density is cosinusoidal over an extrapolated length equal to the actual chamber length plus perhaps 3/2 of a transport mean free path for the ions. For example, the experimental extrapolated length is 72 cm with argon at 10^{-3} torr. This result is again in agreement with the assumed classical diffusion model, but not in agreement with measurements under rather similar conditions at other laboratories.

2. Oscillations in the plasma external to the hollow cathode line source

Strong oscillations and harmonics in the tens-of-kilocycles range have been documented previously as a function of gas pressure, magnetic field, arc current, position, and distance between electrodes. These oscillations showed some of the properties expected of longitudinal standing ion sound waves. However, the frequency variation with electrode spacing was

1. Klaus H. Berkner, Robert V. Pyle, J. Warren Stearns, and Joseph Winocur, "Diffusion from a Line Source in a Magnetic Field," UCRL-10801, June 20, 1963 and Proceedings of the VIth International Conference on Ionization Phenomena in Gases, Paris, July 8-13, 1963, to be published.

not quantitatively correct and no amplitude variations were observed in the axial direction. Lashinsky[2] has reported that rather similar oscillations observed in a "Q device" with cesium plasma may be in agreement with a recent universal instability analysis by Silin[3] for waves propagating perpendicular to B. If the discharge chamber is long compared with the radius, $T_e >> T_i$, and other assumptions are fulfilled, then Silin finds that oscillations in phase along the axis have frequencies given by

$$\int_{r_1}^{r_2} \frac{dr}{r_{bi}} \left[\frac{kT}{\omega} \frac{\ell c}{B|e|} \frac{1}{r} \frac{d}{dr} \ell n N - 1 \right]^{1/2} = n\pi ,$$

where r_1 and r_2 define the radial limits of transparency, r_{bi} is the ion cyclotron radius, N is the density, ℓ an azimuthal quantum number, and n a radial quantum number. The electron temperature has been assumed constant throughout the plasma, which is not true in our case.

The fundamental and harmonic frequency spectra observed in our plasma are sometimes similar to that shown in Fig. 2 of Ref. 2, and are in reasonable agreement with the predictions of the above equation if plausible but nonunique assumptions about the constants are made. The rotation and B dependence also are in qualitative agreement with the universal instability analysis. However, it will be necessary to include temperature gradients, finite length, and incomplete ionization before a quantitative comparison is possible.

Segmented electrodes have been installed in the discharge apparatus to permit an investigation of the effects of boundary conditions on the oscillations and on diffusion.

3. Positive column in a magnetic field

A formal application of the Kadomtsev-Nedospasov dc instability theory to an ac plasma column predicts critical magnetic fields, B_c, in agreement with experiment,[4] and also predicts that the first mode to grow may be $m > 1$ rather than $m = 1$ as in the dc case. Streak-camera photographs did not contradict the latter idea, but individual modes could not be identified. More recently we have attempted to investigate the instability modes by a harmonic analysis of the probe and photomultiplier signals. With conditions for which the fastest growing mode is, for example, $m = 3$ we have been able to conclude only that a large number of high-frequency modes are present immediately above B_c.

2. H. Lashinsky, Universal Instability in a Fully Ionized Inhomogeneous Plasma, MATT-234, Dec. 1963.
3. V. P. Silin, Sov. Phys. JETP 17, 857 (1963).
4. Henry F. Rugge and Robert V. Pyle, Instability of an Alternating-Current Positive Column in a Magnetic Field, UCRL-10698 Rev., Oct. 1963.

The spectrum analyzer does permit us to estimate how far above the critical magnetic field, B_c, it is necessary to go before measurements in a dc column can be compared with the Kadomtsev "turbulence" theory.[5] We have previously noted that streak-camera and photomultiplier traces become hashy at fields perhaps 10% above the critical magnetic field, indicating the onset of several higher modes. In a typical case--e.g., argon at 0.2 torr in a 2.75 cm radius tube--the mean axial electric field rises rapidly up to $B \approx 2\ B_c$, and then continues to rise slowly up to our maximum field measurements of $B \approx 7\ B_c$. The frequency analysis shows that the fundamental ($m = 1$) mode is the dominant signal up to $B \approx 2\ B_c$, above which point no single line stands out above the hash. Approximately $2\ B_c$ is therefore the lowest field at which "turbulence" measurements should be made in this case.

B. Cross Sections

Measurements of the cross sections for exciting fast neutral hydrogen atoms in nonionizing collisions with neutral hydrogen molecules have been reported.[6] These measurements have now been extended to nonionizing collisions with the charged particles of a plasma. Measurements were made with the target neutral or ionized on alternate accelerator beam pulses so that the minimum error would be introduced in the comparison of charged and neutral targets. A preliminary analysis of the data shows, for example, that $\sigma_{6,7}$ is about 500 times as great for a charged as for a neutral target, in reasonable agreement with current theoretical expectations. Similar techniques have been used to obtain H_2^+ breakup cross sections and the excited-state distributions of the resulting neutral hydrogen atoms in H_2, He, N_2, and Ar. Small differences were observed between results from neutral or ionized targets.

---

5. B. B. Kadomtsev, Zh. Tekhn. Fiz. 31, 1273 (1961).
6. Klaus H. Berkner, John R. Hiskes, Selig N. Kaplan, George A. Paulikas, and Robert V. Pyle, The Excitation and Lorentz Ionization of 10-MeV Hydrogen Atoms, UCRL-10802, June 19, 1963, and Proceedings of Third International Conference on the Physics of Electronic and Atomic Collisions, London, July 22-26, 1963, to be published.

6. THEORETICAL STUDIES

A. On Finite Gyration Radius Effects in Hydromagnetics

Alan Macmahon

Finite gyration radius corrections (to second order in gyration radius) to the hydromagnetic equations have been found for an arbitrary configuration. The perpendicular electric field is allowed to be of zero order. The simple hydromagnetic equations must be modified in three ways: inclusion of the first-order terms (collisionless viscosity) of the pressure tensor in the momentum equation, inclusion of the Hall term and zero-order pressure effects in Ohm's law, and first-order corrections (heat flow and kinematical effects) to the adiabatic equations of state of Chew, Goldberger, and Low.[1] The transverse and parallel thermal energies [$P_{xx} + P_{yy}$ and P_{zz} if $\underline{B}(\underline{r}) = B(\underline{r})\underline{z}(\underline{r})$] are found from the equations of state, while the remaining components of the pressure tensor ($P_{xx} - P_{yy}$, P_{xy}, P_{xz}, P_{yz}) and the transverse heat flows are given by Thompson.[2] (Thompson's P_{xz} and P_{yz} are incorrect, however.) The heat flow parallel to the magnetic field is not determined. For the special case of a uniform, constant magnetic field and density and the absence of gradients along the magnetic field, these equations reduce to those used by Roberts and Taylor[3] in discussing the gravitational instability.

Thompson's[2] calculation of the pressure tensor and heat flow is based on the solution of the Vlasov equation in inverse powers of magnetic field strength.[1] It has been observed that if this expansion converges then the distribution function is uniquely determined to any order for all time if the ϕ-independent part of the distribution function is given to the same order at an initial time (ϕ is the azimuthal angle of the velocity about the local magnetic field direction). In particular the ϕ dependence of the initial distribution function cannot be chosen independently of the dependence on the other variables. The physical reason for this constraint is that the distribution function performs a nonrigid rotation in velocity space at the cyclotron frequency. For the expansion to converge this rotation must not produce fluctuation at the cyclotron frequency in the time dependence of the distribution function.

---

1. Chew, Goldberger, and Low, Proc. Roy. Soc. (London), A236, 112 (1956).
2. W. B. Thompson, Rept. Progr. Phys. 24, 363 (1961).
3. K. V. Roberts and J. B. Taylor, Phys. Rev. Letters 8, 197 (1962).

B. Stability of a Charged Plasma in Magnetic Field

John C. Price

The stability of the sheath formed by a plasma with a magnetic field in contact with an electrode was considered. The problem was simplified to an unbounded charged (nonneutral) plasma with charges not permitted to escape along the magnetic field lines. The resulting shear in the E x B drift of the charges was shown to be unstable to small perturbations. A dispersion relation was obtained by integrating effects of perturbed fields along the unperturbed orbits of the particle.

For a nearly neutral plasma ($n^+ \approx n^-$) there are two growing modes occurring at the upper and lower hybrid frequencies with growth rates $(\omega_{pe}^2/\omega_{ce}^2)\,(2\pi e^2|n^+ - n^-|)/m_e\omega_{ce}$ and $(2\pi e^2|n^+ - n^-|)/m_e\omega_{ce}$ respectively. If we consider a possible anode sheath consisting entirely of electrons, the growing mode occurs at ω_{ce}, with maximum growth rate $\frac{1}{2}\,\omega_{pe}^2/\omega_{ce}$.

C. Collisional Effects on Ion-Cyclotron Waves

David L. Sachs

Thermal and collisional effects on transverse electromagnetic waves in a magnetoplasma are studied, with use of the IBM 7094 to determine the existence and importance of poles and branch cuts of the integral

$$E(z,t) = -\frac{ie^{-i\omega t}}{\pi}\int_{-\infty}^{\infty}\frac{KdKe^{iKz}}{K^2 - \frac{\omega^2}{c^2}n^2(K,\omega)}\,,\quad (\text{for } z \geq 0)\,,$$

where n^2, the dielectric function of the plasma, is determined from the Vlasov equation plus phenomenological collision terms for both ions and electrons.

V. THEORETICAL AND BASIC EXPERIMENTAL PLASMA PHYSICS

1. COMPUTATIONAL STUDY OF ELECTRON INJECTION IN THE ASTRON DEVICE

V. Kelvin Neil and Warren Heckrotte

Further numerical investigation of the injection mechanism in Astron has been carried out. The initial results of this program were described in a previous progress report.[1] Since this work is currently being prepared for publication, no detailed presentation is made here. Attention has centered on the initial bunching of electrons injected into the resistor region. The present code simulates the injection of 150 A of 5-MeV electrons with velocity components $v_\theta \approx c$ and $v_z = 0.05\ c$, where c is the speed of light. The initial azimuthal surface current density is thus 15 A/cm.

Two values for the conductivity of the resistive layer have been used. The lower value corresponds to the "focusing" resistors described by Christofilos.[2] With this lower value there is an initial bunching as the electrons at the front of the bunch slow down and those subsequently injected overtake them. In this early stage a maximum surface current density of about 40 A/cm is obtained. But then, as the first electrons continue to slow down, the later-injected ones pass through them, and a doubly peaked distribution results. The average velocity decreases to a value of 0.04 c as the front of the bunch approaches the mirror region 200 cm from the injector. The maximum current density has decreased to 32 A/cm at this time, and the spread in axial velocity is of the order of 0.2 c.

The higher value of the conductivity corresponds to the "slowing down" resistors in Ref. 2. With this value in the code, the surface current density reaches a somewhat higher value, around 55 A/cm, but this is again short-lived. The maximum density is about 35 A/cm when the particles enter the mirror region. The average axial velocity is reduced to 0.03 c in this case, and the spread is somewhat less.

An attempt was made to increase the bunching by allowing the electrons to pass through a region of increasing axial magnetic field. This inverse mirror caused no significant increase in bunching. In fact, the two-humped distribution appeared earlier because many particles were actually reflected.

Bunching sufficient to yield a surface current density of about 100 A/cm was anticipated in Ref. 2. The basis for this was the assumption that the bunching occurs adiabatically, thus the area occupied in z-v_z phase space remains constant. Our work demonstrates that this is not correct. If the current density is reduced by a factor of 3 from the value used in Ref. 2, the fraction of total energy lost by the particles in traversing the mirror region is considerably below the predicted 10%. The relationship between the trapping efficiency of this injection system and the energy absorbed by the resistors has not been established. The answer to this question is being sought.

1. Warren Heckrotte and V. Kelvin Neil, in Controlled Thermonuclear Research Semiannual Report, UCRL-10852, July 1963, p. 100.
2. N. Christofilos, Astron Electron Injection, UCRL-5617-T, June 1959.

2. A COMPUTATION FOR STUDYING THE FORMATION OF THE ASTRON E LAYER

John Killeen

During the past six months the LARC code called LAYER has been revised considerably. The mathematical model of the E layer has not been changed, but the difference methods used to solve the equations have been modified. The Vlasov equations for the E layer are solved numerically in a four-dimensional phase space (r, z, u_r, u_z). The difference equation for the electron distribution function had to be changed because the old one introduced an artificial diffusion of particles inward, which was quite unrealistic. The new difference equation is completely centered in space, velocity, and time at each point in phase space. This means carrying data at two previous time steps; however, by proper use of the LARC drums this is accomplished with no increase in computation time. The new equations have been in use now for the past 3 months and appear to be working correctly. No unrealistic inward diffusion spoils the calculations. Electrons of 5 MeV energy are injected into a given mirror field. They are trapped in this field and form an E layer. In the most recent calculations the difference mesh consists of 62 370 points--21 in the z coordinate, 10 in the radial coordinate, 33 in u_z, and 9 in u_r. At each time step an integration over velocities is carried out to compute the current density, and the field due to this current is added to the vacuum field. A time step of the order 10^{-10} sec or smaller must be used in order that the calculation be stable, which means that many steps are required for substantial buildup of the current. Several test runs have been made with the injection current increased considerably in order to get a substantial effect. In these cases a self-consistent distribution of electrons was obtained with a reversed field. We are planning to refine the mesh further and to make further modifications in the equations to improve accuracy.

3. INVESTIGATION OF CERTAIN MINIMUM-B FIELDS

Cornelius H. Woods and Terry Kammash*

We have examined several magnetic field configurations having the "minimum-B" property with the ultimate objective of investigating microinstabilities, which may exist in such systems. Particular attention has been given to the stuffed cusp,

$$\vec{B}_1 = \frac{B_c}{\sqrt{2}} \left[-\frac{r}{r_c}\,\vec{i}_1 + \frac{r_c}{r}\,\vec{i}_2 + \frac{2z}{r_c}\,\vec{i}_3 \right],$$

and to a special (but to any desired degree realizable) field,

$$\vec{B}_2 = \frac{B_c}{2} \left[-\left(\frac{r}{r_c} + \frac{r_c}{r} \right) \vec{i}_1 + \frac{2z}{r_c}\,\vec{i}_3 \right].$$

---

*Department of Nuclear Engineering, University of Michigan, Ann Arbor, Michigan.

For both these fields the minimum value of B is B_c, and occurs at $r = r_c$, $z = 0$. That particle motion tends to be adiabatic in minimum-B fields if the adiabatic parameter $pc/eB_c r_c$ is not too large suggests that for fields such as $\vec{B}_1$ and $\vec{B}_2$, having relatively simple analytic form, one may be able to express the orbits in suitable form for determining a perturbed distribution f_1. For these fields we have been able to determine the path of the guiding center in analytic form, but the unperturbed orbit itself turns out to be somewhat cumbersome to handle.

We have considered several equilibrium distribution functions, expressed in terms of the constants of motion, which lead to particle densities with maxima at the minimum-B point.

4. STABILITY OF LONGITUDINAL OSCILLATIONS IN A UNIFORM MAGNETIZED PLASMA WITH ANISOTROPIC VELOCITY DISTRIBUTION

Laurence S. Hall and Warren Heckrotte

We have considered the longitudinal oscillations of a uniform magnetized plasma in which the particles are allowed to have anisotropic distributions in velocity-space, corresponding to the two temperatures $T_\perp$ and $T_\parallel$ perpendicular and parallel to the magnetic field. It was shown that no instabilities can exist unless $T_\perp > T_\parallel$ for at least one of the species of plasma particles. An additional theorem, of use in surveying for possible unstable roots to the dispersion equation when $T_\perp > T_\parallel$, was also proved. A report of this title by these authors has been written describing the results (UCRL-7627, Dec. 9, 1963).

5. TIME-DEPENDENT RESISTIVE INSTABILITY CALCULATIONS OF A SHEET PINCH

John Killeen

The existence of resistive instabilities for the sheet pinch has recently been reported in some detail.[1] In that paper perturbations of the form

$$f_1(y) \exp[\, i(k_x x + k_z z) + \omega t \,]$$

are assumed. The problem is then to solve an eigenvalue problem for ω, the growth rate of the instability. If instead we assume

$$f_1(y,t) \exp[\, i(k_x x + k_z z) \,],$$

then the problem becomes an initial-value problem for the perturbed quantities $f_1(y,t)$. A series of programs has been written to solve these equations. The first version, RIPPLE I, demonstrated the "tearing" mode. A second version, RIPPLE II, included resistivity gradients. Recently, two new programs have been brought into operation. RIPPLE III includes the first two programs, but also includes gravitational terms, and demonstrates all three of the basic modes described in FKR[1] as well as the mixed modes. Many cases have been run with this program and detailed comparison made with the analytic theory. The growth rates obtained for the rippling and

1. H. P. Furth, J. Killeen, and M. N. Rosenbluth, Phys. Fluids 6, 459 (1963).

tearing mode agree with the analytic theory. The gravitational modes have also been obtained, but the growth rates differ from the analytic theory. In general, they are higher. Detailed results and solutions will be presented in a separate report.

Another program solves the problem in cylindrical coordinates. It is called RIPPLE IV.

6. TIME-DEPENDENT RESISTIVE INSTABILITY CALCULATIONS IN CYLINDRICAL GEOMETRY

John Killeen

The hydromagnetic model that has been used[1] to study the resistive instabilities of a sheet pinch is applied in cylindrical geometry in order to study specific pinch and hard-core devices. The magnetohydrodynamic equations of an incompressible fluid are used with an isotropic resistivity. The plasma equilibrium configuration is assumed known. It is specified by $B_{\theta_0}(r)$, $B_{z_0}(r)$, and $\eta_0(r)$. These functions are chosen to describe a particular experiment. Perturbations of the form $f_1(r,t)\exp[i(m\theta+k_z z)]$ are used for all the plasma and field variables. A set of five partial differential equations for B_{r1}, $B_{\theta 1}$, v_{r1}, $v_{\theta 1}$, and η_1 are then obtained. The resulting initial-value problem is solved numerically by using an implicit difference method. The program is called RIPPLE IV. To start the calculation an initial perturbation--e.g., v_{r1}--is given. The boundary conditions correspond to either pinch or unpinch cases. In addition to the geometry and equilibrium, which are given from experiments, the parameters m, k_z, and $S = \tau_R/\tau_H$, the ratio of resistive diffusion time to hydromagnetic transit time, are used to specify a problem. In certain cases an exponential growth develops. From such cases a growth rate $p(m, k_z, S)$ is determined. Detailed results will be presented in a separate report.

7. THE COMPUTATION OF SELF-CONSISTENT POTENTIAL DISTRIBUTIONS IN A COLLISIONLESS PLASMA

Laurence S. Hall

The problem of obtaining the self-consistent potential distributions about an electrode in an infinite collisionless plasma in the absence of a magnetic field has been considered. In such a plasma, the charge density that appears on the right-hand side of Poisson's equation can be expressed as a complicated integral functional of the whole potential distribution and of the electron and ion velocity distributions at infinity. Because of the tendency of a plasma toward charge neutrality everywhere except in sheath regions near physical boundaries, however, subtraction problems make it exceedingly difficult to integrate the equations numerically in terms of the boundary condition at infinity. A technique has now been devised which allows one to obtain a self-consistent solution iteratively by a method based on an integral form of Poisson's equation, using the boundary condition at infinity. The method is especially useful in application to the theory of the electrostatic probe, as it avoids the alternative of introducing an artifical semiquantitative boundary condition at the sheath edge, and can

1. H. P. Furth, J. Killeen, and M. N. Rosenbluth, Phys. Fluids 6, 459 (1963).

be used to obtain a potential distribution and associated parameters, accurate to within about 5% of critical quantities, in less than 1 hour IBM 7094 computation time.

A report has been prepared describing the technique of the numerical solution.[1] Numerical work is now proceeding on a parametric study of cylindrical and spherical probes that, when completed in a year or two, should allow quantitative determination of plasma parameters from laboratory measurements of probe current-voltage characteristics.

8. MAGNETIC SHOCKS

S. A. Zwick and D. E. Gonzales

Numerical solutions for the equal-mass magnetic pulse problem have been attained for singly and doubly overlapped loop trajectories. Representative solutions for Mach 10 are shown in Fig. V-1 in terms of the reduced equal-mass displacements $\bar{x}/R$, $\bar{y}/R$, and the reduced magnetic field $b = B/B_0$.

The parametric relations connecting the Alfvén-Mach number a and the stress parameter σ for touching solutions of various orders are presently being calculated on the LARC computer.

Models for a plasma in which the electrons are treated adiabatically are being investigated.

9. MAGNETIC SUSCEPTIBILITY OF AN IMPERFECT GAS

Allan N. Kaufman and Toshio Soda

For a perfect gas of molecules, in thermal equilibrium at temperature Θ and density n, the magnetic permeability $\mu(n, \Theta)$ satisfies the Clausius-Mossotti formula

$$\frac{\mu - 1}{\mu + 2} = \frac{4\pi}{3} n a_1(\Theta) , \tag{1}$$

where $a_1(\Theta)$ is the effective magnetic polarizability of a single molecule, including both the paramagnetic and diamagnetic effects. The present work is a study of the effect of short-range molecular interaction, leading to a virial expansion

$$\frac{\mu - 1}{\mu + 2} = \frac{4\pi}{3} [n a_1(\Theta) + n^2 a_2(\Theta) + \cdots] , \tag{2}$$

where a_2 represents the correction due to two-molecule clusters.

1. Laurence S. Hall, The Computation of Self-Consistent Potential Distributionsin a Collisionless Plasma, UCRL-7660-T.

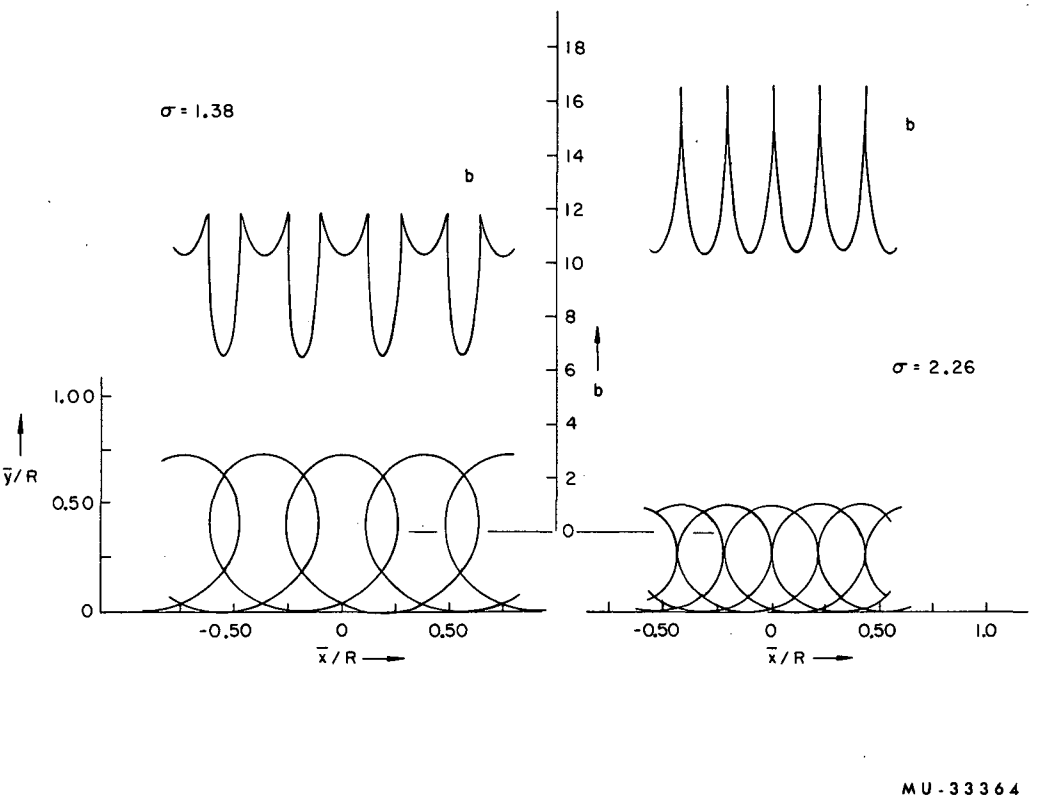

Fig. V-1. Single overlap solution (σ = 1.38) and second-order touching solution (σ = 2.26) with corresponding field ratios, b = B/B_0, for Mach 10.

The main problem of this study was the determination of an appropriate Hamiltonian for the molecular interaction. Inasmuch as magnetic effects are of order v^2/c^2 relative to the Coulomb interaction, a consideration of relativistic and radiative effects was necessary. The effective particle-interaction Hamiltonian has different forms, depending on the molecular separation. For separations $R \approx a_0$ (the molecular size), we use the Darwin Hamiltonian in its conventional form; for separations $a_0 < R < \lambda$ (where $\lambda \approx 137\, a_0$ is a typical atomic wave length), the Darwin Hamiltonian can be reduced to a magnetic dipole-dipole interaction, which falls off as R^{-3}, plus many other terms, proportional to R^{-1}, R^{-2}, and R^{-3}. These terms, which involve multipole moments other than the magnetic dipole, can be eliminated by a summation of graphs which is a generalization of the conventional gauge transformation, and by use of the Wigner-Eckart theorem for irreducible tensors of different rank and parity. Finally, for $R > \lambda$, the Darwin approximation is invalid, and an effective dipole-dipole interaction is obtained from quantum electrodynamics.

A paper on this work will be submitted to the Physical Review.

10. REARRANGEMENT COLLISIONS

Marvin H. Mittleman

The usual method for describing low-energy charge-transfer collisions is a pair of coupled equations. These have always obtained in an approximate form. The exact form has been derived.[1] The method has been applied to resonant charge transfer in the P + H system.[2] Since the starting equations are exact, one can make systematic approximations, thereby determining the errors. A new term is obtained of the same order in the expansion parameters as previously obtained terms, and it is shown that neglected terms are too small to account for the difference between this theory and an existing experiment. The method is being applied to more complicated systems in which the Pauli principle is of importance.

The reaction $P + H_2 \rightarrow H^- + 2P$ has been measured. The Born approximation for this cross section is almost finished. It shows crude agreement with the experiment. A more refined calculation is in progress.

11. BUMPY TORUS

Gordon Gibson,† Willard C. Jordan,‡ and Eugene J. Lauer

Tests of the injection apparatus were continued during this report period.

Additional Observations on the Discreteness in the Pattern of "Injected" Electrons

On the basis of the explanation given earlier[3] for the discrete circles,

1. Marvin H. Mittleman, Coupled Equations for Rearrangement Collisions, UCRL-7629, Dec. 1963, to Ann. Phys. to be published.
2. Marvin H. Mittleman, Resonant Charge Transfer in P + H, UCRL-7655-T, Jan. 1964, to be submitted to Phys. Rev.

† Westinghouse Electric Corporation, Atomic Power Division, Pittsburgh, Pa.
‡ The Bendix Corporation, Research Laboratories Division, Southfield, Mich.

3. Gordon Gibson, Willard C. Jordan, and Eugene J. Lauer, in Controlled Thermonuclear Research Semiannual Report, UCRL-10852, July 1963, 116-123.

it is predicted that the flux lines passing through a bright circle outside one mirror should pass through a dark region (between bright circles) outside the other mirror. This prediction was tested by simultaneously photographing the patterns outside the two injection coils. The points of intersection of a flux line with the two plates were established by using electrons from a small thermionic emitter. The result was that bright circles on the two sides seemed to be connected by common flux lines (this result could be established only for the most widely separated circles). This observation suggests that the guiding centers were distributed among a discrete set of drift paths--a most surprising result.

Millisecond Persistence of Signals after Switching off the Beam in the Injection Test

The containment of charged particles was searched for in the injection test using the technique which is planned with the complete torus. One torus coil on each side of the injection coil set was energized at from 1 to 3 times the design current. Steady injection of about 1 mA of 120-keV beam was used. (A modification to the anode structure has removed the previous voltage limitation.) After the beam was suddenly turned off ($\approx$ 0.2 msec turn-off time), low-energy electrons and ions were collected on metal plates outside the torus coils with a mean persistence time of about 5 msec when a base vacuum of about 10^{-5} mm Hg was used. When the base vacuum pressure was raised, the mean time became shorter, which would be consistent with the containment time's being limited by gas scattering. An x-ray detector, which is sensitive to the energetic particles and not to the ionization products, failed to show a signal that persisted after the beam was turned off. Probably the primary high-energy electrons hit the wall promptly; however, it is possible that some were contained for a measurable time, since parts of the wall are well shielded from the x-ray detector.

Torus Assembly and Test

The assembly of the torus was completed near the end of this report period. The apparatus that was used in the injection test has been incorporated. (This is the injection apparatus with injection coils having mean radii 1.5 times the mean radii of the torus coils.) The base ion gauge reading in the torus is about 5×10^{-6} torr (which is adequately low for the tests that are planned). The torus magnet has been run up to 800 A/turn (500 A/turn is about the maximum that can be used with the present injection apparatus because of "saturation" in the flux leader to the iron poles). Tests for particle confinement have been started.

12. ATOMIC SCATTERING AND CROSS-SECTION MEASUREMENTS

Gilbert O. Brink,* Edmund S. Chambers,
and Robert H. McFarland

Work has continued during this period toward the completion of moving the group into Building 180B. The electron crossed-beam machine has been moved and modified for providing a lower vacuum, and is presently undergoing final leak detection and elimination. A newly designed version of a combined pump and trap, "Puap," utilizing liquid-nitrogen-cooled zeolites, has been installed in the forepump section of the vacuum system. Extrapolation from our previous results as well as from comparable work of the Vacuum Engineering Laboratory predicts an improvement of pressure in this machine by an order of magnitude.

Two papers[1,2] prepared by this group have been accepted by The Physical Review for early publication and one[3] has been accepted by Review of Scientific Instruments. Two other papers[4,5] have been submitted to The Physical Review.

Dissociation of Hydrogen Molecular Ions on H_2

The present experimental work on these reactions is a refinement of preliminary work completed in this Laboratory in 1962. Since then the work of McClure[6] has been published. He has found that dissociation cross sections of H_2^+ and H_3^+ vary with ion source pressure, apparently as a result of molecular excitation. Since ion source type may affect the cross sections, our work with an rf ion source is of value in comparison with McClure's work with a Penning source. There is added incentive to establish these dissociation cross sections, as they may affect previously determined charge-transfer cross sections.

---

*Cornell Aeronautical Laboratory, Buffalo, New York.

1. R. H. McFarland, The Cause of the Observed Polarization of Electron Induced Radiation from Helium (UCRL-7264, May 15, 1963), Phys. Rev. (to be published February 17, 1964).
2. E. S. Chambers, Secondary-Electron Yield on Copper-Beryllium for H^+, H_2^+, H_3^+, H^0, H_2^0, and H_3^0 (UCRL-7421, August 28, 1963), Phys. Rev. (to be published February 17, 1964).
3. E. S. Chambers, Power Calorimetry of Fast-Particle Beams (UCRL-7459, August 28, 1963), Rev. Sci. Instr. (to be published January 1964).
4. E. S. Chambers, Charge-Transfer Cross Sections for H^+, H_2^+ or H_3^+ on H_2 from 2 to 55 keV (UCRL-6987, June 25, 1963), submitted to Phys. Rev.
5. G. O. Brink, Absolute Ionization Cross Sections of the Alkali Metals (UCRL-7492, August 29, 1963), submitted to Phys. Rev.
6. G. W. McClure, Phys. Rev. 130, 1852 (1963).

A narrow hydrogen beam was passed through a collision region containing H_2. Reactants and products were then magnetically analyzed and the components measured with a Faraday cup having an entrance aperture wide enough to include slightly deflected product ions. The resulting e/m and energy analysis is shown for positive ions in Fig. V-2 and for negative ions in Fig. V-3.

Preliminary results at 15 keV differ somewhat from McClure's work.

Reaction	σ_d in Å^2	
	Present	McClure
$H_2^+ \xrightarrow{H_2} H^+ + H$	1.3	2.3
$H_3^+ \xrightarrow{H_2} H^+ + H_2$	0.9	1.3
$H_3^+ \xrightarrow{H_2} H_2^+ + H$	4.2	1.1

H^+ charge transfers to H^0, which can then acquire an additional electron. For this latter reaction the data yield $\sigma_{0\bar{1}} = 1.3$ Å^2 (15 keV). The corresponding reaction for H_2^0 is improbable, as no H_2^- was detected. The H^- E/2 must result from charge transfer of H^0 E/2. This yields a lower energy but less accurate value, $\sigma_{0\bar{1}} = 1.4$ Å^2 (7.5 keV). The H^- E/3 similarly yields $\sigma_{0\bar{1}} = 0.1$ Å^2 (5 keV).

A trace of H_5^+ was detected and also its dissociation product H^+, E/5. Although the system base pressure was about 2×10^{-6} mm Hg, a gamut of oxygen, hydrogen, and nitrogen compound ions was detected. The most prominent was OH^+, and, as shown in Fig. V-2, its dissociation product H^+ E/17 was detected.

Secondary Electron Emission from Hydrogen Ions and Neutrals on Copper Beryllium

The final report[2] was written and issued. The calorimetric technique used in this work was written up and issued.[3]

Electron Scattering

Absolute cross sections for ionization by electron impact of sodium, potassium, rubidium, and cesium have been measured by use of the modulated crossed-beam machine. Values obtained for maximum cross sections have been tabulated,[5] and were observed to increase with increasing atomic number. An unsuccessful attempt, due to inadequate signal-to-noise ratio, to measure the absolute ionization cross section of lithium should become successful with improved vacuum.

During the "down period" of the electron crossed-beam machine, an attempt has been made toward a better understanding and improvement of

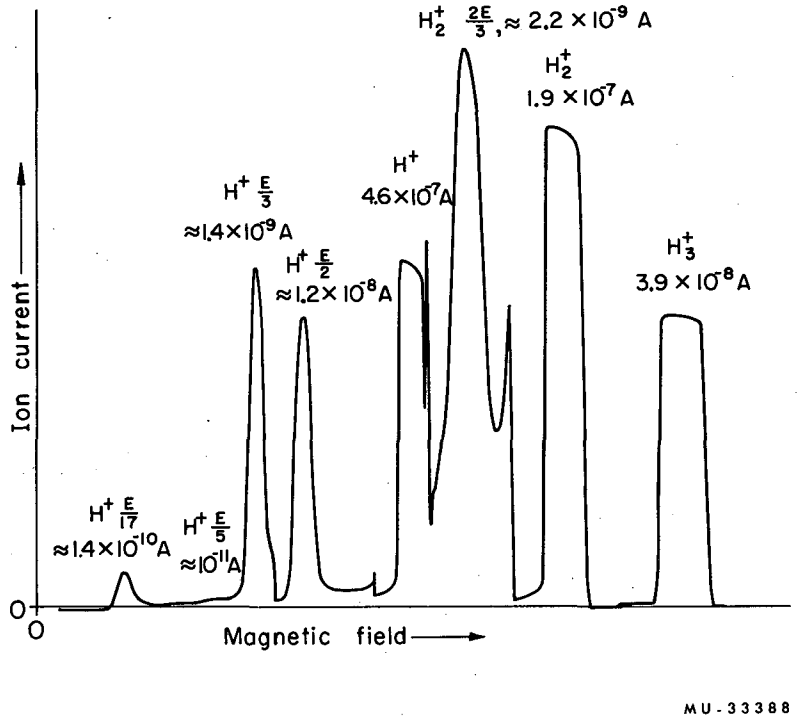

Fig. V-2. Positive ion e/m, energy spectrum.

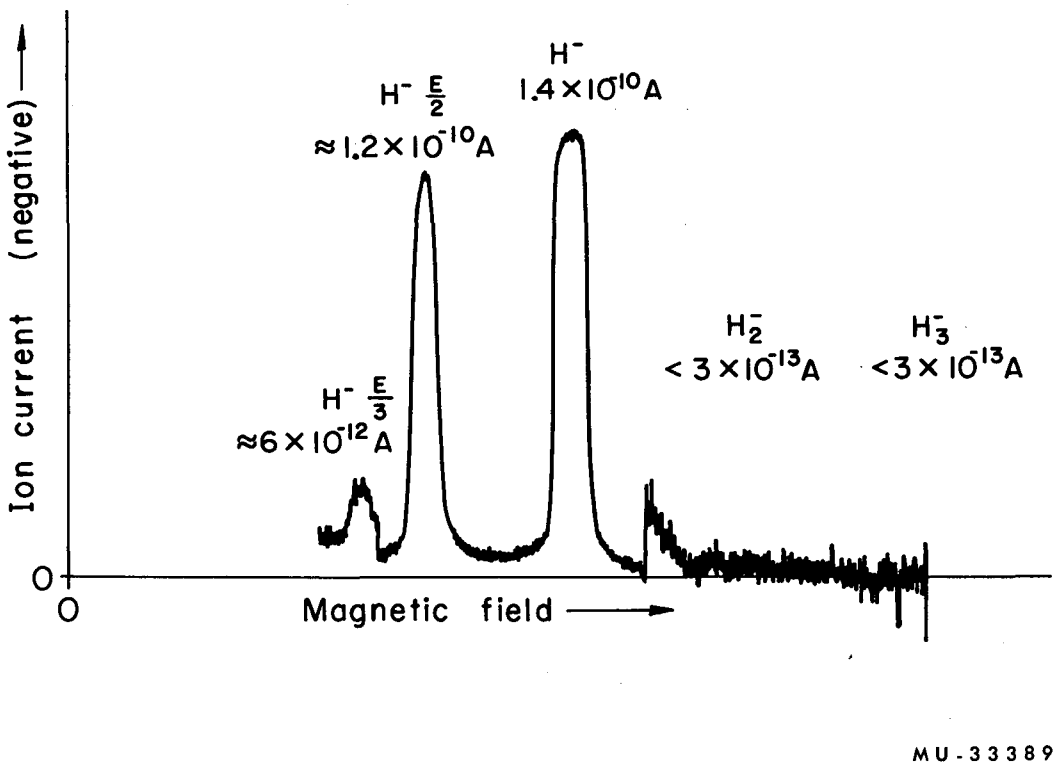

Fig. V-3. Negative ion e/m, energy spectrum.

an electron gun satisfactory for crossed-beam experiments. Such a gun has been in use and described[1] in connection with optical measurements in which the half-breadth resolution, somewhat improved by the optics, was of the order of 0.1 volt. The elastic scattering resonance in helium observed by Schultz[7] was ultilized, and the electron beam energy resolution was shown better than 0.2 V at the resonance energy of approximately 19.5 V. The gun utilizes 0.030-in. apertures, and the beam is focused by a 15-gauss magnetic field with 98% efficiency to a 0.25-in. cup at 2 in. distance. Currents as great as a few microamperes were available at 2 V, and excitation onset potentials were observed to be shifted by as little as 0.2 V at 24 V.

This gun as presently developed should be satisfactory for the majority of planned crossed-beam experiments to 500 V or higher.

Measurements made with this gun on the elastic scattering resonance of helium have used the onset potentials of both the 4922- and 4388-Å lines of helium and the 5400- and 5852-Å lines of neon as potential calibration points. Best results to date indicate a resonance potential of 19.67±0.1 V, in contrast to Schultz's measurement of 19.3±0.1 V.

7. G. J. Schultz, Phys. Rev. Letters 10, 104 (1963).

VI. ENGINEERING AND TECHNOLOGICAL DEVELOPMENT

1. ULTRAHIGH-VACUUM DEVELOPMENT

Norman Milleron

We have devoted the last six months to the following projects:

1. Diffusion pump jet design.
2. Stainless steel to stainless differentially pumped valve closures.
3. A leak detector for large leaks.
4. A trigger gauge responding to overpressure.
5. A method for opening welded joints.

A separately issued report[1] contains a summary of the work done up to October on diffusion pump jets and stainless steel to stainless steel valve closures. Within the past 2 months more understanding was obtained about the stainless-to-stainless type of valve closure. A separate report summarizing this information is being prepared.

A report[2] presented before the American Vacuum Society covers much of the work done with the leak detector. Additionally, a grating monochromator was set up and chart records of emission spectra using a 1P28 PM tube covering the range from 7000 to 3500 Å were made. Air leaks established equilibrium pressures between several torr and $< 10^{-3}$ torr. Over this same pressure range, varying amounts of helium gas were admitted along with the air. These data remain to be analyzed.

Following the publication by McClure, a trigger device for sensing overpressure was constructed and tested. In addition, this device was made in a nude form. In this nude version, the solid cylindrical cathode and solid end caps were replaced by stainless steel wire screen of No. 10 mesh of 0.015-in.-diameter wire. This overpressure sensor was powered by three 300-V batteries in series. A Townsend discharge current less than a μA was drawn when the pressure was below the threshold of the device. Perhaps this battery-powered device can function in fail-safe applications.

One of the problems in using make-and-break welded joints[3] is in opening the joint. A device that cuts open a welded seal with a tubing cutter wheel was built and used successfully for removing the weld from the seal.

1. Norman Milleron, Progress Report on Diffusion Pump Development (UCRL-7505T, Sept. 16, 1963) to be published in Vacuum.
2. Norman Milleron, Detection of Leaks and Mercury Vapor in Vacuum Systems by Analyzing Light from Discharges (UCRL-7399T, Aug. 1963), 1963 Vacuum Symposium Transactions, to be published.
3. Controlled Thermonuclear Research Quarterly Report, UCRL-9002, Dec. 10, 1959, p. 116.

This seal was made by fusing together two 1/16-in. -thick stainless flanges about 11 in. o.d. Each cut and reweld used up ≈ 1/64 in. of the seal radius.

It is my pleasure to acknowledge the outstanding contributions of Elmer L. Borden and Glen S. Matteson in the vacuum laboratory.

2. MECHANICAL ENGINEERING DEVELOPMENT

Thomas H. Batzer

2 X Multistage Compression Facility

James N. Doggett and John Benapfl

Design and test work was aimed at improving the vacuum in the 2X vessels. Pumping tests were made on the 5500-liter east vessel with a mild bake (180° F). The four liquid-nitrogen-trapped 10-inch mercury diffusion pumps yielded a pressure of 4×10^{-8} torr. Maximum pumping speed was 4000 liters/sec at 8×10^{-5} torr, and the speed at 3×10^{-7} torr was 2000 liters/sec. Gettering in this same tank with molybdenum provided a base pressure of 3×10^{-9} torr.

Three additional 5-ft-diameter vacuum vessels, each 3 ft long, were designed and ordered. These will make the length of the machine for various experiments adjustable in shorter increments.

Liquid-nitrogen-cooled liners for the 5-ft-diameter vacuum vessel sections are on order. These liners will be used in conjunction with molybdenum or titanium evaporation to improve the system base pressure and pumping speed.

Arrangements of components for an initial experiment have been decided upon and the assembly should be in operation in the first quarter of 1964.

Low-Energy Neutral Beam Experiment

William S. Neef, Jr.

Magnet performance has been entirely satisfactory in the "B" version of Alice. During extended operational periods the magnet temperature was kept near 100°K at all times. This reduced thermal cycling has apparently extended coil operating life. Ice formation in thermal cracks was the cause of the previous shorting failures. The new bifilar winding technique has been used on one new coil section, which was completed during December. This coil will be tested in January 1964.

The axial limiter and radial profile detector has performed very well both electrically and mechanically. Spring-loaded Teflon chevron seals have been successfully employed on the 5-in-diameter shaft. Other diagnostic tools were evaluated and are being replaced with new types of instrumentation such as solid-state neutral detectors and a microwave horn and reflector.

Tests on the 40-kV Von Ardenne source showed the need for a large "searchlight" focusing magnet to be remotely positioned while inside the source vacuum tank. This system has been released for fabrication. In addition a pair of quadrupole magnets in a "strong focusing" arrangement have been suspended on gimbals to be mounted just in front of the 20-kV beam source. Assembly is nearly complete.

The electrostatic preionizer has been installed in the Alice beam tube. Preliminary tests and small insulator alterations permitted 110 kV to be held across the beam gap. Initial tests with beam injection should be completed by late December.

A substantial positive plasma potential exists under present trapping conditions. A large cathode is being designed to mount outside the mirror on the magnetic axis. It is hoped that the deficiency of electrons in the plasma can be corrected by using hot tantalum wires as a source. The very low system pressure which must be maintained during cathode operation presents serious design obstacles.

A second major design study was started in November. In order to reverse the magnetic field gradients around the plasma, one can use four large magnet coils mounted in a quadrupole formation around the plasma trapping chamber--that is, superimposed on the normal mirror field. The forces on these magnets and their support structure are of the order of 150,000 lb. A structure capable of satisfying the requirements is nearing design completion. Several changes in the beam tube are also needed to accommodate the magnet support structure.

The design of a 4°K shielded target assembly has been completed for use by Alice in wall-plasma interaction studies. The apparatus consists of a 6-in. diam × 4-in.-long target chamber, surrounded by a 10-liter helium Dewar shielded by liquid nitrogen. Various target assemblies may be installed within the chamber; the latter also contains a beam access port and focusing lens to an adjacent mass spectrometer, operating at 77°K. This apparatus is contained within a high-vacuum vessel, which in turn, is coupled to the existing experimental apparatus.

Astron

Charles F. Hurley, James F. Ryan, and Carl J. Anderson

Astron Main Chamber

The final assembly of the Astron main chamber was completed on December 17, 1963. Diagnostics that have been included in the initial assembly are as follows:

(a) Nine rf antennas, installed in ports designed to minimize field perturbations. These may be rotated or withdrawn from the tanks with minimum down time.

(b) Twelve resistors in the resistor arrays, modified and installed to make it possible to monitor the resistor response.

(c) Three ports installed on the tanks for TV cameras. Two cameras have been installed to monitor visible effects of the E layer.

(d) A system consisting of a gas supply, leak valve, pulser valves, and nozzles, which has been installed. This system is designed to admit a desired gas in pulses synchronized with the electron injection, to allow possible visible control of the E-layer buildup.

(e) A system designed to dump a measured amount of gas into the tanks. The higher pressure will destroy the E layer, again making possible visible diagnostics.

(f) A seven-layer slat target of the type being used in the current beam experiments. This target will be used when all magnet power is off to monitor the injected electron location.

(g) A 32-slat target in the tanks at the end opposite to the point of electron injection. This target will be used with a level field to monitor the electron orbit radius. Sixteen Hall-effect magnetometers were installed in the system at various locations both on the machine axis and outside the tanks. One probe was located at the machine axis at the plane symmetry so as to monitor the E-layer field directly.

The auxiliary or negative-flux cantilever coils, one 20 ft long and the other 29 ft long, have been fabricated but were not installed in the initial assembly.

In order to install the 30 trapping resistor modules within the 1 mm on center required, special assembly jigs were developed. These were then inserted in the tanks and aligned as a unit with the machine axis.

The thin 50-mil copper jackets covering the cantilevered coils have been very difficult to maintain vacuumtight. Several techniques have been developed to leak-check these jackets. The jacket ends are 42 ft from the accessible ends of the machine when assembled, making it impossible to pinpoint leaks after final assembly; however, the base pressure of the system with one pump on either end is about 5×10^{-7} torr.

The nylon tubing used to supply cooling water to the 120 cantilever coils has developed leaks. The manufacturer states these are stress cracks and cannot assure complete freedom from them. About 4000 feet of this tubing is installed. Copper tubing with a polyethylene jacket has been procured to replace the nylon tubing, and will be installed when the machine is disassembled to install the negative-flux coils over the existing cantilever coils.

720-kV Electron Gun

In the past two years four accelerating columns have been purchased, and only one of these is vacuumtight. This unit, although not dimensionally correct, is the only one on hand that will permit operation of the gun. Eitel McCullough Company is trying to fabricate one unit that will be used in the spare gun assembly.

The Freon blower continues to be a problem. Four months is the maximum trouble-free operating time we have achieved. This seems to warrant investigating a more reliable blower, which is being done.

An additional 10-in. mercury pumping system was added to the gun cathode chamber and accelerating column.

Bumpy Torus

Eugene T. Bradley and Manuel Calderon

Mechanical assembly of the Bumpy Torus apparatus has been completed and the torus and its associated pumping equipment has been leak-tested. The vacuum attained thus far is 3.5×10^{-6} torr in the torus and 7×10^{-7} torr at the 32-in. diffusion pump. The 32-in. diffusion pump bases at 3.6×10^{-9} torr. It is expected that with further pumping the base pressure in the torus will come down considerably. These measurements have all been made without use of the 6-in. pumping system for the electron gun--that is, with only the 32-in. diffusion pump in operation.

It is expected that the entire system will be in operation before the end of the year. Design has been completed for a new injection box, but owing to long delivery time required for fabrication and other considerations, the present box has been installed in the torus.

Pinch and Shock

James F. Ryan and David C. Holten

Levitron

The cryogenic pump developed for use on the Levitron has been installed on that apparatus and is now fully operational. The liquid helium transfer system is automatic and maintains the cold pumping finger near 5°K. Pumping speed is estimated between 300 and 400 liters/sec. Initial cool-down of the pump result in an

approximate magnitude reduction in system pressure, from 10^{-7} to low 10^{-8} torr. Though not measured, the ability of the finger to pump hydrogen is readily evident during normal Levitron operation. It is felt that this effect is due to trapping or to adsorption by other condensed system impurities.

Hard-Core Cusp

A Hard-Core Cusp machine has been designed and most of the parts are being fabricated. Recent improvements in ultrahigh-vacuum technique are being incorporated in the vacuum vessel design, and very low base pressures are expected.

Magnet Development and Fabrication

Arthur H. Harvey

Table Top Line Coils

The first coil of this type was constructed of 1/4-in. square hollow conductor in a hexapole arrangement, series connected. Because of the unusual geometry of this type of coil, a large number of layout, machining, forming, and laminating operations were necessary. The coil operated for several months. During this time two coil failures occurred when the coil was pulsed in a sense such that the mirror field and the field in the return bends of the coil were opposing. This put elements of the coil separated by two axial slots in compression. The subsequent yielding and buckling crushed the vacuum chamber. Although the laminated form was fractured in some locations, no repairs to the coil were necessary. Final failure occurred when the conductor opened at the terminal; however, the coil was not internally shorted.

The second coil was constructed of 7/16-in. square hollow conductor in a four-element quadrupole series-connected arrangement. Because of the larger conductor cross section it was not practical to attempt to form the conductor in place. The coil was therefore constructed on a jig by making miter solder joints between the elements and their adjacent bends. This coil is now in operation.

The third coil is now under construction. It consists of 0.340-in. square hollow conductor in a six-element hexapole arrangement, series connected.

Alice Quadrupole Magnets

The first coil of the bifilar type has been wound and placed in the potting fixture. It is now being blocked and sealed in preparation for impregnation. The new coil provides the same length cooling path as the previous mirror coils without the necessity of discharging the liquid nitrogen into a center annulus. The coils have a more rugged cooling and electrical terminal arrangement than the previous mirror coils.

Astron Aluminum Cantilever Coils

The 20-ft coil has been wound. After minor adjustments the new winder constructed for this job performed without incident. With proper tension and guide-roller adjustment the winder moves down the rails as the coil is being wound. Much less tension was required to wind the coil than was originally estimated (approximately 300 pounds). Also a test section indicated that stress in the conductor material relieves itself over a period of days at room temperature. Therefore to maintain maximum springback in the coil, it must be placed in its container within a short period of time after winding. Some cracking and checking developed in the terminal conductor joint during winding. These were repaired and leak-tested after the coil had been wound. The 29-ft coil is now in the process of being wound.

Component Development

Thomas H. Batzer and James F. Ryan

Further development of ultrahigh-vacuum aluminum vessels, reported in UCRL-7393,[1] was presented at the American Vacuum Society meeting at Boston in October. Tests since that report verify the suitability of 6061 alloy as well as 5456 for ultrahigh vacuum. Outgassing of a 50-liter vessel was so low that a B-A type nude ion gauge alone maintained the pressure at 2×10^{-9} torr when valved off from the diffusion pumps and molybdenum getter.

A movable baffle has been added to the current design of the liquid nitrogen trap. It can be lowered to cover the oil diffusion pump during start-up. This prevents oil from splashing into the trap during the erratic starting phase while the oil is being heated and outgassed. The arrangement can be seen on LRL drawing AAA-63-101261-00.

The evaluation and accident recovery tests of an Alice-type pumping system on a 75-liter volume have been completed. These tests were made with a 6-in. mercury diffusion pump in place of the 1440 PMC (6-in. CVC oil diffusion pump). The following is a summary of the results:

1. Mercury lost to the liquid-nitrogen-cooled ultrahigh vacuum elbow trap is negligible, as the system ran for 69 days at 2 to 3×10^{-10} torr.
2. Recovery from catastrophic up-to-air accidents is simple and complete if all the high-vacuum surfaces are bakable.
3. Pumping speed for air at 1×10^{-5} torr was about 350 liters/sec.

Further runs were made on the same system except that a converted 720 PMC (4-in. CVC oil diffusion pump) was installed in place of the 6-in. mercury pump. The conversion consisted of replacing the aluminum jets with geometrically identical mild-steel jets to permit operation with mercury. A simple forearm condenser was also added to reduce the loss of mercury to the backing pump. Base pressure and speed runs were made, first with only water cooling on the upper barrel and forearm condenser and then with Freon cooling to -30°C. A summary of the results to date is as follows:

1. Thomas H. Batzer and James F. Ryan, Some New Techniques in Ultrahigh Vacuum, UCRL-7393, Aug. 1963.

	H_2O-cooled	Freon-cooled
Base pressure	5×10^{-10} torr	1.6×10^{-10} torr
Pumping speed at 10^{-5} torr	250 1/sec	———

Speed tests Freon-cooled have not yet been taken.

Cryogenic Project

Clyde E. Taylor and Robert L. Nelson

A series of techniques has been developed for practical fabrication of a 6-in. i.d. sodium coil in "pancake" sections. Seventeen "pancake" sections, each wound from a 25-ft-long, 3/8-in. square, 0.010-in.-wall tube, with 99.99% purity copper terminals, have been filled with ultrahigh-purity sodium and wrapped on a grooved mandril. These sections are now being heat-treated, fabricated into rigid mounting rings, "potted" with a Pb-Bi eutectic filler metal, and individually tested for electrical resistivity using the Collins gas refrigerator for cooling to 10°K. Resistivity tests to date have been satisfactory. The completed coil will be tested by using the refrigerated transport Dewar-cooled helium expansion facility. Assembly of the machined aluminum mold for casting a coil of different design has been postponed pending development of a bubble-free casting technique.

A simple technique for cryogenic heat transfer using closed natural convection loops has been developed. Experiments were made on a series of loops using various geometries, heat transfer fluids, and charging pressures. This technique is now being used for several vacuum system liquid nitrogen traps around the Laboratory.

The "Kirk-cooler" refrigerator, a unique liquid-nitrogen-temperature cooling machine, has been actively developed under P Division sponsorship in Building 153.

A preliminary design study and cost estimate was made on a "minimum-B" low-energy containment machine using liquid-nitrogen-cooled coils and cryogenic vacuum system.

Various general mechanical engineering studies of a short-term nature were made for other divisions of the Laboratory.

3. ELECTRONICS ENGINEERING DEVELOPMENT

Hugh W. Van Ness

Pyrotron

David R. Branum

Table Top III

The experiment has been in operation all during the past 6 months with no major electrical or electronic failures.

A main pulse coil system of lower inductance was installed early in the period. The main capacitor bank discharge switch system was reconnected so there are now two positive and two negative type-5555 ignitrons.

Construction was started on the Solatron capacitor bank and its control system. The bank is now a 50-unit positive and a 50-unit negative 20-kV capacitor bank, each capacitor unit being 7.5 μF. The positive section is 60% complete. The negative section is 40% complete. The banks will be completed when the remaining hardware is received from outside fabrication.

Toy Top III's

The experiment has been in a continuous operating mode for the past 6 months. There have been several capacitor failures in the banks made up of the old 7.5-μF General Electric units.

There was one capacitor failure in one of the 200,000-joule banks. These banks are made up from 14.5-μF 20-kV Tobe Deutschman capacitors. These capacitors have been discharged 60,000 times at various voltage levels. In the 60,000 discharges, five capacitor units have failed in the shorted condition out of a total of 180 units installed.

2X Multiple-Stage Compression Experiment

The past 6 months have been devoted to construction of the control system, the bank charging supplies, the dc magnet supply output and control, and the capacitor bank sections in Building 156.

In Building 180, a 1-megajoule capacitor bank is 80% complete. All that remains to complete this bank is 146 14.5-μF capacitor units from the Toy Top III's experiment.

All of the remaining capacitor banks in Building 180 are complete and are ready to connect to their respective load coils.

In Building 156, one 1.25-MJ 30-kV capacitor bank is complete and a second 1.25-MJ 30-kV section is 85% complete.

Four 25-kV 4-A dc charging supplies for the bank sections in Building 156 are complete and ready for use.

Two 25-kV 6-A dc charging supplies are complete and are now connected to five capacitor banks in Building 180.

The control and output leads for three 25-kV 6-A dc bank charging supplies are complete. These supplies are now in use by Toy Top III's and will be connected to the remaining five capacitor banks in Building 180 when Toy Top III's is deactivated.

Five 300-kW dc magnet supplies are now connected to the 2X experimental area. Three of these supplies are now in use by the 2X source development experiments.

An additional 300-kW dc magnet supply that was connected to the 2X area has now been disconnected and temporarily connected to the Alice experimental area in Building 180. The control and output leads for five additional 300-kW dc magnet supplies have been installed from Building 156 to the 2X area in Building 180. When Toy Top III's is deactivated, the leads will be connected to the supplies.

The diagnostic cable system has been installed.

The main control system in Building 180 is now 100% complete, and is now in a checkout "debugging" phase.

A 15-μF 50-kV fast capacitor bank has been designed, and a prototype section was constructed and tested for 2,000 operations. The complete capacitor bank is now under construction. This bank will be used in the 2X source development area.

Atomic Scattering and Cross-Section Measurements

The installation of the experimental facilities in Building 180B are now complete. The three experimental areas are now in operation.

Design work has been completed on two detectors. The 100-cycle mercury relay phase detector and the solid-state phase detector have been constructed and tested. Both units are now ready for use on the experiments.

Design work on two lock-in amplifiers has been completed. The low-frequency unit has been constructed and tested and is ready for use. The high-frequency unit is now under construction.

Pyrotron

G. Gordon North

Alice

Operation of the Alice machine was resumed the latter part of August following a long shutdown for work on the vacuum system and replacement of the sections of the mirror field coils, which had previously failed.

Variable ac heater power was provided for heating a large titanium target plate located in the beam burial chamber.

New high-density push-button control panels were built and installed in the control console where control function panel space was becoming scarce.

The General Electric partial-pressure analyzer equipment was successfully adapted to the Alice vacuum system for analysis of the residual gas constituents. This equipment uses a combination mass spectrometer tube and photomultiplier detector capable of extreme sensitivity, 10^{-14} to 10^{-16} torr, and fast scan rates up to 1 msec per mass scan.

Planning and design began in October to provide power and control for a "minimum B field" coil configuration. For this arrangement, four or six 16-inch i.d. modular liquid-nitrogen-cooled coils will be used to provide the mirror field. In addition, four Alice modular coils of new design will be mounted in a quadrupole configuration around the confinement chamber. The mirror coils are to be powered by a 300-kW Perkin dc supply borrowed from the 2X Group. The quadrupole coils will be powered by the existing Alice mirror coil dc supply.

The calutron-type ion source has continued in operation. Palladium leak-type hydrogen gas purifiers with sufficient flow rate capacity for use in the gas system for this source were ordered and installed. Experimental operation of the source in a so-called accel-decel mode is currently in progress. In this arrangement, a third electrode, operated at a high negative potential, is located between the arc chamber at positive high voltage and the grounded extraction slit.

Satisfactory regulation of the ion source magnetic field has been accomplished by using a Bell Model 240 incremental gaussmeter as the field-sensing and error-signal-producing device. A permanent installation using this instrument would require a special probe with a long cable and a factory modification of the gaussmeter which would render it unusable with the standard probes. Because of this difficulty, the J. C. Carter rotating-coil fluxmeter instrument has been sent back to the factory for inspection, repair, and recalibration. When returned, it will be placed in the now existing mount and connected for this field-regulating function.

A decision was made to use a Von Ardenne duo-plasmatron-type ion source as the initial "Piggy Back" source. Design and installation of the electrical system for this facility has been in progress. All purchased parts required are now on order.

Ion source development in the 100-kV injector facility is to continue as time permits.

The installation of a third pair of 16-in. i.d. modular coils powered by a third 200-kW Bart-Messing dc supply has been completed in the P-3 experimental area. This will make possible a cusp field configuration for off-axis injection experiments with the P-3 occluded gas type of ion source. For the last 4 months, this area has been used for the experimental operation of a Puffatron-type hydrogen ion source. A 0.5-μF 30-kV capacitor bank, charging supplies, and control system were provided for this project.

The plasma potential monitoring system has been improved and satisfactorily operated during this period of operation of the Alice machine.

Solid-state charged-particle detectors are being employed in several of the diagnostic devices.

A fast-response very-low-current sensitive transistor amplifier of Oak Ridge design is being built for use with the radial profile detector system. The reported performance of this amplifier is as follows: Gain 10^{-7} A/V; it will drive a 90-ohm line to ±1 V; rise time about 1 μsec; rms noise corresponds to a signal of about 2×10^{-10} A. Power is supplied by 4-V mercury cells.

Pinch Program

Levitron Experiment

Except for routine maintenance, the Levitron experiment has been in almost continuous operation since July. Operation of the high-voltage capacitor banks during this same period has been excellent, with only minor failures.

Early in July, the high-voltage ignitron crowbar units on banks 1, 2, and 3 were modified. This modification, along with an automatic hi-pot check of the ignitrons, is primarily responsible for the improved bank operation at the long rise times presently used.

Work on a pulsed electron source for Levitron plasma diagnostics has been completed. This effort resulted in a high-field emission electron gun which produced a 100-kV 200-A 0.2-μsec electron burst. A flash x-ray pulser was used to supply the gun.

A 100-kc induction heating oscillator has been modified for rf heating of the Levitron plasma. This unit is presently used to supply a 30-kW 3-Mc 5-msec rf pulse to the plasma. Indications are that an increase in ion temperature occurs when the oscillator is used in the experiment. Radio-frequency plasma-heating experiments will continue at both the low ion cyclotron frequencies around 3 Mc, and the electron cyclotron frequencies around 10 kMc.

Hard-Core Cusp

Electronic design and installation is now in progress on the "Hard-Core Cusp" experiment. This experiment will investigate the properties of a ring of plasma confined in a cusp field with a central current-carrying copper core.

The experiment will be located in the old "Beta Pinch" area and will use the existing control racks and screen room. The recently completed eight-section high-voltage capacitor bank will be used to provide the pulse core current, and two existing Perkin power supplies will supply the cusp field coils.

The electronic system configuration has been established and design of nonstandard chassis has been completed.

Final design of the various control chains will be completed shortly, along with the necessary cross-connect diagrams.

Special chassis and nonstandard items are now being fabricated or purchased. Except for the above items, rack installation and wiring has been completed.

Bumpy Torus Experiment

During the past month effort has been devoted to completing the electrical and mechanical installation of the full torus and injection section. This effort is now essentially complete and full-scale operation should begin shortly.

Until recently, experiments were being carried out on the injection section only. The results demonstrated the feasibility of the injection method and provided useful operating information.

Pyrotron

Cryogenics

Only minor electronic effort has been required for the cryogenic coil experiment, since the experimental effort has been devoted to sodium coil fabrication techniques.

With actual coil tests expected in the near future, fabrication and installation of a new diagnostic patch panel system is being completed.

Astron

D. O. Kippenhan

Astron Accelerator

Six sections of the accelerator and the 760-keV electron gun are operating at an average pulse-forming network voltage of 31 kV. Operating time averages 30 to 35 hours per week, on swing shift to allow construction to continue on the Astron tank. Operation has been satisfactory, at a repetition rate of five pulses per second, with a 140-A average beam of 4.12 MeV energy.

We expect to raise the repetition rate to 30 pulses per second after January 1, 1964. This will introduce erratic operation owing to thermal drift within the thyratron switches powering the magnetic cores. Work is now in progress to anticipate this type of operation and take the necessary corrective action.

Work done by English Electric Valve Company indicates that filling thyratrons with a mixture of deuterium and hydrogen stabilizes the thermal

drift and reduces the prefire or early-breakdown tendencies. Ratios of 0 to 100% deuterium have been evaluated. Preliminary results indicate that an increase in voltage-holding capabilities of 25% may be gained from any mixture, with the 30% and 100% ratios exhibiting the optimum thermal drift properties and lowest prefire rates. A larger sample of both ratios has been ordered and will be evaluated. The successful completion of this work should reduce the prefire rate and permit higher-voltage operation. A more reliable higher-energy beam will then be obtained.

The core monitor system, used to detect prefires, monitor core voltages, and aid in the timing, is approximately 75% complete. Many of the required chassis are installed and all cabling work is done. The cabling required almost 50,000 ft of RG-213/U coaxial cable. This system is expected to be operational by April, 1964.

This system will aid also in the gathering of statistics on the Astron machine for improving the reliability. At the present repetition rate this is not a serious problem, but as the rate is increased, mean-time-to-failure is 0.5 hour at 60 pps. This figure is the result of the failure reporting system implemented in February 1963, but does not include the resonance-charging system for the pulse-forming networks.

The pulse-forming networks are pieces of RG-218/U coaxial cable cut to the proper length for a 0.4-μsec pulse. They are charged to 32 kV by a dc command resonance-charging power supply. The Astron experiment requires that the networks be charged to this voltage 60 times per second with ±0.2% regulation. These power supplies will not produce this regulation and therefore the regulation system must be redesigned. This is approximately 95% complete and is awaiting manpower to construct the prototype regulation system. The major design features have been checked in actual operation and the required regulation obtained.

Improvement of the beam can be obtained by improvement of the magnetic cores, which is the key to the Astron accelerator. We are working with suppliers of magnetic material and testing new types. None so far has shown any improvement over the present 50-50 nickel-iron core.

Astron Reaction Chamber

The Astron concept of plasma containment and heating is based on a stable dense rotating layer of relativistic electrons (the E layer). This layer is formed and contained by an external solenoidal field. The resultant field of the spinning layer of electrons and the external solenoid create a region of closed magnetic field lines. Within these closed lines, or magnetic bottle, a plasma of tritium or deuterium can be trapped and heated by collision to the required temperature for thermonuclear fusion reactions.

A 90-ft-long, 5-ft o.d. vacuum liner, surrounded by a single-layer solenoid winding and having two cantilevered solenoids on the inside, forms the reaction chamber. The center of the liner is the E-layer region where the plasma will be formed. The external solenoid is composed of water-cooled modular coils. Each module is 6 in. long and is powered by an individual power supply. The inner cantilevered coils are identical in construction.

Forty-nine 15-kW, sixteen 30-kW, and one 200-kW remotely programmed, current-regulated power supplies feed the outer layer. These supplies were purchased on outside contracts and installed along with the necessary cabling by Laboratory personnel.

Thirty-three 4-kW, nine 2.25-kW, thirteen 1-kW, and seventeen 0.25-kW remotely programmed, current-regulated power supplies are used on the inner coils. The cost of these supplies was reduced substantially by using one large unregulated, nonadjustable dc power source and pulse-width modulation on the multiple outputs to obtain the regulation, fast response, and filtering required. These power supplies were built by LRL Berkeley and installed by LRL Livermore.

All inner and outer coils, power supplies, and cabling are installed and operating satisfactorily. Approximately 55 man-months of electrician effort was expended in the installation and cabling.

Trapping the electrons requires a mirror geometry on the external and internal solenoid fields. This can be accomplished by programming the reference voltage to the power supplies. This reference has been designed and installed so that the operator can adjust the reference (i. e., the output current) to any of the 100 power supplies individually. Not only can the mirror shape be changed by individual power supplies by the use of a large common reference supply, a linear tapped resistor, and variable resistors all tied together by computer-programming patch boards, but the entire shape may be changed in less than 10 minutes by inserting a new program board.

Diagnostics for the reaction chamber are developed and installed. Three closed-circuit TV cameras will observe the buildup of the E layer and its destruction by an air injection. Nine rf pickup loops will pick up rf energy of the beam and indicate stable plasma conditions. Fifteen Hall probes will monitor the external field, and one Hall probe will indicate field reversal that occurs when the E layer is formed. A 32-slat target will pick up the beam before the mirror is applied to indicate that the beam energy and the magnetic field are compatible. Loops attached to deceleration resistors that provide rf mode rejection will monitor the amount of energy lost by the beam to the deceleration resistors.

All systems have been installed and checked and the beam deflected into the reaction chamber on December 20, 1963. The results were considered highly successful.

VII. TALKS AND PUBLICATIONS

Sixth International Symposium on Ionization Phenomena in Gases, Paris, France, July 8-13, 1963

Charles W. Hartman, Electrode Sheath Effects in Pulsed, High-Current Discharges (UCRL-7357, June 13, 1963).

John R. Hiskes, Cascade Processes in Energetic Neutral Hydrogen Beams (UCRL-7356, July 2, 1963).

Wulf B. Kunkel and Gary A. Pearson, On the Heating of Electrons in Crossed Electric and Magnetic Fields (UCRL-10800, June 19, 1963).

Klaus H. Berkner, Robert V. Pyle, Henry F. Rugge, J. Warren Stearns, and Joseph Winocur, Diffusion from a Line Source in a Magnetic Field (UCRL-10801, June 20, 1963).

International Meeting on Plasma Confinement in Mirror Fields, Fontenay-aux-Roses (Seine), France, July 15-19, 1963

F. H. Coensgen, Plasma Confinement in the Toy Top Experiment, invited paper.

C. C. Damm, Containment and Stability in the Alice Machine, invited paper.

W. A. Perkins, Observation of Plasma Instability with Rotational Effects in a Mirror Machine, invited paper.

R. F. Post, Plasma Instability and Its Stabilization in a Simple Mirror Machine--Comparison between Experiment and Theory, invited paper.

Third International Conference on the Physics of Electronic and Atomic Collisions, University College, London, England, July 22-26, 1963

Robert H. McFarland, The Cause of the Observed Polarization of Electron-Induced Radiation from Helium (UCRL-7264, May 1, 1963).

Klaus H. Berkner, John R. Hiskes, Selig N. Kaplan, George A. Paulikas, and Robert V. Pyle, The Excitation and Lorentz Ionization of 10-MeV Hydrogen Atoms (UCRL-10802, June 19, 1963).

Marvin H. Mittleman, High Energy Charge Exchange

Cryogenic Engineering Conference, Boulder, Colorado, August 19-21, 1963

David C. Holten, The Static and Dynamic Behavior of Helium Gas Thermometers Below 77° Kelvin (UCRL-7327, April 16, 1963).

Wescon Conference, San Francisco, California, August 21-23, 1963

K. A. Saunders and R. L. Sewell, Command Resonance Charging System for the Astron Accelerator (UCRL-7363, May 14, 1963).

Tenth National Symposium of the American Vacuum Society, Boston, Mass., Oct. 16-18, 1963

Thomas H. Batzer and James F. Ryan, Some New Techniques in Ultra-High Vacuum (UCRL-7393, August 12, 1963).

Norman Milleron, Detection of Leaks and Mercury Vapor in Vacuum Systems by Analyzing Light from Discharges (UCRL-7399-T, August 20, 1963).

International Symposium on Plasma Phenomena and Measurements, Annual Meeting of AIEE Professional Group in Nuclear Science, San Diego, California, October 29-31, 1963

R. F. Post, High Temperature Plasma Measurements, invited paper.

David B. Cummins, A Stabilized Ignitron (UCRL-7391-T Abstract, June 4, 1963).

A. F. Waugh and A. H. Futch, A Method for Continuous Measurement of Plasma Potential Over a Range of 0 to 4 kV (UCRL-7414, June 19, 1963).

APS Division of Plasma Physics, Fifth Annual Meeting, San Diego, California, November 6-9, 1963

Harold P. Furth, Plasma Confinement Configurations with Finite Minima in Magnetic Field, invited paper, G2.

Frederic H. Coensgen, Plasma Losses in Magnetic Compression Experiments, invited paper, T1.

Terry Kammash and Warren Heckrotte, Stability of Longitudinal Oscillations in Anisotropic Plasma, A1 (UCRL-7439-T Abstract, July 17, 1963).

Forrest I. Boley and William S. Cooper III, The State of a Highly Ionized Hydrogen Plasma Produced by an Ionizing Switch-On Shock, C5 (UCRL-11022 Abstract, September 19, 1963).

William S. Cooper III and Wulf B. Kunkel, Experimental Study of the Recombination of a Highly Ionized Hydrogen Plasma, C6 (UCRL-11021 Abstract, September 19, 1963).

John Killeen, Time-Dependent Resistive Instability Calculations in Cylindrical Geometry, D5 (UCRL-7509-T Abstract, September 17, 1963).

Harold P. Furth and Marshall N. Rosenbluth, Hydromagnetically Stable Containment of Low-β Plasma in Toroidal Configurations of Minimum Plasma Energy, I, G4 (UCRL-7508-T Abstract, September 19, 1963).

Norman L. Oleson, James F. Steinhaus, and William L. Barr, Electron Cooling and Neutral Density Determination in a Plasma from an Occluded Gas, Cold Plasma Source, H2 (UCRL-7511-T Abstract, September 18, 1963).

R. F. Post, Finite Orbit Effects and the Stability of "Hollow" Plasma, J6 (UCRL-7514-T Abstract, September 19, 1963).

Laurence S. Hall, Self-Consistent Potential Distributions in Low Density Plasma. I--How to Integrate Poisson's Equations, M3 (UCRL-7483-T Abstract, August 26, 1963).

Alan Hoffman and Laurence S. Hall, Self-Consistent Potential Distributions in Low Density Plasmas. II--Preliminary Results of a Cylindrical Probe Problem, M4 (UCRL-7484-T Abstract, August 26, 1963).

Walton A. Perkins and William L. Barr, Plasma Stability Studies with a Complex Mirror Machine, O5 (UCRL-7507-T Abstract, September 17, 1963).

Oscar A. Anderson, Finite-Conductivity Hydromagnetic Instability of a Reverse-B_θ Pinch, O7 (UCRL-11020 Abstract, September 18, 1963).

Stirling A. Colgate, Dale H. Birdsall, and Harold P. Furth, Levitron Confinement and Instabilities, O8 (UCRL-7518-T Abstract, September 20, 1963).

V. Kelvin Neil and Warren Heckrotte, Astron Electron Injection System, Q10 (UCRL-7510-T Abstract, September 18, 1963).

A. H. Futch, Jr., Plasma Potential in a Neutral Injection Experiment, T11 (UCRL-7512-T Abstract, September 19, 1963).

George R. Spillman, A Study of Hydromagnetic Waves in Cylindrical Plasma, U9 (UCRL-11023 Abstract, September 18, 1963).

Meeting of American Society of Mechanical Engineers, Philadelphia, Pa., November 19, 1963

R. F. Post, Status of Research Toward Controlled Fusion Power, invited paper.

U. S. Naval Postgraduate School, Monterey, California, December 13, 1963

Harold P. Furth, Recent Progress in Controlled Fusion Research, invited paper.

APS 1963 Winter Meeting in the West, California Institute of Technology, Pasadena, California, December 19-21, 1963.

Klaus H. Berkner, Selig N. Kaplan, and Robert V. Pyle, Electron Detachment from 20-MeV D^0 and D^- Ions, Bull. Am. Phys. Soc. Ser. II 8, 605 (1963) (UCRL-11053 Abstract, October 8, 1963).

Publications

The Physical Review

Robert H. McFarland and Edward A. Soltysik, Alternate Method of Measurement of Polarization of Light Emitted by He Atoms Excited by Energetic Electrons, 129, 2581 (1963) (UCRL-7037, August 22, 1962).

Selig N. Kaplan, George A. Paulikas, and Robert V. Pyle, Electron Detachment from 20-MeV D^- Ions by a magnetic Field, 131, 2574 (1963) (UCRL-10746, April 19, 1963).

Physical Review Letters

Harold P. Furth, Existence of Mirror Machines Stable Against Interchange Modes, 11, 308 (1963) (UCRL-7452, August 30, 1963).

The Physics of Fluids

W. A. Perkins and R. F. Post, Observation of Plasma Instability with Rotational Effects in a Mirror Machine, 6, 1537 (1963) (UCRL-7302, March 26, 1963).

Allan N. Kaufman, Statistical Derivation of Hydrodynamics for a Coulomb System, 6, 1574 (1963) (MATT-190, May 1963).

Forrest I. Boley, John M. Wilcox, Alan W. DeSilva, Peter R. Forman, Gordon W. Hamilton, and C. N. Watson-Munro, 6, 925 (1963) (UCRL-10381, October 12, 1962).

The Review of Scientific Instruments

Frank J. Gordon and Charles C. Damm, High Intensity Source of 20-keV Hydrogen Atoms, 34, 963 (1963) (UCRL-7095-T, January 12, 1963).